IMPACT OF ANTI-S2 PEPTIDES ON A VARIETY OF MUSCLE MYOSIN S2 ISOFORMS AND HYPERTROPHIC CARDIOMYOPATHY MUTANTS REVEALED BY FLUORESCENCE RESONANCE ENERGY TRANSFER AND GRAVITATIONAL FORCE SPECTROSCOPY

Negar Aboonasrshiraz, B.S.

Dissertation Prepared for the Degree of

DOCTOR OF PHILOSOPHY

UNIVERSITY OF NORTH TEXAS

August 2020

APPROVED:

Douglas D. Root, Major Professor
Robert C. Benjamin, Committee Member
Amie Lund, Committee Member
Ed Dzialowski, Committee Member
Xiaoqiang Wang, Committee Member
Jyoti Shah, Chair of Department of Biological Sciences
Su Gao, Dean of the College of Sciences
Victor Prybutok, Dean of the Toulouse Graduate School

Aboonasrshiraz, Negar. *Impact of Anti-S2 Peptides on a Variety of Muscle Myosin S2 Isoforms and Hypertrophic Cardiomyopathy Mutants Revealed by Fluorescence Resonance Energy Transfer and Gravitational Force Spectroscopy*. Doctor of Philosophy (Biochemistry and Molecular Biology), August 2020, 89 pp., 7 tables, 28 figures, references, 81 titles.

Myosin subfragment-2 (S2) is an intrinsically unstable coiled coil. This dissertation tests if the mechanical stability of myosin S2 would influence the availability of myosin S1 heads to actin thin filaments. The elevated instability in myosin S2 coiled coil could be one of the causes for hypercontractility in Familial Hypertrophic Cardiomyopathy (FHC). As hypothesized FHC mutations, namely E924K and E930del, in myosin S2 displayed an unstable myosin S2 coiled coil compared to wild type as measured by Fluorescence Resonant Energy Transfer (FRET) and gravitational force spectroscopy (GFS). To remedy this, anti-S2 peptides; the stabilizer and the destabilizer peptides by namesake were designed in our lab to increase and decrease the stability of myosin S2 coiled coil to influence the actomyosin interaction. Firstly, the effectiveness of anti-S2 peptides were tested on muscle myosin S2 peptides across MYH11 (smooth), MYH7 (cardiac), and MYH2 (skeletal) with GFS and FRET. The results demonstrated that the mechanical stability was increased by the stabilizer and decreased by the destabilizer across the cardiac and skeletal myosin S2 isoform but not for the smooth muscle isoform. The destabilizer peptide had dissociation binding constants of 9.97 × 10-1 μM to MYH7 isoform, 1.00 μM to MYH2 isoform, and no impact on MYH11, and the stabilizer peptide had dissociation binding constants of 2.12 × 10-2 μM to MYH7 isoform, 3.41 × 10-1 μM to MYH2 isoform, and no impact on MYH11 revealed by FRET. In presence of the stabilizer, FRET assay, affinity of the E930del and E924K increased by 10.23 and 0.60 fold respectively. The force required to uncoil muscle myosin S2 peptides in the presence of the stabilizer peptide was more than in its absence

in muscle myosin S2 isoforms of MYH7 (1.80 fold higher), MYH2 (1.40 fold higher), and E930del (2.60 fold higher) and no change for MYH11 compared to control. The force required to uncoil muscle myosin S2 in presence of the destabilizer was less than in its absence in both MYH7 (2.00 fold lower) and MYH2 (2.5 fold lower) but the same for MYH11 compared to their controls. Both FRET and GFS assays demonstrated that both anti-S2 peptides do not have any impact on smooth muscle myosin S2 isoform. In FRET assay, there was no significant difference in the lifetime value in the presence or absence of anti-S2 peptides in smooth muscle myosin S2. In GFS assay, there was no significant difference in the force required to uncoil the dimer in presence or absence of the anti-S2 peptides smooth muscle myosin S2. Effectively, the stabilizer peptide improved the stability of FHC mutant (E924K and E930del) myosin S2 peptide. FHC mutations showed high lifetime value in FRET assay and low force to uncoil coiled coil myosin S2 in GFS assay. In the presence of the stabilizer, lifetime value decreased in FRET assay and more force was required to uncoil myosin S2 coiled coil in GFS assay. This study demonstrated that structure of muscle myosin S2 can be altered by small peptides. The stabilizer peptide enhanced dimer formation in wild type and mutant cardiac, and skeletal myosin S2 peptides, and destabilizer increased flexibility of cardiac and skeletal myosin S2 wild type peptide. Neither anti-S2 peptides had impacts on smooth muscle myosin S2 isoform. The study thus effectively demonstrates the mechanical stability of myosin S2 coiled coil in striated muscle system could be modified using the specific anti-S2 peptides. Stabilizer of the anti-S2 peptide was effective to remedy the dampened stability of FHC myosin S2 coiled coil thus providing a new dimension of treating cardiovascular and skeletal muscle disorders by targeting the structural property of muscle proteins.

ACKNOWLEDGEMENT

I would like to express my deepest gratitude and acknowledge the efforts of my major professor, Dr. Douglas D. Root, for all his unconditional help and valuable guidance towards my better understanding of scientific concepts and successful completion of doctorate degree.

I would also like to thank my committee members, Dr. Robert C. Benjamin, Dr. Amie Lund, Dr. Ed Dzialowski, and Dr. Xiaoqiang Wang for their precious time and guidance in my pursuit of doctoral degree and I would like to extend my thanks to all my lab family.

I would like to extend my special thanks for my former colleague, Rohit R Singh, in helping me in all possible aspects of my doctorate degree and believing in me.

Lastly, my thanks and appreciations go to my family, my parents and sisters, for their support throughout my life and I will always be indebted to them.

تقدیم به

پدرم به خاطر زحمات بی دریغش و

مهربانی بی انتهایش با دریایی از

سپاسگزاری و تشکر

و

مادرم که مرا درس محبت ، پشتکار،

ایستادگی و گذشت آموخت با سبدی از

گل یاس

و

ستاره های آسمان زندگیم ،

خواهران عزیزم که شادترین لحظات زندگیم

در کنار آنان سپری شد .

TABLE OF CONTENTS

Page

LIST OF TABLES

Page

LIST OF FIGURES

Page

ABBREVIATIONS

ΔE930	Glutamate deletion at 930^{th} residue
^0C	Degree Celsius
A band	Anisotropic band
ADP	Adensoine diphosphate
ATP	Adenosine triphosphate
DCM	Dilated cardiomyopathy
d_{max}	Maximum length of molecule
d_{min}	Minimum length of molecule
DMSO	dimethylsulfoxide
DRX	Disordered Relaxed State
DTPA	Diethylene Triamine Pentaacetic Acid
DVB	Divilobenzene
E	Efficiency of Energy Transfer
E9240K	Glutamate substitution to lysine at 924^{th} residue
FHC	Familial hypertrophic cardiomyopathy
FITC	Fluorescein Isothiocyanate
FPLC	Fast Protein Liquid Chromatography
FRET	Fluorescence Resonance Energy Transfer
GFS	Gravitational Force Spectroscopy
HMM	Heavy meromyosin
I band	Isotropic band
J	Overlap Integral
K_d	Dissociation constant
LMM	Light meromyosin

M	Molar
mM	Millimolar
MYH11	Smooth Muscle Myosin S2 Isoform
MYH2	Skeletal Muscle Myosin S2 Isoform
MYH7	Cardiac Muscle Myosin S2 Isoform
nm	Nanometer
nM	Nanomolar
P	Concentration of peptide
PDB	Protein data bank
P_i	Inorganic Phosphate
PMT	photomultiplier tube
pN	Piconewton
Q	Quantum yield of the donor
R	Separation Distance
R_0	Critical Transfer Distance
RPC	Reverse Phase Chromatography
S1	Myosin subfragment 1
S2	Myosin subfragment 2
SR	Sarcoplasmic reticulum
SRX	Super Relaxed State
T	Temperature
TFA	Trifluoroacetic acid
T_D	Lifetime of donor in absence of acceptor
T_{DA}	Lifetime of donor in presence of acceptor
UV	Ultraviolet

VOC	Voltage operated calcium channel
α	Proportionality Constant
γ	Damping Constant
η	Refractive Index
κ^2	Orientation Factor
μL	Microliter
μm	Micrometer
μM	Micromolar
ϕ	Phase
ω	Oscillation Frequency

CHAPTER 1

INTRODUCTION

Familial Hypertrophic Cardiomyopathy is a sarcomeric protein disease that causes thickening and enlargement of left ventricle which leads to the fibrosis within muscle tissues. This disease is mostly due to mutations within cardiac myosin binding protein C and muscle myosin heavy chain. The FHC heart displays a hypercontractile sarcomere and impaired relaxation during diastole. It occurs among children and elderly. The individuals suffering from FHC die due to heart failure by lower stroke volume. This dissertation focuses on the study of FHC causing mutations in myosin heavy chain and efficacy of proposed therapeutic peptides to combat hypercontractility and hypocontractility.

1.1 Muscle and Sarcomere

Muscle is a fibrous soft tissue that contracts to give humans the capability of movement and activity. There are three different categories of muscles: cardiac, skeletal, and smooth muscle. Physiological functions are closely related to contraction of these muscles. In the presence of Adenosine Tri-Phosphate (ATP), the actomyosin interaction causes contractions of all muscle types by myosin thick filament and actin thin filament interactions; thus, to provide energy ATP is hydrolyzed by the ATPase activity of myosin subfragment 1 (S1) head (Huxley, A.F., 1964; Lymn, R.W. and Taylor, E.W., 1971; Huxley, A.F. and Niedergerke, R., 1954).

The functional unit of muscle present in both skeletal and cardiac muscles, but absent in smooth muscle, is a sarcomere (Wang, K., 1985). Muscle contraction involves proteins available in this muscle unit. Schematic of a sarcomere is shown below (Figure 1.1). Cardiac muscle has involuntary control, branches, striations, and uninucleated cells that interdigitate at intercalated

discs. As cardiac muscle contracts, it ejects blood into the circulation. Cardiac muscle can be found within walls of the heart (Marieb, E.N., 12th Edition).

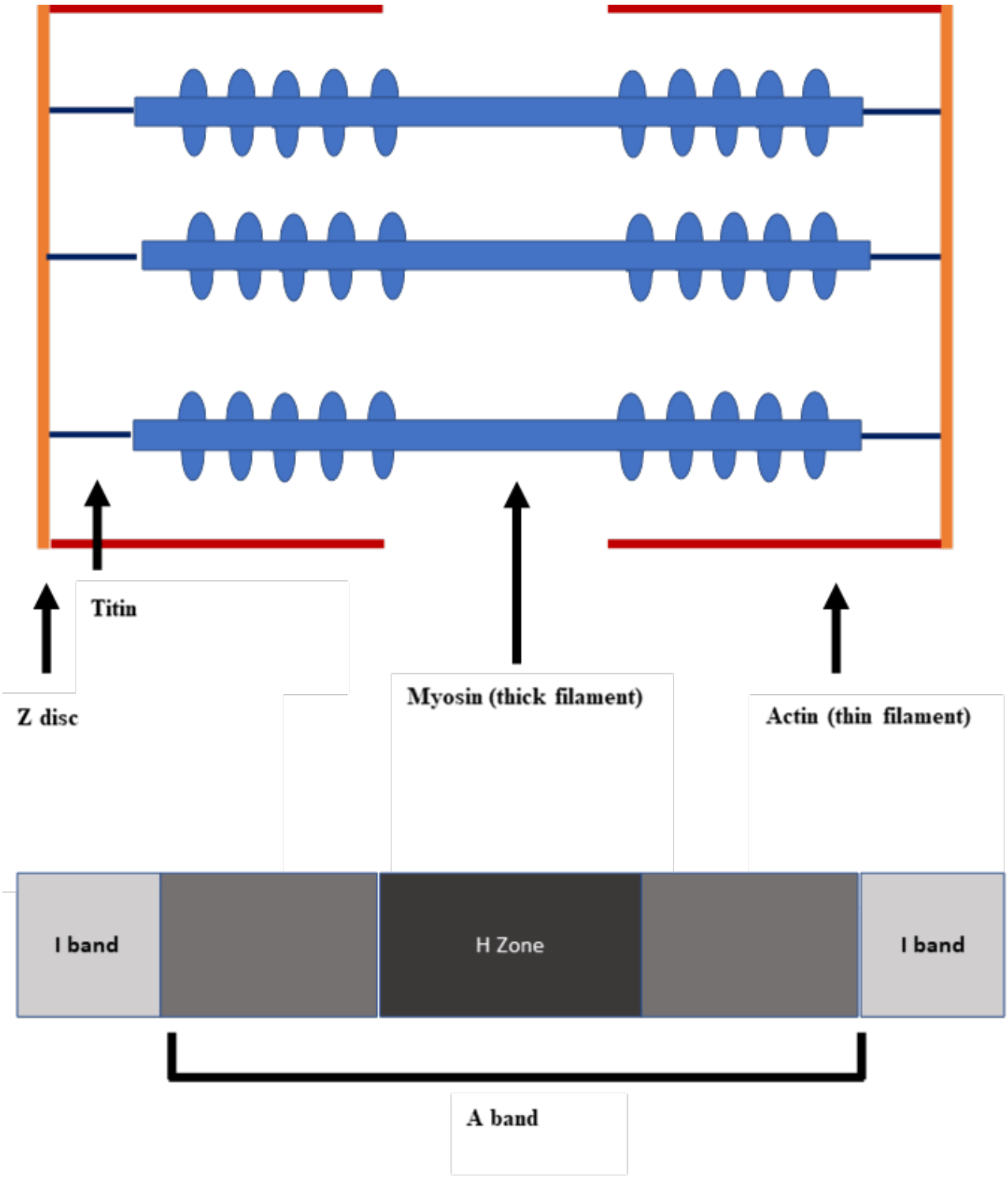

Figure 1.1: Schematic of a Sarcomere

Skeletal muscle contains long, cylindrical, multinucleated cells or fibers, and has apparent striations. Skeletal muscle are under voluntary control involved locomotion and day to day activities. Skeletal muscle can be found attached to the bones or occasionally to the skin (Marieb, E.N., 12th Edition). Skeletal muscle has more regular striations compare to cardiac muscle due to tight bundles within myofibrils (Price, H.M., 1963). Actin thin filaments, myosin thick filament, tropomyosin, troponin complex and myosin binding protein C are parts of both striated muscles', cardiac and skeletal, contractile system.

Involuntary smooth muscle has spindle-shaped cells with central nuclei. This type of muscle has no striations and cells are arranged closely to form sheets. Smooth muscle helps in the bodily process of ejecting substances such as food though the digestive tract, urine, and labor inducing contractions. Smooth muscle can be found within walls of hollow orangs such as digestive and urinary tract organs, uterus, and blood vessels (Marieb, E.N., 12th Edition). Although smooth muscle has no striations, contractile parts are similar to skeletal and cardiac muscle (Cooke, P., 1976).

1.2 Myosin

Myosin is a motor protein that depends on ATP to function. Binding of myosin to actin takes place subsequent to hydrolysis of ATP (Ruppel, K.M., and Spudich, J.A., 1996). Myosin filament consist of two heavy chains and four light chains. Muscle myosin heavy chain is categorized in to light meromyosin (LMM) and heavy meromyosin (HMM). HMM further divides to subfragment 1 (S1) region at proximal end, and subfragment 2 (S2) region at distal end (Figure 1.2). S1 and S2 are connected to each other by myosin S1-S2 hinge (Rayment, I., and Holden, H.M., 1994). LMM contains tight coiled coil at distal C terminus to make thick filament backbone (Goodson, H.V. and Spudich, J.A., 1993). The more N terminal part of the

myosin tail, within the HMM, contains coiled coils that are more flexible than LMM and link it to the globular heads (Root et al., 2006).

There are mutations within the amino acid residues 900-940 of the myosin S2 that are responsible for Familial Hypertrophic Cardiomyopathy (FHC) (Semsarian *et al*., 2015**;** Root et al., 2006**;** Erdmann *et al*., 2003). Although this region does not have a direct role in actomyosin interaction, the mutations within this region lead to FHC thus, hinting at a role for the myosin S2.

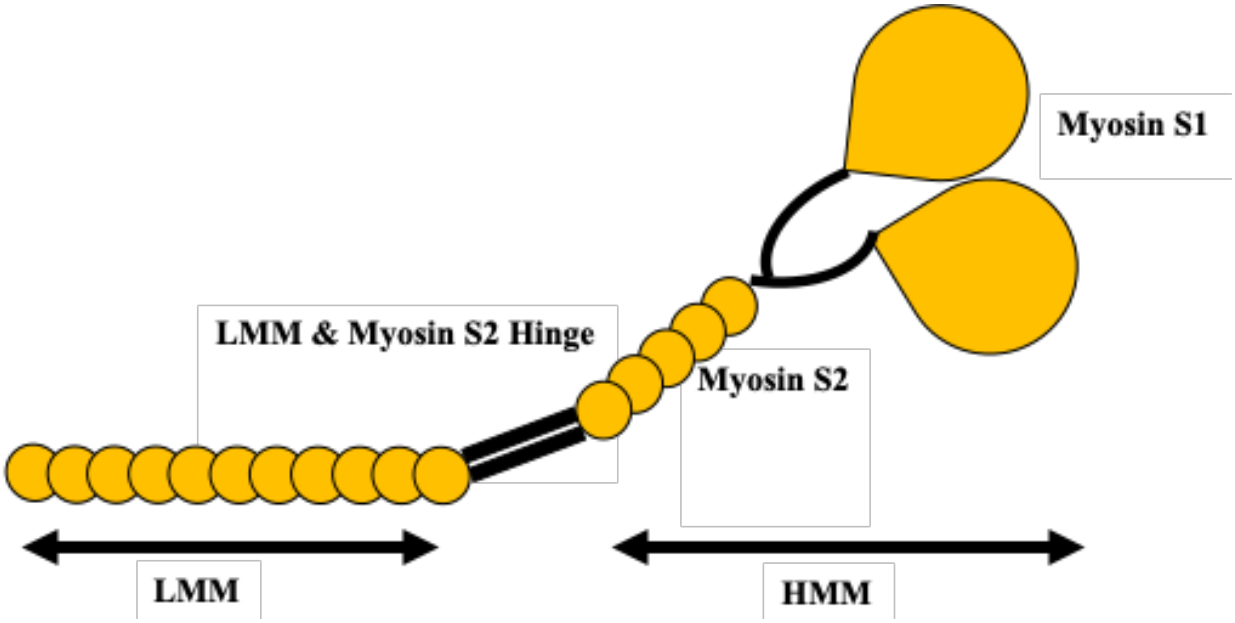

Figure 1.2: Myosin coiled coil structure representation from N terminal to C terminal (right to left) with different parts labelled.

There is amino acid residue conservation along cardiac (MYH7), skeletal (MYH2), and smooth (MYH11) muscle myosin S2 isoforms. MYH7 with UNIPROT ID: P12883 and MYH2 with UNIPROT ID: Q9UKX2 are 81.09% identical (generated from UNIPROT and multi-sequence alignment) and MYH7 and MYH11 with UNIPROT ID: P35749 are 41.15% identical (generated from UNIPROT and multi-sequence alignment).

1.3 Actin

F-actin is polymerized from G-actin by binding to ATP (Rees, M.K., and Young, M.,

1967). Troponin and associated tropomyosin bind to actin thin filament at every 7th position of actin (Ebashi *et al*., 1969). The actin thin filament starts from Cap Z and goes to H zone of sarcomere. Thus, the actin thin filament can be seen from I band to A band of sarcomere.

1.4 Muscle Contraction and Its Regulation

1.4.1 Cardiac and Skeletal Muscles

Striated muscle, cardiac and skeletal muscles, contraction has a four stage cycle. Illustration of muscle contraction cycle is summarized in figure 1.3 (Lymn, R.W. and Taylor, E.W., 1971**;** Taylor, E.W.,1977). First, myosin S1 head binds to actin thin filament after power stroke. Myosin S1 heads get released from actin after binding of ATP. Second, ATP gets hydrolyzed to adenosine diphosphate (ADP) and inorganic phosphate (P_i)**;** resulting in myosin S1 heads assuming a cocked position. Myosin now binds to actin thin filament weakly in Z line direction (Rayment *et al*., 1996). Third, power stroke takes place as P_i gets released from myosin S1 heads, allowing the actin thin filaments to be pulled towards the M-line of the sarcomere (White and Taylor, 1976; Siemankowski *et al*., 1985; Goldman, 1987). Within this stage, myosin S1 heads bind stiffly in a new conformation on to the actin thin filament. Lastly, as ADP gets released, the myosin switches to rigor state where another cycle of force generation can take place.

Muscle contraction is through hydrolysis of ATP by the myosin S1 heads and influx of calcium ions in the cytosol. In skeletal muscle, influx of calcium ions happens in result of signals coming through nervous system going to calcium channels located within sarcoplasmic reticulum (SR) of the muscle fibers (Walker, S.M., and Schrodt, G.R.,1967). Calsequestrin that is located within SR is a storage protein for calcium (Hill, R. W. *et al.*, 2008). As the calcium channels open, calcium ions flow into the cytosol of the muscle fiber. Calcium ions bind to the

troponin C of troponin complex. As a result the troponin I shifts the troponin T which displaces the tropomyosin off the actin thin filament f now which allows myosin S1 heads dock on to the actin thin filament (Vibert *et al*., 1997).

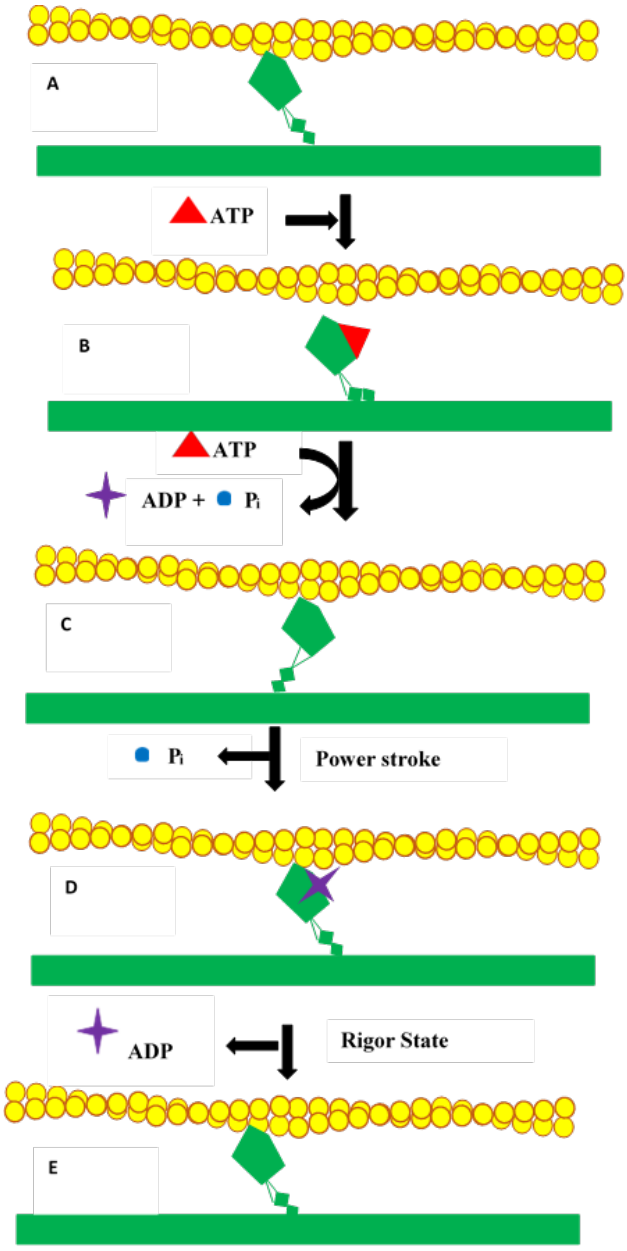

Figure 1.3: Actomyosin interaction step in muscle contraction. (A) Myosin S1 head (green) binds to actin thin filament (yellow) after power stroke. (B) Myosin S1 heads get released from actin after binding of ATP. (C) ATP gets hydrolyzed to ADP and P_i; myosin S1 heads assume a cocked position which leads to binding to actin thin filament weakly. (D) Power stroke takes place as P_i gets released, allowing the actin thin filaments to be dragged towards the M-line of the sarcomere. (E) As ADP gets released the myosin switches to rigor state where another cycle of force generation can take place.

1.4.1 Smooth Muscle

Within interior of smooth muscle cell, actin filaments do not attach to z-line. Actin filaments attach to small transverse structures called dense bodies. Dense bodies are bound to the surface membrane by intermediate filaments. Myosin filaments are unsystematically distributed between smooth muscle actin filaments. Contractile filaments move sideways to the long axis of the cell wall. In smooth muscle, binding of calcium to calmodulin that binds to caldesmon activates calcium signaling. Calmodulin- caldesmon complex would detach from actin thin filament which clears of the myosin binding site on actin thin filament. The main mode of regulation in smooth muscle myosin is phosphorylation of light chains by myosin light chain kinase. This phosphorylation frees myosin S1 heads from one another. The myosin S1 binds to actin thin filament through hydrolysis of ATP and generates the power stroke. Myosin light chain phosphorylation enables cross-bridge formation and cycling during which energy from ATP is used for tension development and shortening. The action potential is built slowly similar to the slow type cardiac action potential. The Voltage Operated Calcium channel (VOC) is for uptake of Ca^{2+}. The repolarization happens by an outgoing flux of potassium ion through both delayed K^+ channels and calcium activated K^+ channels.

1.5 Familial Hypertrophic Cardiomyopathy

Cardiomyopathy is a heart related genetic disorder. Mutations in sarcomeric proteins cause pathological changes, which leads to sudden death (Crilley, J.G. *et al*., 2003; Redwood, C.S., 1999, Semsarian, C. *et al*., 2015). Throughout the molecule of the myosin, there are many different mutation distributions (Semsarian *et al*., 2015**;** Nag *et al*., 2015). Point mutations along muscle myosin can impact wide range of ages, young and old, with or without any symptoms (Barsheshet, A. *et al.*, 2011). The majority of mutations are located within the myosin thick

filament, and a few of them are located within the actin thin filament. Studies show majority of cardiomyopathy mutation are found within MYH7, myosin heavy chain beta isoform (Erdmann, J. *et al.,* 2003; Cirino, A. L., and Ho, C., 2003).

There are different classifications of cardiomyopathy including: Familial Hypertrophic Cardiomyopathy (FHC) and Dilated Cardiomyopathy (DCM). In FHC, the left wall of the heart ventricle thickens. Thickening of the left ventricle wall of the heart results in the left ventricle chamber decreasing in volume, thus the stroke volume of the heart decreases (Wigle, E.D. *et al*., 1995). This results in death by heart failure, syncope or asymptomatic (Semsarian, C. *et al*., 2015; Cirino, A. L., and Ho, C., 2008). In DCM, the wall of the left ventricle gets thin and loosens. The left ventricle wall gets thin causing the space within the left ventricle to increase, but the myocytes within the left ventricle are weak to pump blood out of the heart sufficiently, resulting in death by heart failure (Semsarian, C. *et al.,* 2015; Cho, K.W. *et al.,* 2016). Figure 1.4 illustrates the anatomy of normal human heart compared to FHC and DCM hearts.

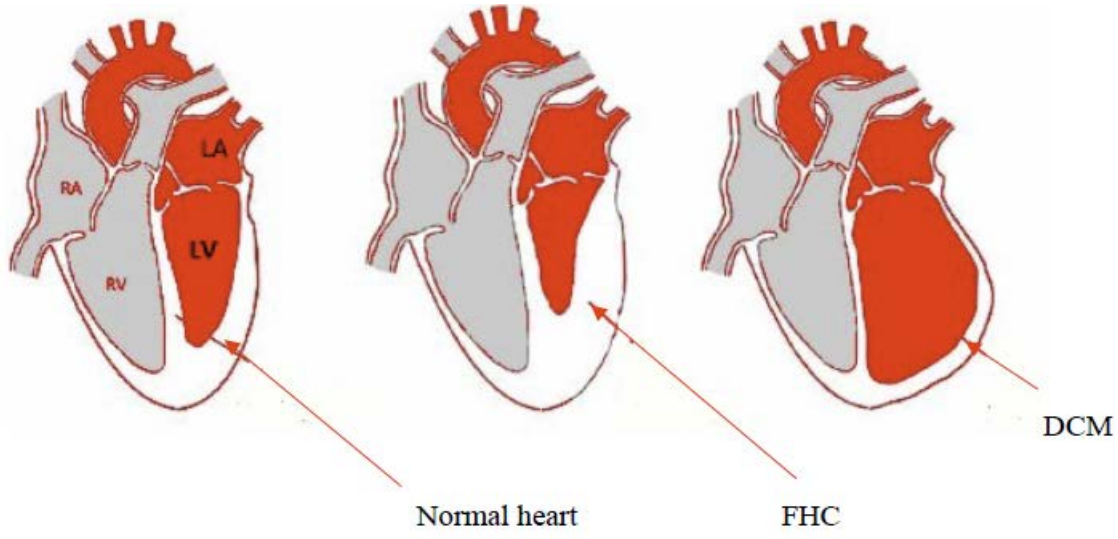

Figure 1.4: Anatomy illustration of normal human heart (left) compared to FHC (middle) and DCM (right) hearts.

The majority of disease causing mutations are located within the S1 region and have critical functional properties. Mutations within S1 head can impact binding of myosin S1 heads

to actin thin filament during muscle contraction, which impacts the force generated by cardiac muscle. A few mutations are located within the N terminal region of the myosin S2. It has been reported that there are mutations within the proximal region of myosin S2, which leads to cardiomyopathy (Richards, P. *et al*., 2004). Anyone suffering from these mutations has a chance of sudden cardiac arrest (Jean, M.,2003; Tesson, F. *et al.*,1998). FHC impacts contractile apparatus of cardiac muscle which can be either point or missense mutations. Two mutations within the S2 region of myosin which cause FHC are glutamate substitution to lysine at 924th residue (E924K) and glutamate deletion at 930th residue (ΔE930) (Richards, P. *et al*., 2004). A familial hypertrophic cardiomyopathy distribution hotspot on MYH7 gene is illustrated on figure 1.5. These mutations intensely obstruct dimerization and thus destabilize the coiled coil structure of S2 region of myosin.

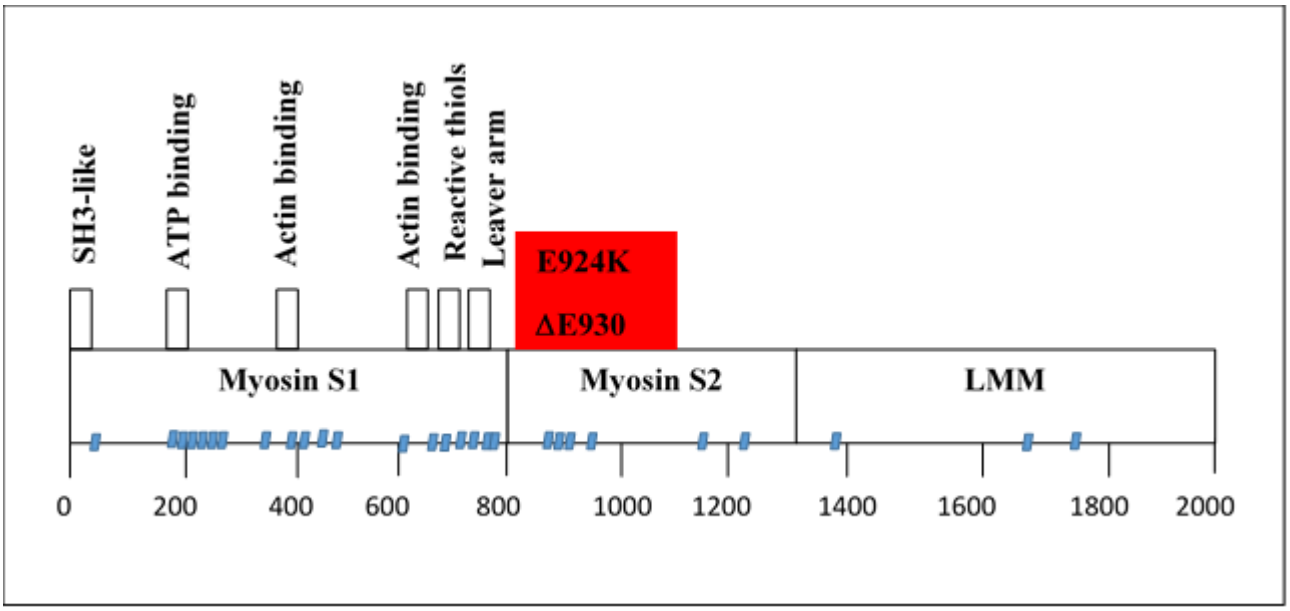

Figure 1.5: Familial hypertrophic cardiomyopathy distribution hotspot on MYH7 gene. Each blue box represents a FHC point mutation. Red highlights the FHC mutation studied throughout this study.

The S2 region of myosin is a coiled coil linker between light meromyosin (LMM) and the (S1) region of myosin. Although the S2 region of myosin is not directly involved in actomyosin

interaction, mutations in this region are responsible for cardiomyopathies. Which raises the question: what characteristics does the S2 region of myosin have that cause such a huge impact on the overall actomyosin interaction and over all force produced?

1.6 Hypothesis and Testing

Myosin subfragment 2 is an intrinsically unstable coiled coil. The mechanical stability in the S2 region of myosin 2 might have a key role to play in regulating the amount of myosin S1 heads available for binding to the actin, thus having an overall impact on actomyosin interaction and net force production of myosin S2 during contraction. On the other hand, the destabilized myosin S2 would lose this regulation resulting in an increase in force production due to excess availability of myosin S1 heads (Gundapaneni, D. *et al*., 2005). This elevated instability could underlie one of the causes for FHC. To remedy this, anti-S2 peptides, stabilizer and destabilizer peptides by namesake are designed to increase and decrease the stability of myosin S2 coiled coil to influence the actomyosin interaction. It can be hypothesized that a stabilizing peptide would increase stability of the myosin S2 region of the myosin coiled coil by wrapping around the myosin S2, and the destabilizing peptide would decrease stability of the myosin S2 by pulling the coiled coil to opposite directions. The FHC point mutation; E924K and ΔE930 in myosin S2 peptides increases the instability in myosin S2 coiled coil compared to wild type. The efficacy of anti-S2 peptides were tested on myosin S2 peptides across MYH11, MYH7, and MYH2.

Previous electron micrograph studies have shown that myosin S1 heads of both smooth and skeletal muscle myosin can fold back on their long tail domain, thus they can have a bent conformation (Waldmüller *et al*., 2003). Cryo-electron micrograph and atomic modellings of thick filaments have shown that myosin S1 heads bind to each other and fold back and bind to proximal myosin S2 region (Elliott, A., and Offer, G. 1978). Further, in smooth muscle, calcium

mediated phosphorylation of myosin light chain shifts myosin S1 heads to on state.

It is hypothesized that a stable myosin S2 provides a conformation for S1 heads to fold back and rest on myosin S2 region, thus regulates availability of S1 heads. In the presence of any mutations, the myosin S2 coiled coil could be either more stable or more flexible. A more stable myosin S2 extends switch off state of myosin S1 heads, thus limits the number of active myosin S1 heads available to bind to actin. This even causes hypo-contraction of cardiac muscle which leads to DCM.

With more flexible myosin S2 excessive amount of active myosin S1 heads would be available, thus causes hypercontraction which leads to FHC. Hypercontraction leads to diastolic dysfunction which results in impaired relaxation. Over a period of time this impairment leads to development of fibrosis and slowly leading to thickening of ventricle walls. It is believed that there would be a decrease in actomyosin interaction in presence of the stabilizer and there would be an increase in actomyosin interaction in presence of the destabilizer. To test properties of myosin S2 two assays were designed:

- Experimental Assay 1: The first aim is to test whether different concentrations of the stabilizer and the destabilizer peptide change the distance between two helix of coiled coil myosin S2 in muscle myosin S2 isoforms and FHC mutants (E924K & ΔE930) with help of Fluorescence Resonance Energy Transfer (FRET).
- Experimental Assay 2: The second aim is to test whether the stabilizing peptide would increase stability of the myosin S2 isoforms region of the myosin coiled coil by wrapping around the myosin S2 and decrease the amount of force produced and the destabilizing peptide would decrease stability of the myosin S2 isoforms by inhibiting the natural coiled coil formation of S2, thus increasing the amount of force produced with help of Gravitational force spectroscopy (GFS).

The purpose of this study is to compare the force required to unwind coiled coil structure of muscle myosin S2 isoforms in presence and absence of stabilizer and destabilizer, and the distance change between two helix of myosin S2 of these tissues with increase in concentrations. The stability and flexibility of myosin S2 is a key factor in actomyosin interaction. This stability

and flexibility can be measured by force using force spectroscopy to have an insight into function of stabilizer and destabilizer and tests whether there is more or less energy transfer in terms of lifetime when stabilizer or destabilizer is present (Semsarian, C. *et al.*, 2015). Fluorescence resonance energy transfer utilizes efficiency of energy transfer in terms of lifetime. This insight provides details on how the distance between two helix of coiled coil myosin S2 changes in response to different concentrations of stabilizer and destabilizer peptides. Gravitational force spectroscopy (GFS) tests whether unwinding of the myosin S2 coiled coil required more or less force when stabilizer or destabilizer is present.

1.6.1 Different Concentrations of the Stabilizer and the Destabilizer Peptide Changes the Distance between Two Helix of Coiled Coil Myosin S2 in Muscle Myosin S2 Isoforms and FHC Mutants (E924K & ΔE930)

The stabilizer peptide was designed in Dr. Root's laboratory using computer simulations. This peptide binds around the myosin S2 coiled coil within amino acids 924-942. The purpose of designing this peptide was to stabilize the myosin S2 coiled coil, so the amount of available myosin S1 heads for actomyosin interaction would decrease.

On the other hand, the destabilizer peptide, which was also designed in Dr. Root's laboratory using computer simulations, was designed for the same region of the myosin S2 coiled coil to disrupt the natural formation of the dimer. The destabilizer peptide bind to one α-helix of the muscle myosin S2 coiled coil. This peptide was designed to help make the myosin S2 coiled coil more flexible to increase the amount of myosin S1 heads available for actomyosin interaction.

The first test is to check binding affinity of the stabilizer and the destabilizer peptides to cardiac muscle myosin S2 peptide. Florescence Resonance Energy Transfer is performed to measure binding affinity of the stabilizer and the destabilizer to cardiac muscle myosin S2

peptides. A monomer of myosin S2 isoforms was conjugated with the donor probe and another monomer was conjugated to the acceptor probe. For all muscle myosin S2 isoforms, one experiment was done as a control. In control assay, dimer of muscle myosin S2 isoforms were diluted to find minimum optimal dimer concentration to treat with anti-S2 peptides. In experimental assay, minimum optimal dimer concentration of muscle myosin S2 isoforms were titrated with different concentrations of anti-S2 peptides till they saturate. Expected results is to see the stabilizer peptide enhances dimer formation in wild-type and mutant cardiac, and skeletal muscle myosin S2 peptides and the destabilizer peptide increase flexibility of wild-type cardiac and skeletal myosin S2 wild-type peptide. It is also expected to see either of the anti-S2 peptide have an impact on smooth muscle myosin S2 isoform. Also, would be able to measure the dissociation constant of the stabilizer and the destabilizer peptides binding to myosin S2 peptides.

1.6.2 The Stabilizer Peptide is Specific to Myosin S2 Coiled Coil and Stabilizes the Myosin S2 Coiled Coil thus Decreasing the Amount of Force Produced and The Destabilizer Peptide is Specific to Myosin S2 Coiled Coil and Destabilizes the Myosin S2 Coiled Coil thus increasing the Amount of Force Produced

After confirming binding affinity of the stabilizer and the destabilizer peptides to muscle myosin S2 isoforms, next is to check whether the stabilizer and the destabilizer peptide have an impact on myosin S2 coiled coil stability and flexibility.

The GFS assay is performed to confirm the stability and flexibility of muscle myosin S2 coiled coil isoforms in presence of the anti-S2 peptides. In this assay, the myosin molecule is suspended between immobile edge and mobile bead. The assay will uncoil the muscle myosin S2 in presence and absence of anti-S2 peptides. In presence of the stabilizer peptide, more force will be required to uncoil the myosin S2, and in presence of the destabilizer peptide, less force will be required to uncoil the myosin S2 compare to absence of anti-S2 peptides.

All of these experiments performed together validate the binding affinity of the anti-S2 peptides to the muscle myosin S2 isoform regions. The experiments also confirm that the stabilizing and flexibility by binding of the stabilizer and the destabilizer peptide to the muscle myosin S2 coiled coil isoforms. Increases in the stability of muscle myosin S2 isoforms increase the amount of force required to uncoil the dimer, and decreases in the stability of muscle myosin S2 isoforms decrease the amount of force required to uncoil the dimer. The force produce by the striated muscle sarcomere can be altered or modulated by changing the mechanical stability of myosin S2 coiled coil with the help of S2 specific peptides where one peptide can increase the stability and reduce the contraction produced while the other will have an effect vice versa to the previous one.

CHAPTER 2

MATERIALS AND METHOD

2.1 Materials

2.1.1 Myosin

Myosin was extracted from rabbit skeletal muscles using the protocol from Scientist et al. Cold extraction buffer [0.3 molar (M) potassium chloride, 0.072 M sodium phosphate monobasic, 0.063 M potassium phosphate dibasic, and 0.001 M ethylene diamine tetra-acetic acid with pH 6.5] was used to extract myosin from ground rabbit skeletal back muscle. Three times the volume of ground rabbit back muscle the cold extraction buffer was added. For 15 minutes, the combination was stirred gently, followed by addition of distilled water at 4 ^{0}C to bring the volume 10 times the volume of ground rabbit muscle. Stirring was allowed for an additional 20 minutes. Later the muscle slurry was filtered through the cheese cloth covered funnel in to a 28 flask. Distilled water was added to the filtered product (15X the volume) and was allowed to precipitate over night at 4 ^{0}C. The clear supernatant was discarded, and precipitate was centrifuged for 10 minutes in GSA rotor at 7000 rpm. To suspend the precipitate, 5 ml of 2 M potassium chloride was used. The final concentration of potassium chloride was diluted to 0.3 M with cold distilled water after measuring the volume of suspended precipitate. The next step was to precipitate the impurities, the product was centrifuged for 45 minutes to at 9000 rpm. Acquired supernatant was finally diluted to the concentration of 0.033 m potassium chloride with cold distilled water. An extinction coefficient of 0.55 $(mg/ml)^{-1}$ cm^{-1} at 280 nm was used the obtain myosin concentration. Lastly, the rabbit skeletal myosin was flash frozen in liquid nitrogen and kept at -80^0 C in aliquots for experimental use (Xu, J., and Root, D.D.,2000; Gundapaneni *et al*., 2005).

2.1.2 Actin

Acetone powder from the rabbit back muscle was used as described to obtain actin (Xu, J., and Root, D.D. 2000; Spudich, J.A. and Watt, S. 1971; Kron *et al*., 1991; Gundapaneni *et al*., 2005). The filtered material obtained on the cheese cloth of myosin extraction was extracted and added to the two times the volume of cold buffer (0.6 M potassium chloride, 0.4 M sodium bicarbonate and 0.01 M sodium carbonate; pH=7.0). The same volume of distilled water and filtered through the cheese cloth was used to dilute the mixture. For 30 minutes at room temperature, the product was washed with 5X volume of 4% sodium bicarbonate solution and was further filtered through the cheese cloth again. For 5 minutes, the product was washed with 10X volume of distilled water and filtered again using cheese cloth. For 10 minutes, the product was washed with 3X volume of acetone and filtered through cheese cloth. Acetone was repeated two time and product acquired was dried at room temperature overnight. Acetone powder was scratch and stored at -20^0 C. To extract actin from the acetone powder, 5 gram of acetone powder was suspended in 30 ml of G-buffer (2 mM Tris hydrochloric acid, 0.2 mM adenosine triphosphate, 0.5 mM 2-mercaptoethanol, and 0.2 mM calcium chloride with pH 7.6) for 120 minutes at 4^0 C. For 15 minutes the product was centrifuged at 15000 rpm later the supernatant was collected. A 0.45 μm Millipore filter was used to filter the supernatant. Final concentrationa of 50 mM potassium chloride and 1 mM magnesium chloride were added to the filtered supernatant to polymerize actin for 120 minutes at room temperature. Additionally, for 30 minutes, 0.6 M potassium chloride was added and stirred. For 30 minutes at 4 ^{0}C the product was centrifuged at 40,000 rpm. Pellet acquired was put in G-buffer and dialyzed against G-buffer with continuous stirring for 72 hours at 4 ^{0}C. For dialysis, G-buffer was used every 24 hours. For 60 minutes, at 4 ^{0}C, the dialyzed product was centrifuged at 40,000 rpm, the supernatant

containing G-actin was removed. Extinction coefficient of 0.63 $(mg/ml)^{-1}$ cm^{-1} at 290 nm was used to obtain actin concentration (Xu, J., and Root, D.D. 2000). G-actin was polymerized in 50 mM potassium chloride, flash frozen, and was stored in -80 ^{0}C in small aliquots for further use.

2.1.3 Human β-cardiac Myosin S2 Peptide

A small region of myosin subfragment 2 (S2) region of human β-cardiac myosin (MYH7) was selected to be synthesized by BioSynthesis; Inc. The region was selected based on mutations found within this region causing Familial hypertrophic cardiomyopathy (FHC) (Richards, P. *et al.*, 2003)**.** The mutations are located within proximal region of myosin S2 specifically region of 921-939 (Figure 1.5). Myosin S2 is an intrinsically unstable coiled coil and the sequence of this region was acquired from Protein Data Bank (PDB). The 19 residue peptide was chemically synthesized. Generated amino acid sequence used is as follow:

Wild-type: NH2-EMNERLEDEEEMNAELTAK-COOH [1]

2.1.4 Human β-cardiac Mutant Myosin S2 Peptide (ΔE930)

Analysis of the mutation hotspot region of human β-cardiac myosin S2 revealed that the glutamate deletion at 930th residue (ΔE930) is one of several point mutations that cause FHC (Figure 1.5). This mutation causes mechanical instability and an unstable coiled coil (Taei, N., Root, D.D., 2013). Again, the sequence of this mutation was obtained using the PDB. An 18 residue peptide of this region was chemically synthesized. Generated amino acid sequence used is as follows:

ΔE930: NH2-EMNERLEDEEMNAELTAK-COOH2

[1] E = glutamate, M = methionine, N = asparagine, R = arginine, L = leucine, D = aspartate, A = alanine, T = threonine, K = lysine

[2] E = glutamate, M = methionine, N = asparagine, R = arginine, L = leucine, D = aspartate, A = alanine, T = threonine, K = lysine

2.1.5 Human β-cardiac Mutant Myosin S2 Peptide (E924K)

Mutation hotspot region of human β-cardiac myosin S2 revealed that glutamate substitution to lysine at 924th residue (E924K) is one of the several point mutation that cause FHC (Figure 2.1). This mutation also causes mechanical instability and unstable coiled coil (Taei, N., Root, D.D., 2013). Sequence of this mutation was obtained using PDB. A 19 residue peptide of this region was chemically synthesized. Generated amino acid sequence used is as follows:

E924K: NH2-EMNKRLEDEEEMNAELTAK-COOH [3]

2.1.6 Human Skeletal Myosin S2 Peptide

MYH2 gene codes for human skeletal muscle myosin expressed in fast type IIA muscle fibers. This myosin isoform can be found within extraocular muscle. A 19 residue peptide of the S2 region of MYH2 was matched to the previously synthesized S2 peptide of cardiac isoform and chemically synthesized 925 – 945. Generated amino acid sequence used is as follows:

Skeletal: NH2-EVTERAEDEEEINAELTAK–COOH[4]

2.1.7 Human Smooth Myosin S2 Peptide

Human smooth muscle myosin heavy chain (MYH11) is a part of the non-striated muscle. This gene can be found within esophagus, endometrium, duodenum, etc. A 21 residue peptide of the S2 region of MYH11 was matched to the previously synthesized S2 peptide of

[3] E = glutamate, M = methionine, N = asparagine, R = arginine, L = leucine, D = aspartate, A = alanine, T = threonine, K = lysine

[4] E = glutamate, V = Valine, N = asparagine, R = arginine, L = leucine, D = aspartate, A = alanine, T = threonine, K = lysine, I = Isoleucine

cardiac isoform and chemically synthesized 926-946. Generated amino acid sequence used is as follows:

Smooth: NH2-EMEARLEEEEDRGQQLQAERK-COOH[5]

2.1.8 Stabilizer Peptide

Stabilizer peptide is a poly-cation compound that was designed computationally to bind around cardiac muscle myosin (S2) region of 921-939. This specific region of myosin S2 is rich in glutamate. Thus, the positive charge from stabilizer peptide and negative charge from myosin S2 peptide would allow for protein-protein interaction. The molecular model generated from computer simulations using the Macromodel program is shown below (Figure 2.1).

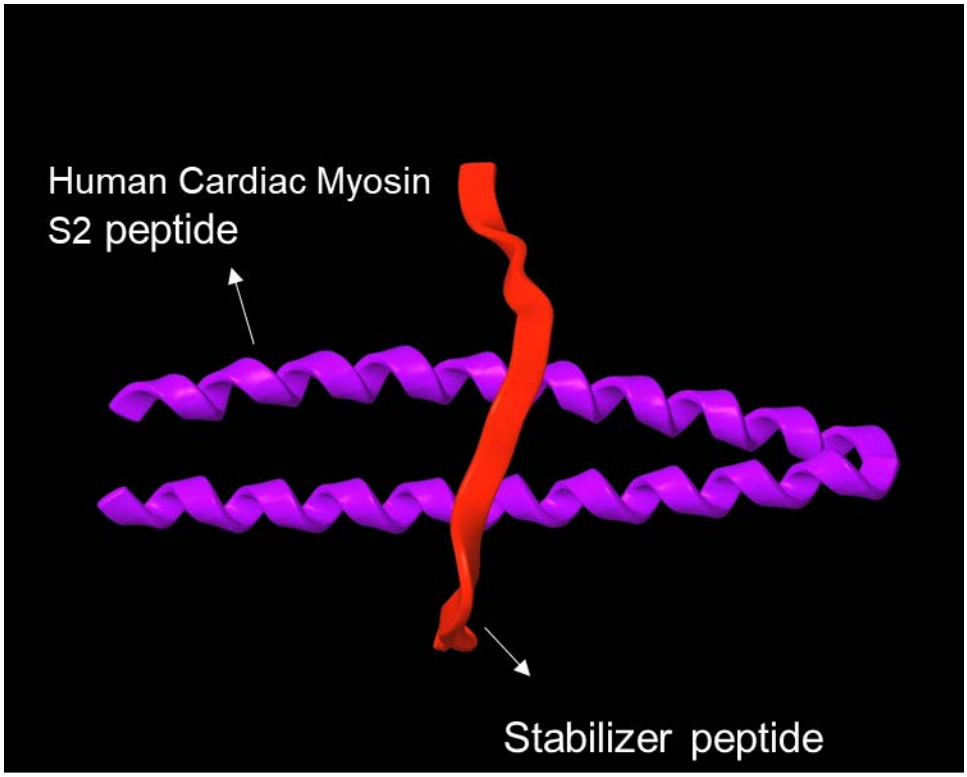

Figure 2.1: Molecular representation of stabilizer peptide (red) bound around cardiac myosin S2 peptide (purple).

[5] E = glutamate, , M = methionine, A = alanine, R = arginine, L = leucine, D = aspartate, G = Glycine, Q = Glutamine, K = lysine

2.1.9 Destabilizer Peptide

Destabilizer peptide is a 19 residue peptide against human cardiac muscle myosin S2 region of 921-939. This peptide has high binding affinity to a single helix of the myosin S2. One molecule of this destabilizer peptide would bind to one α-helix of the cardiac muscle myosin S2 coiled coil and disrupt the natural coiled coil formation. The molecular model representation is shown below (Figure 2.2).

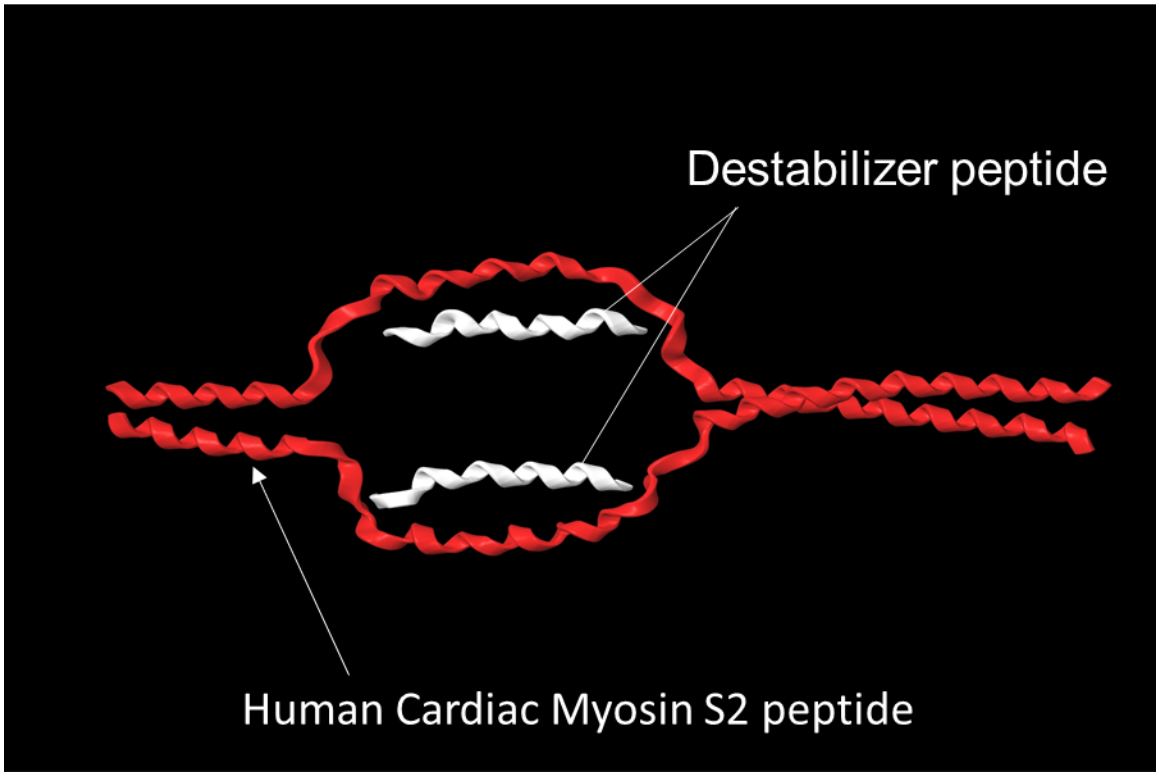

Figure 2.2: Molecular representation of destabilizer peptide (white) pulling human cardiac myosin S2 peptide dimer (red) apart.

2.2 Methods

2.2.1 Fluorescence Resonance Energy Transfer

2.2.1.1 Fluorescence Resonance Energy Transfer Acceptor and Donor Probes

Chelate-lanthanide complex was utilized as the donor probe, which is composed of a lanthanide, an antenna, and a chelate. Organic chromophore antenna (cytosine) will absorb a

photon of light, and it will transfer energy to lanthanide ion (terbium III). This probe excites at 248 nm and emits at 547 nm (Root, D. D., 1997).

Fluorescein was used as the acceptor probe. Fluorescein isothiocyanate (FITC) is composed of a xanthene ring and a reactive thiol group. Xanthene ring has fluorescent characteristics and the reactive thiol group will bind to the biomolecules at their free amino (-NH_2) group. This probe has excitation peak at 495 nm and emits at 520 nm (Taei, N., Root, D.D., 2013).

Resonance energy probes (donor and acceptor) will be covalently attached to synthetic myosin S2 peptides of cardiac muscle, ΔE930 cardiac muscle, E924K cardiac muscle, smooth muscle, and skeletal muscle (Fabiato, A.,1988).

Amino acid sequences of muscle peptides were attached to the resonance probes that were selected through dynamic simulation experiments (Figure 2.4). The same method was used to conjugate probes to mutant peptides (E924K and ΔE930). Muscle myosin S2 peptide synthetic peptide sequences are as follow:

Wild-type	NH_2-EMNERLEDEEEMNAELTAK-COOH
E924K	NH_2-EMNKRLEDEEEMNAELTAK-COOH
ΔE930	NH_2-EMNERLEDEEMNAELTAK-COOH
Skeletal	NH_2-EVTERAEDEEEINAELTAK–COOH
Smooth	NH_2-EMEARLEEEEDRGQQLQAERK-COOH

Acceptor probe was conjugated to muscle myosin S2 peptides at N-terminus. Muscle myosin S2 peptides were dissolved in 20 mM HEPES buffer at pH 8.0. And FITC was dissolved in few drops of N, N dimethyl formamide. Lastly, FITC and muscle myosin S2 peptide was

reacted together in 1 to 1 molar ratio and was let to react for 120 minutes at room temperature. The FITC conjugated S2 peptides were purified using Reverse Phase Chromatography.

Donor probe was conjugated to muscle myosin S2 peptides at the C-terminus. Chelate was attached to a reactive site of cytosine and muscle myosin S2 peptide was attached to another reactive site of cytosine in dimethylsulfoxide (DMSO) as a solvent at room temperature (Root, D. D.,1997). Chelate and cytosine were reacted together in 1 to 1 molar ratio. Later, muscle myosin S2 peptide was reacted with chelate-cytosine mixture in 1 to 1 molar ratio conjugating to primary amine group of lysine. For lanthanide, terbium ion with a longer life-time was used. Titration of terbium ion to chelate labeled peptide was done in 1 to 1 ratio prior to FRET assay.

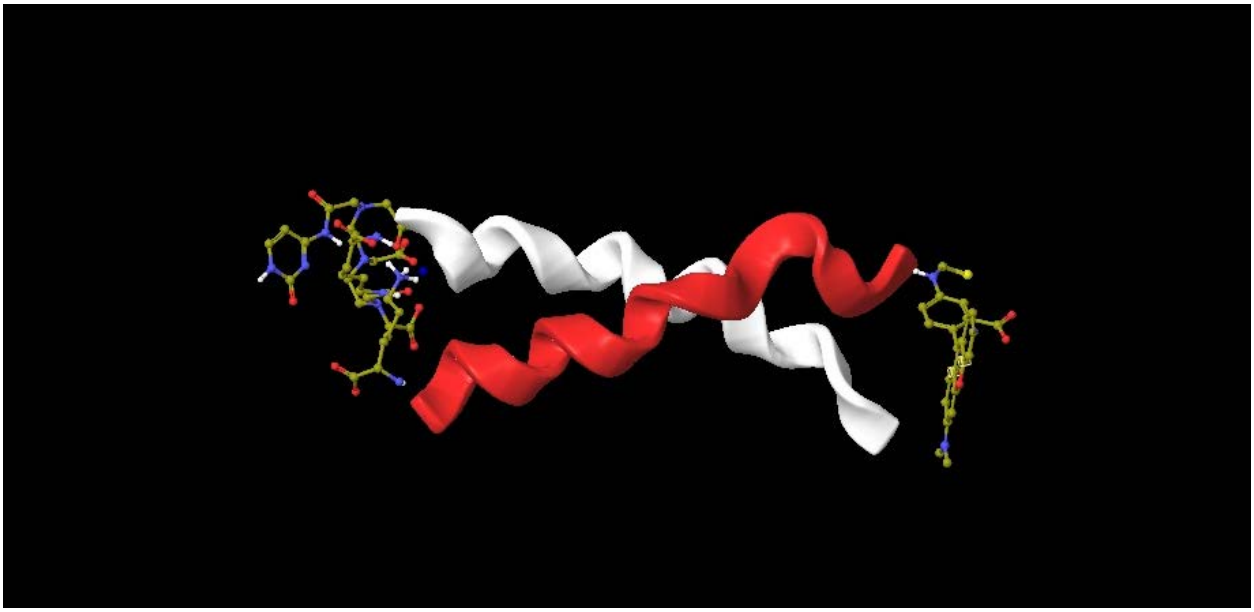

Figure 2.3: Atomic model of myosin S2 peptide. The FITC conjugated to one monomer (red) and terbium chelate complexed conjugated to another monomer (white).

2.2.1.2 Instrumentation

In this experiment, the luminescence spectrometer, AMNICO-BOWMAN SERIES 2 SPECTROMETER, was used to detect resonance energy transfer. This instrument is composed of two light sources: continuous lamp and flash lamp (UV excitation source) and sensitive

detectors for time-resolved detection. Specific experimental settings will be controlled through a connected computer system to the instrument. The connected computer system also enables data storage. Built in gates and filters for further control and monitoring will control intensity of light that will pulse through and emit from the sample. Emission signal generated from decay of molecules was detected by a photomultiplier tube, which contains proper color filters to detect the emitted photons (Gundapaneni, D. *et al.*, 2005).

2.2.1.3 Monochromators

Emission and excitation lights require wavelength and bandpass values. These values were selected using monochromators. Diffraction gratings, mirrors, and slits make up monochromators. Monochromators allowed continuous ranges of an untainted narrow band of excitation and emission light. Monochromators measured fast multiple wavelengths. This was possible with a fast-slewing monochromators that is 12,000 nm per minute, and a bandpass that is controlled through a computer.

2.2.1.4 Bandpass

The bandpass within the instrument is the width of the slit that has a huge impact on intensity and resolution of light. The bandpass setting was used to bring balance between intensity and resolution. It is usually between 0.5 to 16 nanometers. Opening of the bandpass causes more light to pass to the sample, thus an increase in sensitivity.

2.2.1.5 Photomultiplier Tube (PMT)

The luminescence spectrometer is connected to a computer system to collect the data during the experiment. Light from the sample emerges, goes to the emission monochromator, and then into the PMT. The emitted photons energized the photocathode of the PMT and

converts the energy to an amplified DC current. the computer measured an amplified DC current as fluorescent intensity. The PMT was gated to accommodate different wavelengths of light.

The alternative set up was used as well. In this set up, there is an external PMT placed closer to the light that comes out from the sample to avoid light expansion and loss of more light. Instead of the emission monochromator, optical filters were used to select the wavelength.

The proximity of collecting light into external PMT is higher compared to the internal PMT, which is further away from the sample, and there is the possibility of losing light. This alternative set up is hooked on to an amplifier, and the sensitivity is controlled. The emission output goes through an amplifier, which is converted to voltage. The data is stored in digital oscilloscope and used for further calculations and analysis.

2.2.1.6 Fast Protein Liquid Chromatography (FPLC)

Fast protein liquid chromatography is one of the common techniques to purify and separate protein mixtures due to its efficiently of using various properties of protein like charge, size, isoelectric point, and hydrophobicity. FPLC has two main phases: a stationary and a mobile. Beads with pores or conjugated with adjuvant to trap the proteins make up the stationary phase, and any buffer that flows through stationary phase is considered mobile phase. The stationary phase consists of resin beads where the protein of interest binds to with the help of buffer promoting this binding. While the mobile phase buffer will dissociate the bound protein of the beads based on the decreasing affinity of protein to the beads. A FPLC contains one or two pumps, computer system, detection units, and a fraction collector. The pumps within the FPLC run the buffers through stationary phase or the resin beads. UV absorbance and conductivity of the protein mixtures are measured using UV and conductivity detectors attached to the end of the column as sample elutes from the column. Computer system allows modification of methods,

manage ongoing run, and collect and evaluate chromatograms (Robyt, J. F, and White, B. J. (1987).

2.2.1.7 Reverse Phase Chromatography (RPC)

Reacted and unreacted FITC-conjugated peptide was separated from each other using a pepRPC column of reverse phase chromatography. Binding of FITC-conjugated peptide to the column was increased using trifluoroacetic acid (TFA). The TFA enhances the ion paring of FITC- conjugated peptide to the column. There were two buffers used: Buffer A containing 0.05% TFA in water to promote the ion-pairing of FITC-conjugated peptide to pepRPC column. While buffer B containing 0.05% TFA in acetonitrile with gradient of 0% to 100% allowed to elute the FITC-conjugated peptide of the column. The flow rate of buffers through the column was maintained at 0.5 mL/minute.

Collected fractions from the pepRPC column run were purified further to remove TFA. To remove TFA from the fractions, a divilobenzene (DVB) column was used. Buffers used during DVB column purification were water as buffer A and methanol as buffer B with gradient set to 0% to 100% to elute the FITC-conjugated peptide After collecting the fractions, methanol was evaporated with help of a centrifuge, and the sample was later dissolved in appropriate assay buffer of choice.

Reverse phase chromatography, like other chromatographies, consists of two phases: nonpolar stationary and polar mobile. This column elutes protein mixture based on its increasing hydrophobicity. Therefore, polar proteins elute before nonpolar proteins do. The computer system allows setting the gradient from 0% to 100% of the nonpolar solvent for elution to take place. To increase ion-pairing of protein mixtures to the column, trifluoroacetic acid (TFA) was used. TFA is used to increase binding of protein mixture to the nonpolar stationary phase by

allowing the hydrophobic interaction between stationary phase and the protein mixture. Long narrow columns with greater number of theoretical plates can be used to improve separation of protein mixture. In addition, acidic conditions improve separation with high resolution. However, acidic conditions and environments only work for short peptides and if used with nucleic acids or folded proteins, they undergo denaturation. Backpressure that is the result of protein mixture and column interaction is a main issue associated with RPC. Performing RPC at a very low flow rate would decreases the chances of facing backpressure. However, a very slow flow rate would decrease the resolution due diffusion along the column (Amersham Pharmacia Biotech AB., 2001).

2.2.1.8 Anion-Exchange Chromatography

Reacted and unreacted chelate-conjugated peptide was separated from each other using a Q-Sepharose column of anion exchange chromatography. There were two buffers used: Buffer A contained 10 mM imidazole at pH 7, and Buffer B contained 10 mM imidazole and 1 M KCL at pH with flow rate of 1 mL/minute with 0% to 100% gradient.

Anion-exchange chromatography allows protein mixture separation based on molecular charge. This type of chromatography attracts anions that are negatively charged to the stationary phase comprised of positively charged beads (Wilson, K., & Walker, J., 2010). This technique works based on attraction between analyte and stationary phase. The stationary phase and oppositely charged analyte bind together, and the mobile phase alters the binding of analyte to the column with charged ions (salt). There should be at least one pH unit difference between eluent buffer and analytes isoionic point (Wilson, K., & Walker, J.,2010). The right type of buffer allows the maximum number of impurities to stay on the column or elute last. Net surface charges of interested compound plays a big role on media selection. Protein mixture binds to the

matrix. Alterable interaction of charged molecule with oppositely charged column matrix separates the protein mixture. Increase in salt concentration of mobile phase, alters ionic strength within the column, results in compound elution. Salt ions race with bound biomolecules to binding to the matrix leading to elution of protein from the column based on the molecular charge (Amersham Pharmacia Biotech AB., 2001).

2.2.1.9 Spectroscopy

The UV-vis spectrometer was used throughout the experiments to measure the concentration of compounds based on the absorbance of a respective wavelength of light. A spectrometer (Hewlett - Packard) was used to obtain concentration of the peptides conjugated to the acceptor or donor probe from FRET. FITC conjugated peptide had an absorbance peak at 495 nm. The chromatogram monitored by absorbance of the FITC conjugated peptide had two main peaks (Figure 2.4**)**. The first peak signifies the unreacted FITC and the second peak signifies FITC conjugated peptide. Beer-Lambert's law was used find out the concentration of FITC conjugated peptide. In Beer-Lambert's law, "$A=\alpha C l$", A is absorbance read by spectrometer at 495 nm, α is the extension coefficient which is 5900 $M^{-1}cm^{-1}$ for FITC and l distance that light travel through the sample which is 1 cm.

The chelate complex conjugated to the peptide had an absorbance peak at 290 nm. The chromatogram monitored by absorbance of the peptide conjugated chelate complex had four main peaks (Figure 2.5). The first peak corresponds to unreacted cytosine, the second and third peaks correspond to unreacted DTPA and unreacted DTPA with cytosine, and the last peak corresponds to chelate complex conjugated peptide. Concentration of chelate complex conjugated peptide was measured using the same Beer-Lambert's law with $\alpha = 9300\ M^{-1}cm^{-1}$ and l of 1 cm.

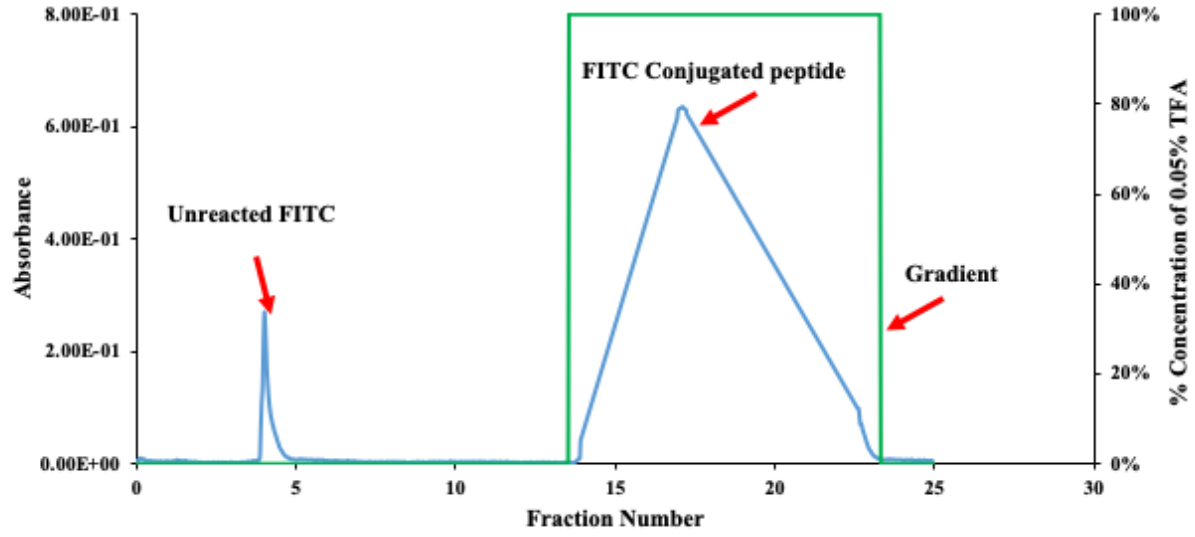

Figure 2.4: Reverse phase chromatogram of FITC conjugated peptide

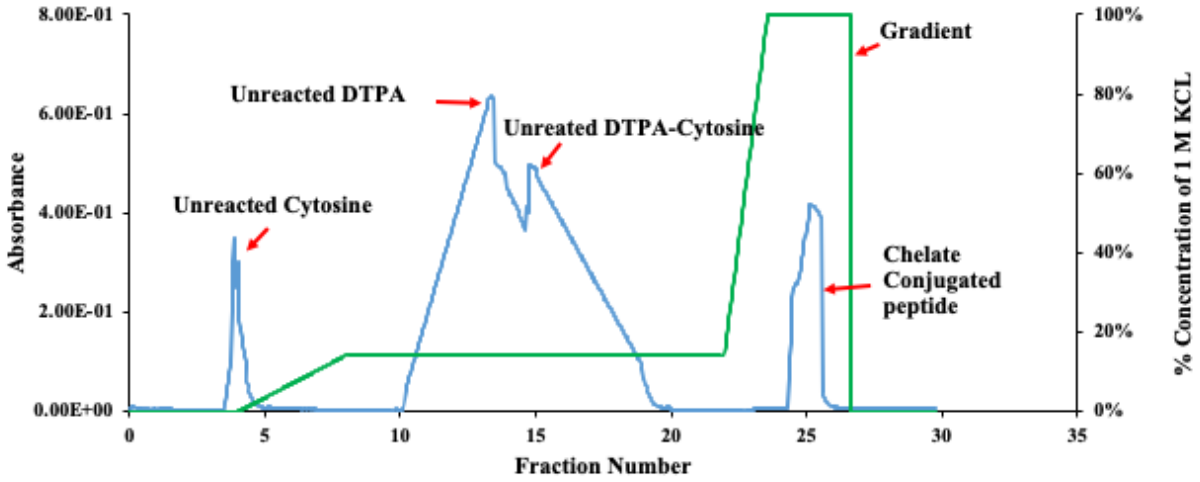

Figure 2.5: Anion exchange chromatogram of chelate complex conjugated peptide

2.2.1.10 Binding Isotherm Equation for Fitting FRET Data

Binding isotherm equations to fit FRET data was derived as below for the control experiments.

$$P + N \leftrightarrow B$$

where B = binding, P = one monomer, and N = another monomer

$K_D = \frac{[P][N]}{[B]}$

where $P = P_t - B$ and $N = N_t - B$

$K_D \rightarrow B = (P_t - B)(N_t - B)$

$0 = B^2 - (N_t + P_t + K_d)B + P_t N_t = (0 = Lx^2 + Mx + N)$

using the quadratic formula to solve for B

$B = \frac{Nt+Pt+Kd \pm \sqrt{(Nt+Pt+Kd)^2 - 4Pt\,Nt}}{2} = \left(x = \frac{-M \pm \sqrt{M^2 - 4LN}}{2N} \right)$

where $L = 1$, $M = \pm (N_t P_t K_d)$, $N = P_t N_t$

Binding isotherm equations to fit FRET data were derived as below for the experiments in presence of the anti-S2 peptides. Below shows the derivation of the equation in presence of the destabilizer peptide specifically.

$D + P = B$

where B = binding, D = dimer, P = anti-S2 peptide

$K_D = \frac{(Concentration\ D)(Concentration\ P)}{(Concentration\ B)}$

$D_t = D + D_B$

$D_B = B$

$P_t = P + P_B \rightarrow P_B = 2B$

$K_D = \frac{(Dt - B)(Pt - 2B)}{(B)}$

$0 = 2B^2 + 2\,D_t\,B - B\,P_t - K_D\,B + D_t\,P_t$

$0 = 2B^2 - B\,(2D_t + P^t + K_D) + D_t\,P_t$

$0 = A\left(\frac{2Dt+Pt+Kd \pm \sqrt{(2Dt+Pt+Kd)^2 - 8Pt\,Dt}}{4} \right) + C$

where $P_t = X$, D_t = concentration of dimer, and K_D (dissociation constant) = B

Derived equations for each experiment is as below:

1) Smooth muscle myosin S2 isoform + Destabilizer

$$F(x) = (0.00207-c)*(x+0.2+b-((x+0.2+b)^2-0.8*x)^{1/2})/0.4+ c$$

2) Smooth muscle myosin S2 isoform + Stabilizer

$$F(x) = (0.00207-c)*(x+0.2+b-((x+0.2+b)^2-0.8*x)^{1/2})/0.4+c$$

3) Smooth muscle myosin S2 isoform control

$$F(x) = (1-(4*x+c-((4*x+c)\text{^}2-16*x\text{^}2)\text{^}0.5)/4/x)*a+(4*x+c-((4*x+c)\text{^}2-16*x\text{^}2)\text{^}0.5)/4/x*b$$

4) Skeletal muscle myosin S2 isoform + Destabilizer

$$F(x) = (0.00207-c)*(x+0.2+b-((x+0.2+b)^2-0.8*x)^{1/2})/0.4+ c$$

5) Skeletal muscle myosin S2 isoform + Stabilizer

$$F(x) = (a-c)*(2-((b+x+2-((b+x+2)\text{^}2-8*x)\text{^}.5)/2))/2+c$$

6) Skeletal muscle myosin S2 isoform control

$$F(x) = (1-(4*x+c-((4*x+c)\text{^}2-16*x\text{^}2)\text{^}0.5)/4/x)*a+(4*x+c-((4*x+c)\text{^}2-16*x\text{^}2)\text{^}0.5)/4/x*b$$

7) Cardiac muscle myosin S2 isoform + Destabilizer

$$F(x) = (a-c)*(x+0.2+b-((x+0.2+b)\text{^}2-0.8*x)\text{^}0.5)/0.4+ c$$

8) Cardiac muscle myosin S2 isoform + Stabilizer

$$F(x) = (a-c)*(.1-((b+x+.1-((b+x+.1)\text{^}2-.4*x)\text{^}.5)/2))/.1+c$$

9) Cardiac muscle myosin S2 isoform control

$$F(x) = (1-(4*x+c-((4*x+c)\text{^}2-16*x\text{^}2)\text{^}0.5)/4/x)*a+(4*x+c-((4*x+c)\text{^}2-16*x\text{^}2)\text{^}0.5)/4/x*b$$

10) Cardiac mutant muscle myosin S2 isoform (E924K) + Stabilizer

$$F(x) = ((1-(4*x + c-((4*x + c)^2-16*x^2)^{1/2})/4/x)*a+ (4*x+ c - ((4*x + c)^2-16*x^2)^{1/2})/4/x*b$$

11) Cardiac mutant muscle myosin S2 isoform (E924K) control

$$F(x) = (1-(4*x + c-((4*x + c)^2-16*x^2)^{1/2})/4/x)*a+ (4*x + c-((4*x + c)^2-16*x^2)^{1/2})/4/x*b$$

12) Cardiac mutant muscle myosin S2 isoform (ΔE930) + Stabilizer

$$F(x) = (1-(4*x+c-((4*x+c)\text{^}2-16*x^2)^{1/2})/4/x)*0.00185619+(4*x+c-((4*x+c)^2-16*x^2)^{1/2})/4/x*0.00114$$

13) Cardiac mutant muscle myosin S2 isoform (ΔE930) + control

$$F(x) = (1-(4*x+c-((4*x+c)\text{^}2-16*x)^{1/2})/4/x)*0.00195619+(4*x+c-((4*x+c)^2-16*x^2)^{1/2})/4/x*0.001$$

2.2.2 Gravitational Force Spectroscopy

2.2.2.1 Materials

The materials included 3-aminopropyltriethoxysilane, acetone, coupling buffer (0.01 M pyridine in water with pH 6.0), 5% glutaraldehyde, quenching solution (1 M glycine in water with pH 7.0), blocking buffer (0.01 M Tris, 0.1% sodium azide, 0.1% bovine serum albumin, 0.15 M sodium chloride, and 0.001 M ethylenediaminetetraacetic acid with pH 7.0), wash buffer (0.01 M Tris, 0.1% sodium azide, 0.15 M sodium chloride, and 0.001 M ethylenediaminetetraacetic acid with pH 7.0) low salt buffer (0.1 M potassium chloride, 0.02 M imidazole, 5 mM magnesium chloride, with pH 7.0), 1-ethyl-3-(3-dimethyaminopropyl) carbodiimide, N-hydroxysuccinamide, iodoacetamide-succinimidyl ester, 8M urea solution (50 mM imidazole and 0.1 mM tris (2-carboxyethyl) phosphine with pH 7.0) monodisperse silica beads, glass slides, glass coverslips, vacuum grease, rabbit skeletal myosin, purified actin (G-actin), 1 μM human β-cardiac myosin S2 peptide, 1 μM human β-cardiac mutants myosin S2 peptide (ΔE930 and E924K), 1 μM human skeletal myosin S2 peptide, 1 μM human smooth myosin S2 peptide, stabilizer peptide, and destabilizer peptide.

A light microscope with an objective lens of 10X was mounted on an alt-azimuthal mount. A digital video camera of Sony, XCD-V60 replaced the ocular lense. Extension springs on steel bracket held the alt-azimuthal mount suspended.

The muscle myosin S2 synthetic peptides were as follows:

KIQLEAKVKEMNERLEDEEEMNAELTAKKRKLEDEC (MYH7)

KIQLEAKVKEMNERLEDEEMNAELTAKKRKLEDEC (MYH7 ΔE930)

KQELEEILHEMEARLEEEEDRGQQLQAERKKMAQQC (MYH11)

KIQLEAKIKEVTERAEDEEEINAELTAKKRKLEDEC (MYH2)

2.2.2.2 Methodology

Gravitational force spectroscopy (GFS), is a single molecule force spectroscopy that utilizes gravitational force to measure absolute length of a single molecule at the given force calculated by the density of the bead suspending the molecule. This technique was discovered and developed in Root lab, which measures the forces in piconewton and sub-piconewton levels. Other than absolute length of a molecule, GFS measures force range required to uncoil, stretch or extend the molecule yielding a force-distance profile for the suspended molecule. Besides that, based on the force-distance profile, number of amino acids within the molecule can be calculated. Also, the other advantage of GFS was that it did not require any prior force calibration step up (Singh, R.R. *et al.*, 2019). Hence, GFS was an ideal choice to test the mechanical stability of all the myosin S2 coiled coil. The GFS allowed to test the flexibility or stability of a single molecule of myosin S2 peptide and also for the S2 peptides treated with anti-S2 peptides. The flexibility of myosin S2 is not dependent on the assembly myosin as a thick filament or myosin in its single molecule form. The flexibility of myosin S2 region was reported to be similar in single molecule form or myosin in a thick filament assembly, thus it could be conceived that the changes seen on flexibility of myosin S2 in presence of anti-S2 peptides would correlate to changes in myosin S2 flexibility for myosin in a thick filament form (Singh, R.R. *et al.*, 2019). The schematic diagram of GFS is shown below (Figure 2.7).

The GFS set up assembly contains a light microscope that is horizontally mounted on an alt-azimuthal which is suspended with help of extension springs on a steel bracket. To capture both images and videos of suspended molecule, a digital video camera has been placed instead of the ocular lenses. The molecule of interest is tethered between an immobile edge of glass coverslip placed on a glass slide and mobile silica or glass bead. Slide with the molecule of interest in inserted into the light microscope component of GFS. The bead with molecule of interest is imaged through the microscope and then oriented to the direction of gravity vector to allow the maximal gravitation force exerted on to the bead. GFS has two modes, one is called rotational mode or an equilibrium mode which measures the absolute length of a single molecule and the second one is called free fall mode which measures the force required to unwind, uncoil, stretch or extend the molecule of interest.

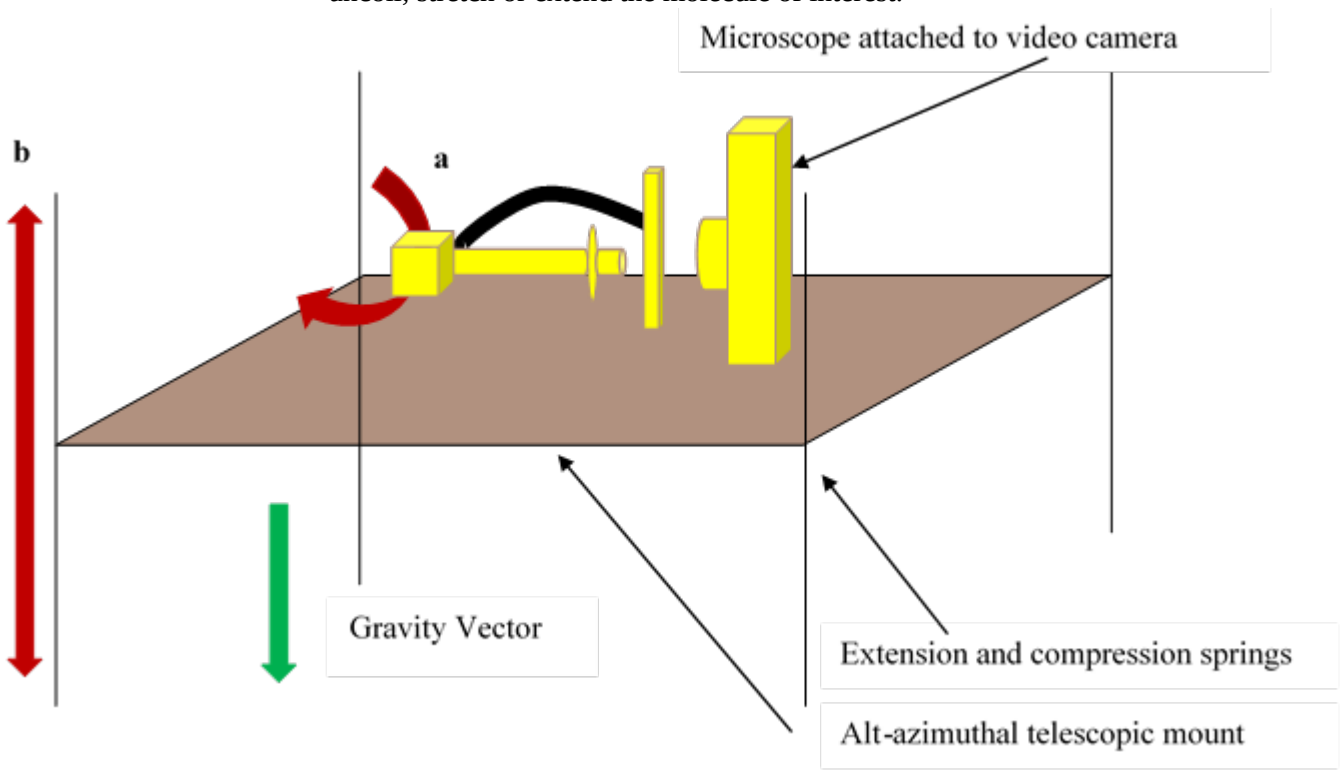

Figure 2.6: Schematic diagram of GFS which has two modes: (a) rotational mode, (b) free-fall mode

2.2.2.3 Rotational Mode

Length of molecule suspended between an immobile edge and mobile bead is measured using rotational mode (Figure 2.8 & 2.9). In rotational mode, the molecule is suspended within mobile and immobile edge on a glass slide and placed on the light microscope. The bead with molecule of interest is tethered to immobile edge and oriented in the direction of gravity vector. To begin the measurement, orientation of the slide was rotated to 45 degrees clockwise or

counterclockwise from starting position (gravity vector). After positioning the start point, 45 degrees clockwise or counterclockwise, rotation of microscope began in opposite direction, counterclockwise or clockwise.

Rotation was stopped when the microscope rotated 90 degrees from the starting point, either counterclockwise or clockwise. For example, if the start point was set in a direction 45 degrees clockwise to the gravity vector, rotation was stopped 45 degrees counterclockwise to the gravity vector. The duration of the rotation was recorded using the mounted video camera and was later analyzed using Image J. Image J is an image processing software for analyzing images and videos. The speed at which the microscope was rotated for measurement purposes was half a degree per second. By analyzing the video an x and y coordinate was measured for each frame of the video; which is the coordinate for the center of bead. Later, these coordinates are further used to determine the length of the molecule suspended by the bead (Figures 2.10 & 2.11).

The exact length of suspended molecule is obtained from analyzing a line equation parallel to the immobile edge and the center of the mobile bead for each video frame. A bell shaped curve is acquired from the distance between the mobile bead and the line plotted versus rotational angel. At the start of the rotation, the molecule has a conformation with minimum length (d_{min}) and during rotation when the mobile bead is parallel to gravity vector the length would be at maximum (d_{max}) and lastly the length would go back to minimum position again. To get the absolute length of the molecule, d_{min} was subtracted from d_{max}. The force exerted on the bead was calculated by the product of mass of the bead and acceleration by gravity where mass of bead was rectified for its buoyancy. Mass of the bead was calculated as follows, radius of the bead was used to calculate the volume of the bead, later the volume was multiplied with the known density of the bead leaving us with the mass of the bead.

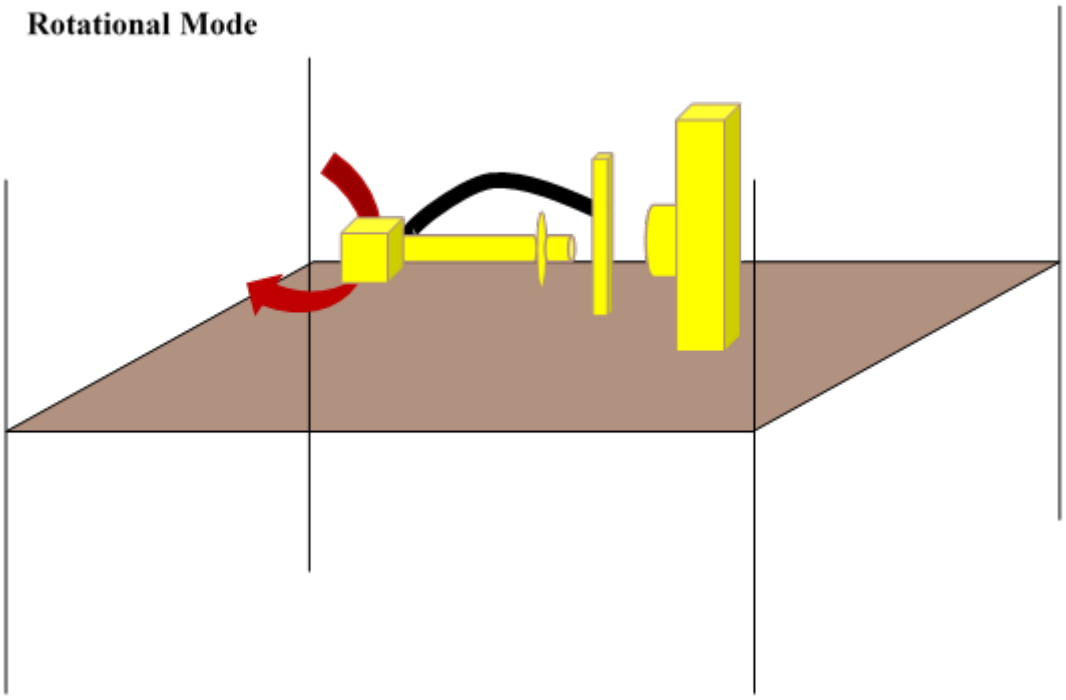

Figure 2.7: Schematic diagram of rotational mode setup. Red arrow indicates rotation of microscope

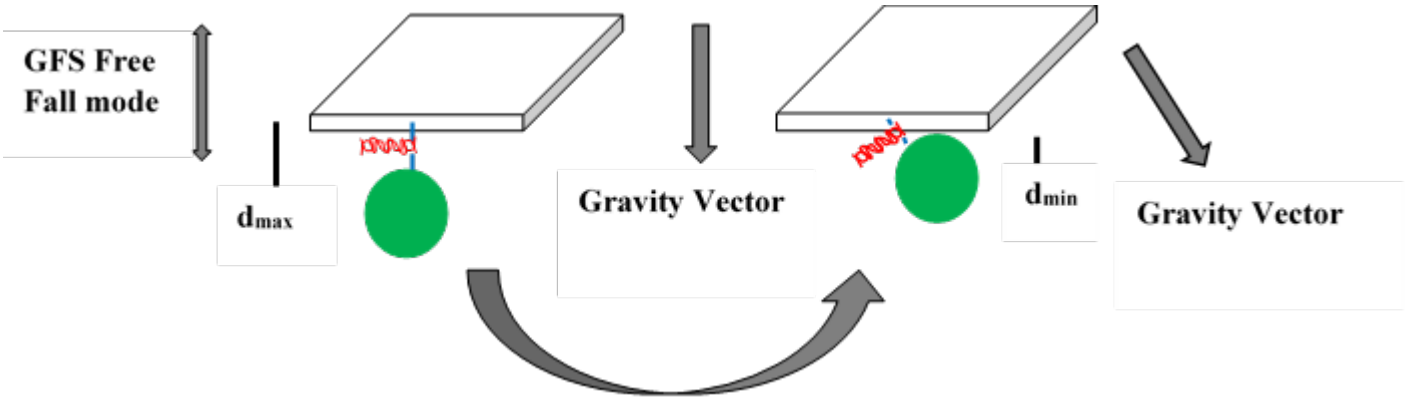

Figure 2.8: Schematic diagram of rotational mode bound to immobile edge

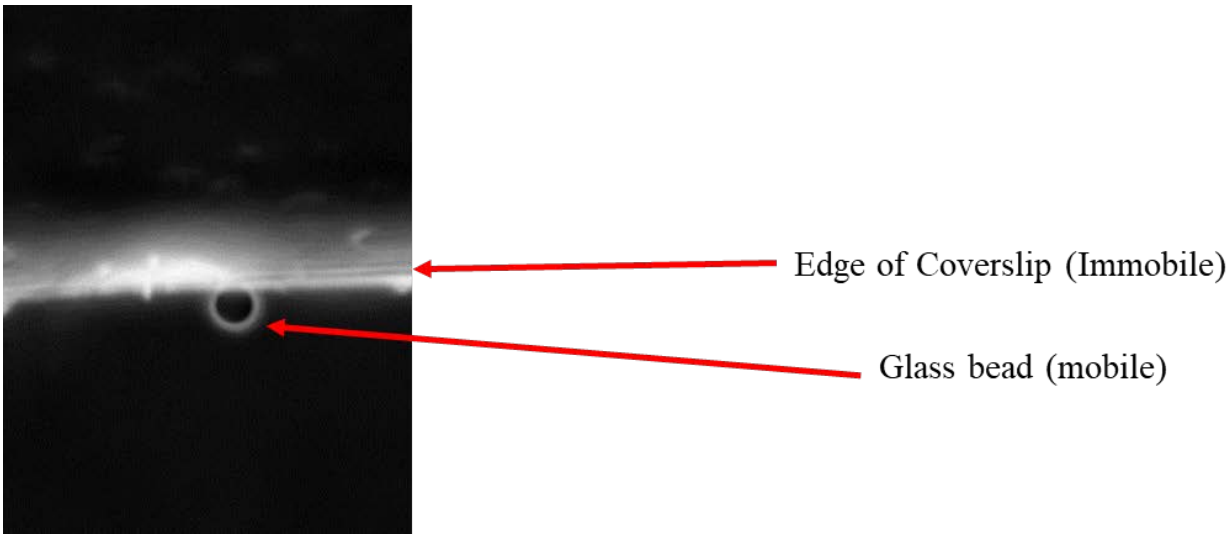

Figure 2.9: Example of mobile bead bound to immobile edge

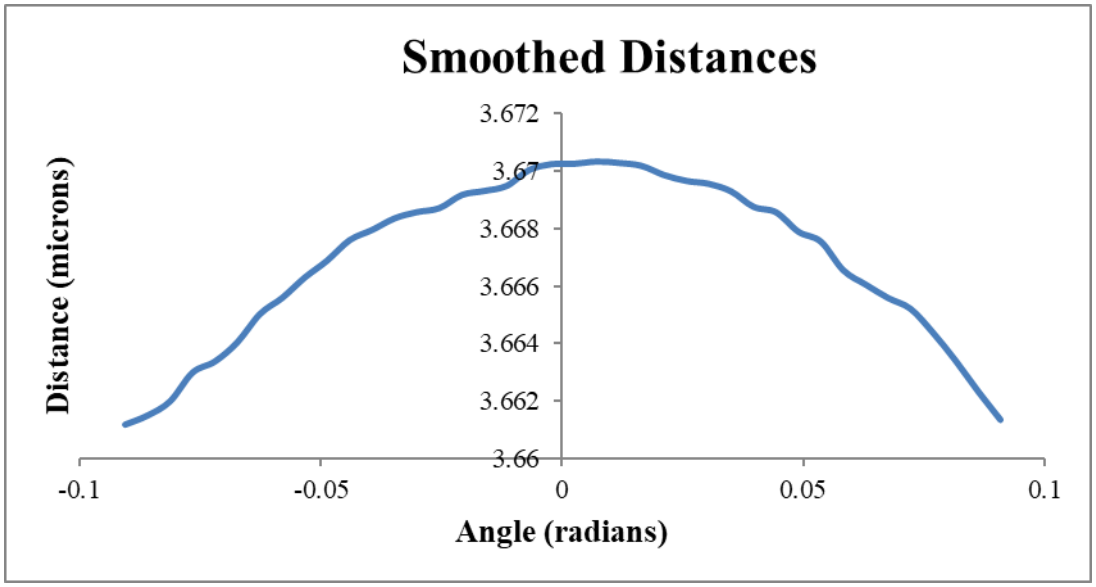

Figure 2.10: Example of bell shaped curve used to get coordinates for the center of the bead. Length of the molecule suspended by the bead is measured based on maximum and minimum length of the curve.

2.2.2.4 Free-Fall Mode

Free fall mode, another measurement variant of GFS which allows the user to get a force distance profile on a single molecule experiencing the gravitational force. Free fall mode allows a variable force by the virtue of gravity to be exerted on a single molecule. The GFS setup, light

microscope with mounted camera on spring on alt-azimuthal platform, can be dropped (Figure 2.12). The start of free-fall mode force applied to the bead is zero or close to zero. The platform dropped during free fall mode experiences an acceleration due to gravity which results in an acceleration trace for GFS, which is the function of spring constant possessed by the spring holding the GFS platform. As the platform goes towards equilibrium, trace of the acceleration decays. During the free fall mode, GFS has a single molecule which is suspended within an immobile edge and mobile bead will now experience the variable force which would be calculated by the product of mass of the bead and the acceleration of the GFS.

Measurement in free fall mode begins with setting orientation of the bead molecule in the direction of gravity vector and then simultaneously dropping the platform while starting the video recording of bead. Recording was stopped as the platform reached steadiness. The video frames were later processed using Image J to get the x and y coordinates of the center of the mobile bead and stationary spot on the immobile edge. Rotational mode data and free fall data work hand in hand. Using the information from both assays, the length of the molecule for every single frame was calculated; later, these information yielded to force-distance graph which distance is indication of the length of the actual molecule.

The product of the GFS acceleration and the mass of the bead will provide a force trace for the single molecule tethered between the immobile edge and mobile bead. The image processing would provide distance trace for the single molecule experiencing the free fall by the GFS. When this force trace is aligned with distance trace will yield the extension or the stretch experience by the single molecule under variable forces. In this case, a coiled coil myosin S2 peptide will have one end of the monomer trapped by immobile edge and the other monomer is tethered to mobile bead. The myosin S2 molecule undergoing the free fall mode will result in a

force distance trace giving the information about amount of force required to uncoil the dimer along its length. Stability and flexibility of myosin S2 peptide coiled coil can be measured by measuring the amount of force required to uncoil the coiled coil. A stable coiled coil would require greater force compared to a much more flexible coiled coil to unwind.

To test stability and flexibility of myosin S2 peptide two different types of conjugation was performed to tether the molecule between the immobile edge and mobile edge. First conjugation was crosslinking the muscle myosin S2 peptides to immobile edge and mobile bead. A different conjugation was benefiting from the binding property of actin to myosin S1. Rabbit skeletal myosin molecule at myosin S1 position was bound with G-actin treated immobile edge and mobile bead.

2.2.2.5 Conjugation with Myosin S2 Peptides

To bind the muscle myosin S2 peptide between immobile edge and mobile bead, both this edge and the mobile bead have to be treated with muscle myosin S2 peptide. Glass coverslips represent the immobile edge and silica beads represent the mobile bead. Both the glass coverslips and silica beads are treated with 0.04% 3 aminopropyltriethoxylsilane in acetone to add aminosilane groups to hydroxyl groups on the surface of both the glass coverslips and silica beads. Both glass coverslip and aminosilanate beads were rinsed with distilled water. To the aminosilane groups, 1 mg/1 ml iodoacetamide-succinimidyl ester was added; this chemical is a biofunctional crosslinker. The surfaces were rinsed with the wash buffer. 1 μM interested muscle myosin S2 peptide was added to both the surfaces in 8 M urea solution (50 mM imidazole and 0.1 mM TCPE with pH 7.0) in separate tubes. The mixture was kept in urea solution to allow muscle myosin S2 in its monomer status. Low salt buffer was exchanged with the urea solution in the slide chamber so the monomers could form a dimer molecule ready for measurement.

2.2.2.6 Conjugation of G-actin

This conjugation was done by first, treating glass coverslips and silica beads with 0.04% 3-aminopropyltriethoxylsilane in acetone to add the aminosilane groups to both glass coverslips and silica beads. To cross link G-actin to the aminosilanated glass coverslips and silica beads 740 mM 1-ethyl-3-(3 dimethyaminopropyl) carbodiimide was used with help of 60 µM N-hydroxysuccinamide. To block any unreacted group, glycine quenching solution was added. Lastly, both glass coverslips and silica beads went over several washes with low salt buffer and were stored in the same low salt buffer for GFS experiments.

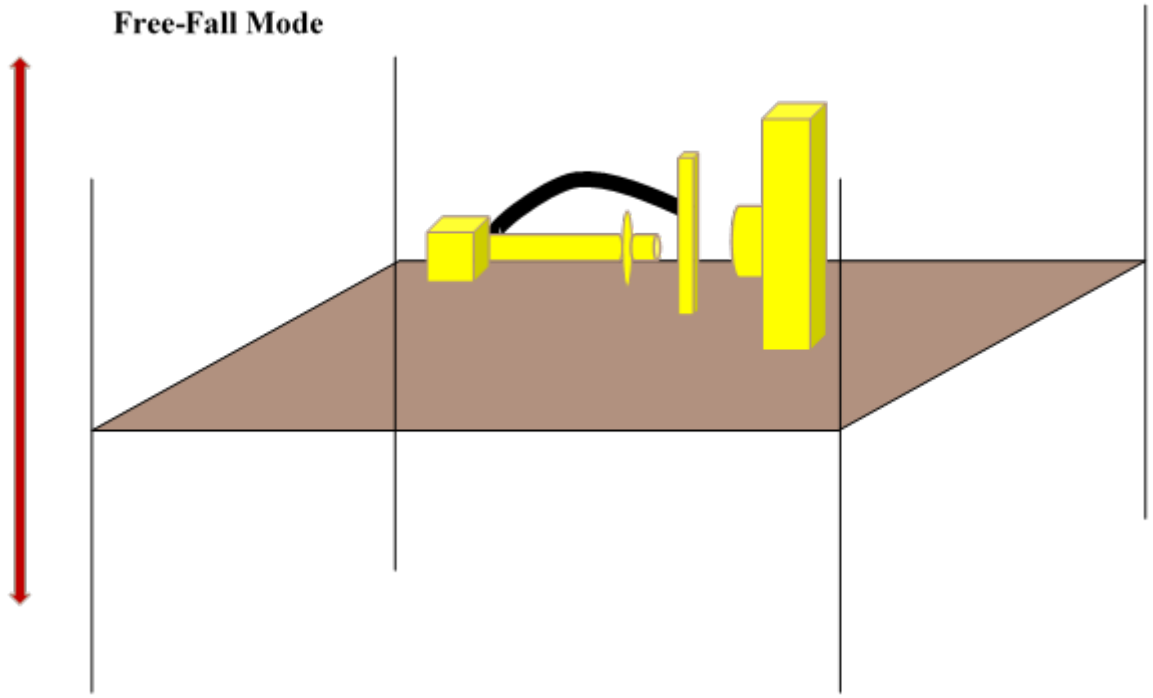

Figure 2.11: Schematic illustration of free-fall mode (red arrow). Platform surface is dropped in direction of gravity vector.

Oscillation of the dropped platform was matched to the gravitational acceleration experienced by the GFS platform to yield force acceleration trace using the formula bellow:

$$x(t) = \alpha e^{-(\gamma t)/2} \cos(\omega t - \phi)$$

where ϕ is the phase, ω is the oscillation frequency, α is a proportionality constant, and γ is a damping constant.

If ϕ equals zero

$$x(t) = \alpha e^{-(\gamma/2)t} \cos(\omega t)$$

$$v(t) = -\gamma/2\, \alpha e^{-(\gamma/2)t} \cos(\omega t) - \omega \alpha e^{-(\gamma/2)t} \sin(\omega t)$$

$$a(t) = (\gamma/2)^2 \alpha e^{-(\gamma/2)t} \cos(\omega t) + \gamma/2\, \alpha\omega e^{-(\gamma/2)t} \sin(\omega t) + \omega \alpha (\gamma/2) e^{-(\gamma/2)t} \sin(\omega t) - \omega^2 \alpha e^{-(\gamma/2)t} \cos(\omega t)$$

$$a(t) = ((\gamma/2)^2 - \omega^2) \alpha e^{-(\gamma/2)t} \cos(\omega t) + \omega \alpha \gamma e^{-(\gamma/2)t} \sin(\omega t)$$

If $\gamma \cong 0$

$$a(t) = -\omega^2 \alpha \cos(\omega t)$$

which is proportional to $x(t) = \alpha \cos(\omega t)$ and also to force (F=ma).

2.2.2.7 Slide Preparation

GFS experimental slide was prepared by first selecting a clean glass slide and making a four walled chamber with edges of coverslip and vacuum grease. (Figure 2.13A). One side of the chamber being the glass coverslip treated with G-actin or the interested muscle myosin S2 peptide. Second, peptide treated or G-actin treated coverslip was placed in the chamber, facing the center of the slide with vacuum grease (Figure 2.13B). Third, within the chamber, around 50 μL of anticipated myosin S2 peptide or actin coated silica beads was added followed by 100 μL low salt buffer, and 5 μL anti-S2 peptide for total concentration of 3.5 nM anti-S2 peptide (Figure 2.13C). Lastly, the chamber was sealed with another clean coverslip and vacuum grease leaving the center of the chamber with suspension buffer, treated bead and molecule of interest untethered (Figure 2.13D). To let molecule of interest to be bound to the edge of the coverslip and mobile bead, the slide was rotated for 120 minutes at room temperature. After 120 minutes, the slide is ready for measurement. By uncoiling the myosin S2 peptides, the stability and flexibility of this region was measured with free fall mode in conjunction with rotational mode of GFS. In addition, impact of anti-S2 peptides on the stability of myosin S2 peptide were tested using the same technique.

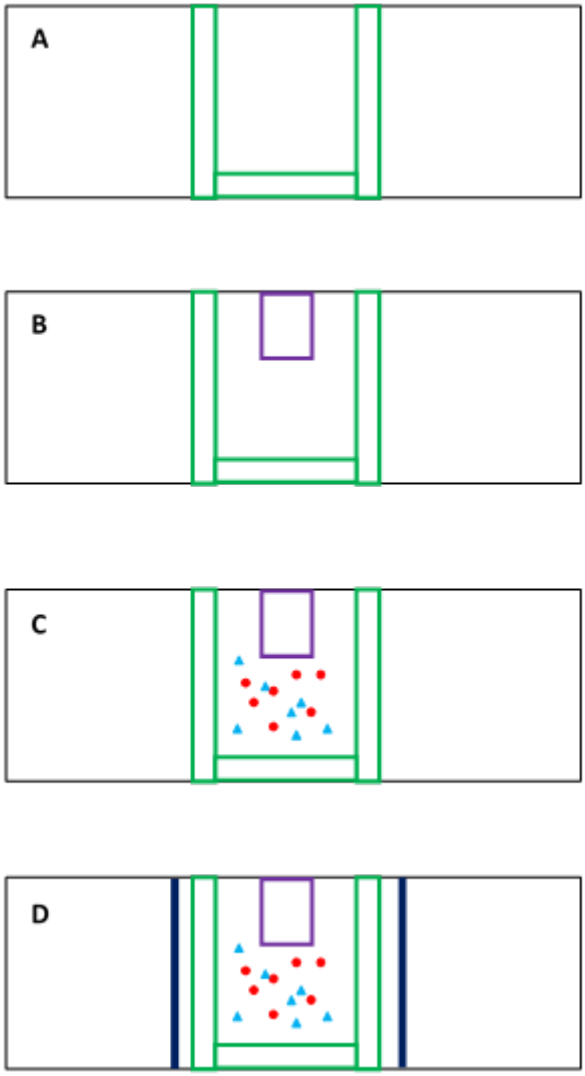

Figure 2.12: Schematic illustration of slide preparation for GFS measurements

2.3 Statistical Analysis

For all the FRET and GFS assays, anti-S2 treatment peptides were compared to its respective control. The statistical significance was calculated by performing Student's t-test. Also, in addition to Student's test, Wilcoxon-Mann-Whitney was performed for GFS. Statistical significance was specified with p-value less than 0.5. The FRET assays had n= 3 (table 3.3) and respective "n" values for GFS assay is provided in Table 3.7.

For the FRET experiment, the error bars represent ± Standard Error of the Mean (S.E.M) for lifetime values calculated by fitting them to exponential decay curve using WinCurveFit (Kevin Raner Software). For the GFS experiment, the error bars represent ± S.E.M which was calculated by dividing the standard deviation for each force distance observation by square root of the number of observations. The S.E.M for each experiment was added to the respective graph.

Shapiro-Wilk normality test was performed on the GFS measurements. Cardiac, skeletal, and smooth muscle myosin S2 isoform treatment with the destabilizer peptide have normal distribution ($p > 0.05$). While the control for cardiac muscle myosin S2 isoform had normal distribution, smooth muscle myosin S2 isoform, skeletal muscle myosin S2 isoform, and ΔE930 did not have normal distribution. Upon the stabilizer treatment, only ΔE930 now had a normal distribution. While skeletal, cardiac and smooth muscle myosin S2 isoform with the stabilizer did not have a normal distribution.

CHAPTER 3

RESULTS

3.1 Fluorescence Resonance Energy Transfer (FRET)

3.1.1 Anti-S2 peptides have an impact on MYH7

FRET measured the dissociation constant (binding affinity) between the myosin S2 dimers and the anti-S2 peptides. The anti-S2 peptides were designed computationally to target S2 region of cardiac muscle β-myosin (MYH7). Anti-S2 peptides were specifically designed against cardiac muscle myosin S2 peptides region 921 to 939. Impact of these peptides were further tested on the other two muscle myosin isoforms namely skeletal (MYH2) and smooth (MYH11). Results indicated that anti-S2 peptides were able to manipulate the coiled coil formation on skeletal and cardiac muscle isoforms. Of the two peptides, one peptide was designed to bind across the dimer of S2 region and other was designed to associate with a monomer of S2. Anti-S2 peptides were designed with the purpose of binding and further stabilizing or destabilizing the myosin S2 coiled coil.

In FRET assay, Fluorescein Isothiocyanate (FITC) functioned as fluorescent acceptor probe and Terbium Diethylene Triamine Pentaacetic Acid-Cytosine (Lanthanide-DTPA-Cytosine) functioned as donor probe. Donor probe was conjugated to C-terminus of a myosin S2 peptide monomer and acceptor probe was conjugated to N-terminus of another myosin S2 peptide. In FRET as lanthanide of the donor probe decays, energy goes to fluorescein and it emits energy in form of light. In addition, as the monomers come closer to each other, lifetime of donor decreases indicating a decrease in distance between donor and acceptor probe; an opposite effect is observed, with an increase in distance between the probes, distance increases. Lifetime of donor probe was measured in milliseconds.

A number of factors impacted the efficiencies of resonance energy transfer as mentioned before (Taei, N., Root, D.D.,2013; Schiller, P.W., 1975; Clegg, R.M., 1992; Selvin, P. R.,1995). Experimental measurements of these factors are summarized as follow:

Probe	$J(M^{-1}cm^{-1}nm^4)$	κ^2_{min}	κ^2_{avg}	κ^2_{max}	Q	η	$R_{o\,min}$ (nm)	$R_{o\,avg}$ (nm)	$R_{o\,max}$ (nm)
FITC ^{MYH7}	1.05×10^{15}	0.66	0.67	0.69	0.47	1.4	4.42	4.43	4.45
FITC ^{MYH2}	1.05×10^{15}	0.66	0.67	0.69	0.40	1.4	4.30	4.31	4.33
FITC ^{MYH11}	1.05×10^{15}	0.66	0.67	0.69	0.40	1.4	4.30	4.31	4.33

Table 3.1: Calculated Critical Transfer Distance Parameters

During FRET assay, cardiac muscle myosin $S2^{pep}$ was treated with increasing concentrations of anti-S2 peptides. The test indicated the dissociation constant of cardiac muscle myosin $S2^{pep}$ control and treated with anti-S2 peptides (Table 3.1). Dilution to decrease the concentration of dimer cardiac muscle myosin $S2^{pep}$ was performed to measure binding affinity of coiled-coil peptide and in turn to measure minimal concentration for stable dimer formation (Figure 3.1A). Concentration of dimer cardiac muscle myosin $S2^{pep}$ used to treat with anti-S2 peptides was 0.1 μM. When treated with the stabilizer peptide, as the concentration of the stabilizer peptide increased, lifetime decreased; which states that it took less amount of time for energy to transfer from donor to acceptor probe thus a decrease in distance between donor and acceptor probe with increase in concentration of the stabilizer. An opposite effect was observed, in presence of the destabilizer peptide, as the concentration of the destabilizer peptide increased, lifetime increased as well. This states that it took longer amount of time for energy to transfer from donor to acceptor probe thus an increase in distance between donor and acceptor probe with increase in concentration of the destabilizer. (Figure 3.1B)

The test indicated K_d of cardiac muscle myosin $S2^{pep}$ control to be $3.08 \times 10^{-1} \pm 6.21 \times$

10^{-2} µM with R value of 0.97. In presence of the stabilizer peptide K_d was $2.12 \times 10^{-2} \pm 6.61 \times 10^{-3}$ µM with R value of 0.96 and in presence of the destabilizer peptide K_d was $9.97 \times 10^{-1} \pm 9.87 \times 10^{-3}$ µM with R value of 0.96. Our results strongly suggest that anti-S2 peptides have an impact on cardiac muscle myosin $S2^{pep}$ (Table 3.3**)**. As mentioned before, anti-S2 peptides are specific to myosin S2 region, decrease or increase in distance between donor and acceptor probe is due to the binding of stabilizer and destabilizer peptide to the myosin S2 peptide.

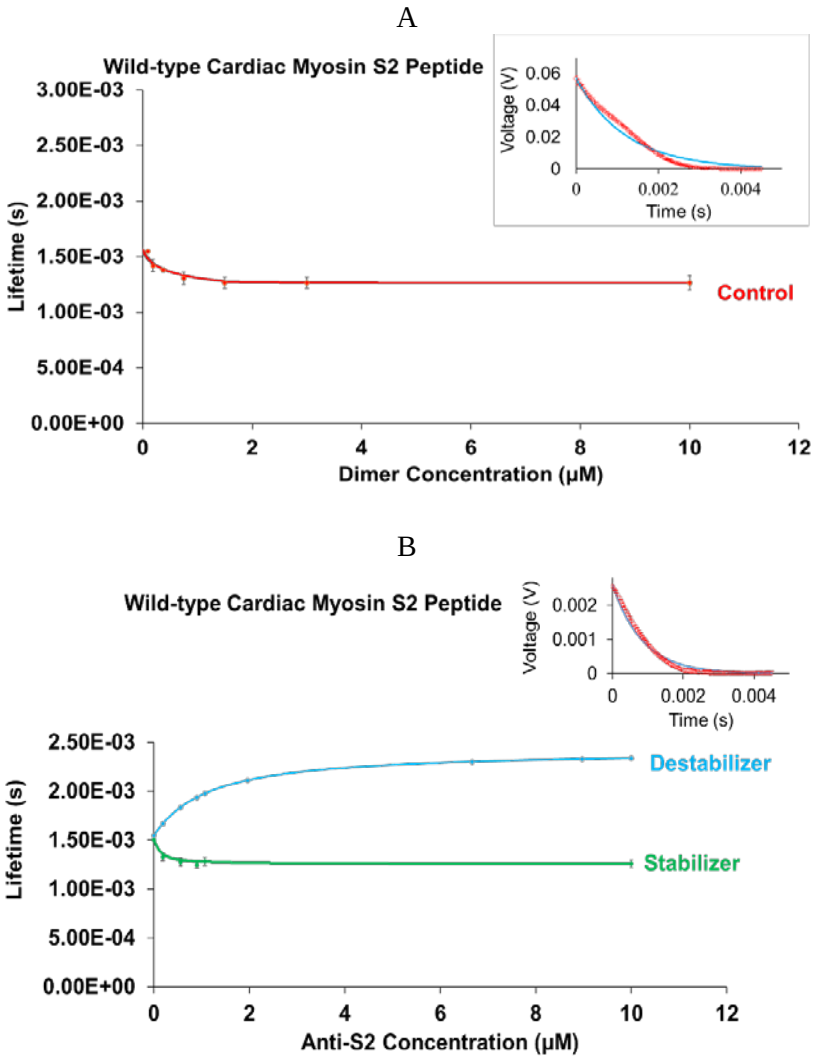

Figure 3.1: The FRET results of MYH7 isoform. (A) Lifetime of cardiac wild-type muscle myosin S2 donor probe. (B) Lifetime of cardiac wild-type muscle myosin S2 donor probe treated with the stabilizer (green) and the destabilizer (blue). *Graph on top right hand corner is an example of exponential graph that was used to measure lifetime at each concentration. * Error bars are standard error mean (S.E.M)

Muscle Peptides with Stabilizer	T_D (μM)	T_{DA} (μM)	EET	R_{min} (nm)	R_{avg} (nm)	R_{max} (nm)
Cardiac	1.73E-03	7.87E-04	5.45E-01	4.29	4.30	4.32
		7.69E-04	5.56E-01	4.26	4.27	4.29
		7.52E-04	5.66E-01	4.23	4.24	4.26
Skeletal	1.73E-03	4.82E-04	7.21E-01	3.67	3.68	3.69
		4.29E-04	7.52E-01	3.57	3.58	3.60
		3.76E-04	7.82E-01	3.47	3.48	3.50
Smooth	1.73E-03	8.69E-04	4.98E-01	4.31	4.32	4.34
		3.09E-04	8.21E-01	3.33	3.34	3.36
		0.00E+00	1.00E+00	0.00	0.00	0.00
E924K	1.94E-03	6.08E-04	6.86E-01	3.88	3.89	3.91
		4.61E-04	7.62E-01	3.64	3.65	3.67
		3.14E-04	8.38E-01	3.36	3.37	3.38
ΔE930	1.89E-03	4.33E-04	7.71E-01	3.61	3.62	3.64
		3.10E-04	8.36E-01	3.37	3.38	3.39
		1.87E-04	9.01E-01	3.06	3.07	3.08

Table 3.2: Experimental measurement of separation distance between the acceptor probe and the donor probe

The distance between the donor and the acceptor probe, separation distance (R), was calculated using the formula below (Taei, N., Root, D.D., 2013):

$$E = R_0^6 / (R_0^6 + R^6)$$

The formula uses critical transfer distance (R_0) and efficiency of energy transfer (E) to calculate separation distance (Förster, T., 1948). Efficiency of energy transfer was measured using lifetime of the donor in presence and absence of the acceptor probe as in

$$E = 1 - (\tau_{da} / \tau_d)$$

Critical transfer distance was measured using summarized formula below:

$$R_0 = [8.785 \times 10^{-11} \kappa^2 J \eta^{-4} Q_D]^{1/6} \text{ nm}$$

where Q is the quantum yield of the donor, η is the refractive index of the medium between the donor and the acceptor probes, κ^2 is orientation factor, and J is the overlap integral (Maliwal, B.P. *et al*, 1994). Experimentally estimation of these parameters are summarized in table 1.

Average of calculated separation distance of cardiac muscle myosin $S2^{pep}$ in presence of the stabilizer was 4.27 nm (Table 3.2). The separation distance is comparable to the peak frequency of 3.9 nm with a range of 2.8 nm to 4.7 (Taei, N., Root, D.D., 2013). The value from separation distance of cardiac muscle myosin $S2^{pep}$ also suggests that monomers represent an equal population of both homodimers and heterodimers. Table 3.2 summarizes three values for T_{DA}, which are minimum, average, and maximum T_{DA} and corresponding efficiency of energy transfer, and minimum, average, and maximum critical transfer distance.

3.1.2 Stabilizer Peptide has an Impact on MYH7 Mutant Peptide

E924K and ΔE930; the myosin S2 FHC mutants, form unstable dimers. Binding affinity of the dimer mutant peptides are lower compare to the dimer wild-type peptide (Table 3.3). Similar to cardiac muscle myosin $S2^{pep}$ wild-type, dilution by decreasing the concentration of both dimer cardiac muscle myosin $S2^{pep}$ mutant was performed (Figure 3.2A & 3.3A). Concentration of dimer cardiac muscle myosin $S2^{pep}$ mutants used to treat with the stabilizer peptide was 0.1 μM. Impact of the stabilizer peptide was tested on both the mutants. E924K was treated with different concentrations of the stabilizer. Increase in concentration of the stabilizer lead to decrease of lifetime (Figure 3.2B). The test indicated K_d E924K control to be 2.54 ± 1.72 μM with R value of 0.96. In presence of the stabilizer peptide K_d was $3.62 \times 10^{-2} \pm 5.59 \times 10^{-3}$ μM with R value of 0.98. Additionally, graph of treated E924K and cardiac muscle myosin $S2^{pep}$ wild type with the stabilizer peptide were compared (Figure 3.2B). The calculated separation

distance in presence of the stabilizer peptide was 3.65 nm. The results strongly suggest that the stabilizer peptide had an impact on E924K mutant muscle myosin S2 peptide by decreased lifetime of donor observed. (Table 3.3).

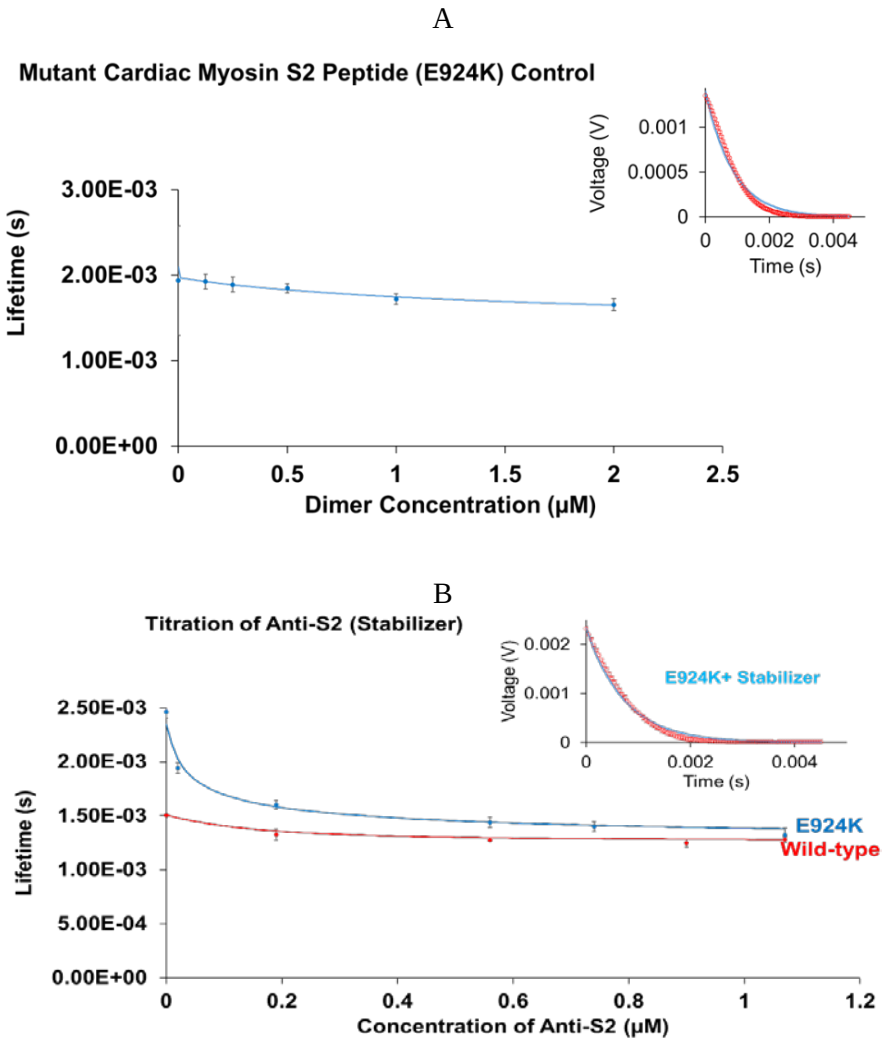

Figure 3.2: The FRET results of mutant MYH7 isoform (E924K). (A) Lifetime of cardiac E924K muscle myosin S2 donor probe.(B) Lifetime of cardiac E924K muscle myosin S2 donor probe treated with the stabilizer peptide (blue) compared to cardiac wild-type muscle myosin S2 donor probe treated with the stabilizer peptide (red).

In FRET assay, like E924K, ΔE930 was treated with different concentrations of the stabilizer. Increase in concentration of the stabilizer lead to decrease of lifetime (Figure 3.3A). The test indicated K_d of ΔE930 control to be 3.24 ± 2.25 μM with R value of 0.99. In presence of

the stabilizer peptide K_d was $2.38 \times 10^{-1} \pm 4.14 \times 10^{-2}$ μM with R value of 0.93. Additionally, graph of treated ΔE930 and cardiac muscle myosin $S2^{pep}$ wild type with the stabilizer peptide were compared (Figure 3.3B). Calculated separation distance in presence of the stabilizer peptide was 3.38 nm. The results state that stabilizer peptide had an impact on ΔE930 FHC mutant of cardiac muscle myosin $S2^{pep}$ (Table 3.2) by decreasing the distance between the FHC mutant dimer.

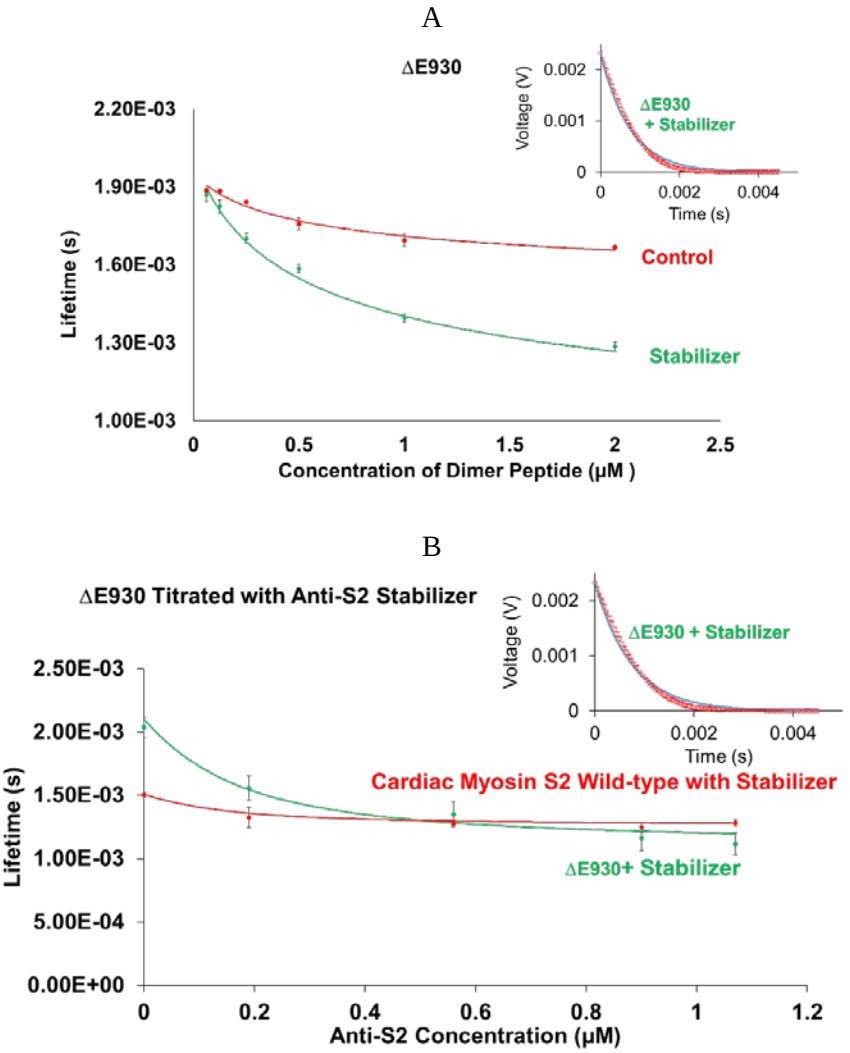

Figure 3.3: The FRET results of mutant MYH7 isoform (ΔE930). (A) Lifetime of cardiac ΔE930 muscle myosin S2 donor probe treated with the stabilizer peptide (green) compared to control (red). (B) Lifetime of cardiac ΔE930 muscle myosin S2 donor probe treated with the stabilizer peptide (blue) compared to cardiac wild-type muscle myosin S2 donor probe treated with the stabilizer peptide (red).

3.1.3 Anti-S2 Peptides have an Impact on MYH2

Like cardiac muscle myosin $S2^{pep}$, dilution by decreasing the concentration of dimer skeletal muscle myosin $S2^{pep}$ was performed and further was treated with different concentrations of anti-S2 peptides (Figure 3.4A & 3.4B**)**. Different concentrations of dimer skeletal muscle myosin $S2^{pep}$ was used with anti-S2 peptides. To treat skeletal muscle myosin $S2^{pep}$ with the stabilizer peptide, dimer concentration of 0.1 μM was used; in presence of the destabilizer peptide dimer concentration of 2 μM was used. Similar results as cardiac muscle myosin $S2^{pep}$ was observed when skeletal muscle myosin $S2^{pep}$ was treated with anti-S2 peptides. Increase in concentration of the stabilizer lead to decrease in lifetime (Figure 3.4B). Oppositely, increase in concentration of the destabilizer lead to increase in lifetime (Figure 3.4C). The test indicated K_d of skeletal muscle myosin $S2^{pep}$ control to be $3.41 \times 10^{-1} \pm 2.91 \times 10^{-2}$ μM with R value of 0.98. In presence of the stabilizer peptide K_d was $1.97 \times 10^{-2} \pm 2.87 \times 10^{-3}$ μM with R value of 0.98 and in presence of the destabilizer peptide K_d was 1.00 ± 1.38 μM with R value of 0.98. Calculated separation distance in presence of the stabilizer peptide was 3.58 nm. Our results strongly suggest that anti-S2 peptides had an impact on skeletal muscle myosin S2 peptide (Table 3.3).

A

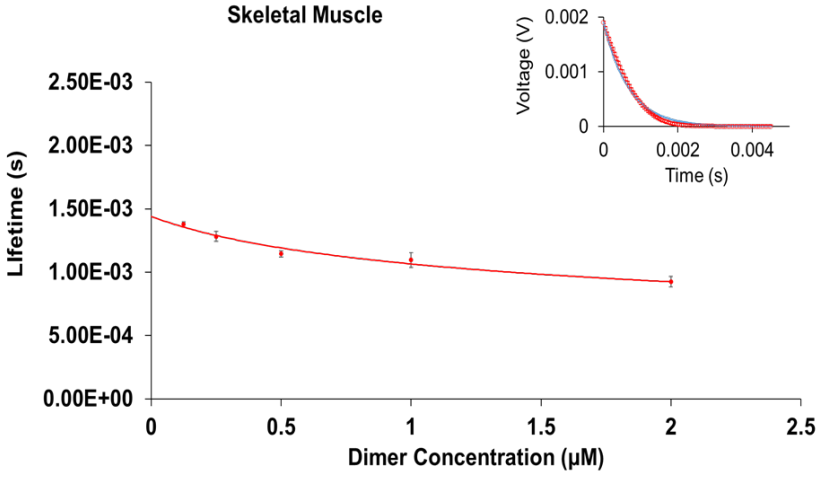

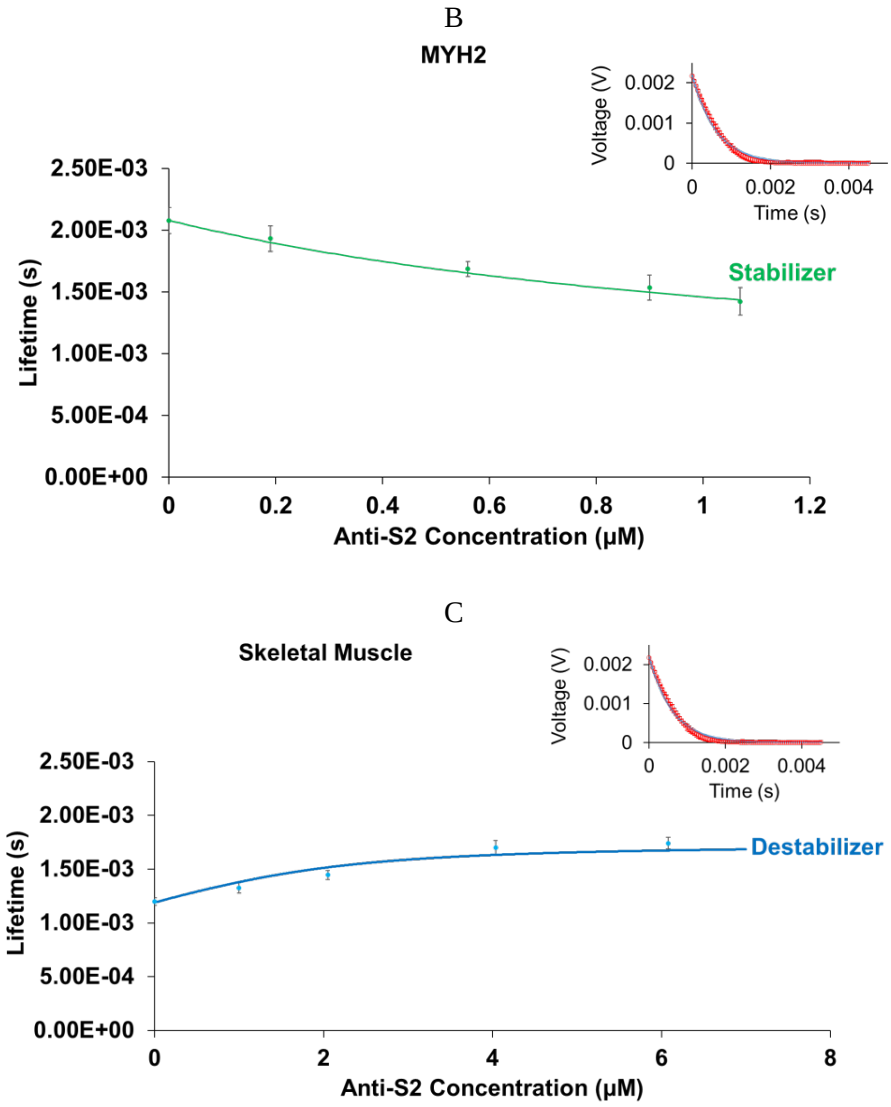

Figure 3.4: The FRET results of MYH2 isoform. (A) Lifetime of skeletal muscle myosin S2 donor probe. (B) Lifetime of skeletal muscle myosin S2 (0.1 uM) donor probe treated with the stabilizer. (C) Lifetime of skeletal muscle myosin S2 (2 uM) donor probe treated with the destabilizer.

3.1.4 Anti-S2 Peptides have No Impact on MYH11

The specificity of peptides were later tested on the myosin S2 of the smooth muscle (MYH11). Dilution by decreasing the concentration of smooth muscle myosin $S2^{pep}$ dimer revealed that 0.1 μM of the peptide was sufficient enough to form a stable dimer (Figure 3.5A). Smooth muscle myosin $S2^{pep}$ was treated with different concentrations of anti-S2 peptides. The

test indicated K_d of smooth muscle myosin $S2^{pep}$ control to be $3.02 \times 10^{-1} \pm 2.02 \times 10^{-1}$ μM with R value of 0.98 and was not able to determine dissociation constant of smooth muscle myosin $S2^{pep}$ treated with anti-S2 peptides (Table 3.3). Calculated separation distance in presence of the stabilizer peptide was 3.34 nm. The data suggested that stabilizing and destabilizing effect of the anti-S2 peptides had no impact on smooth muscle myosin S2 peptide (Figure 3.5B).

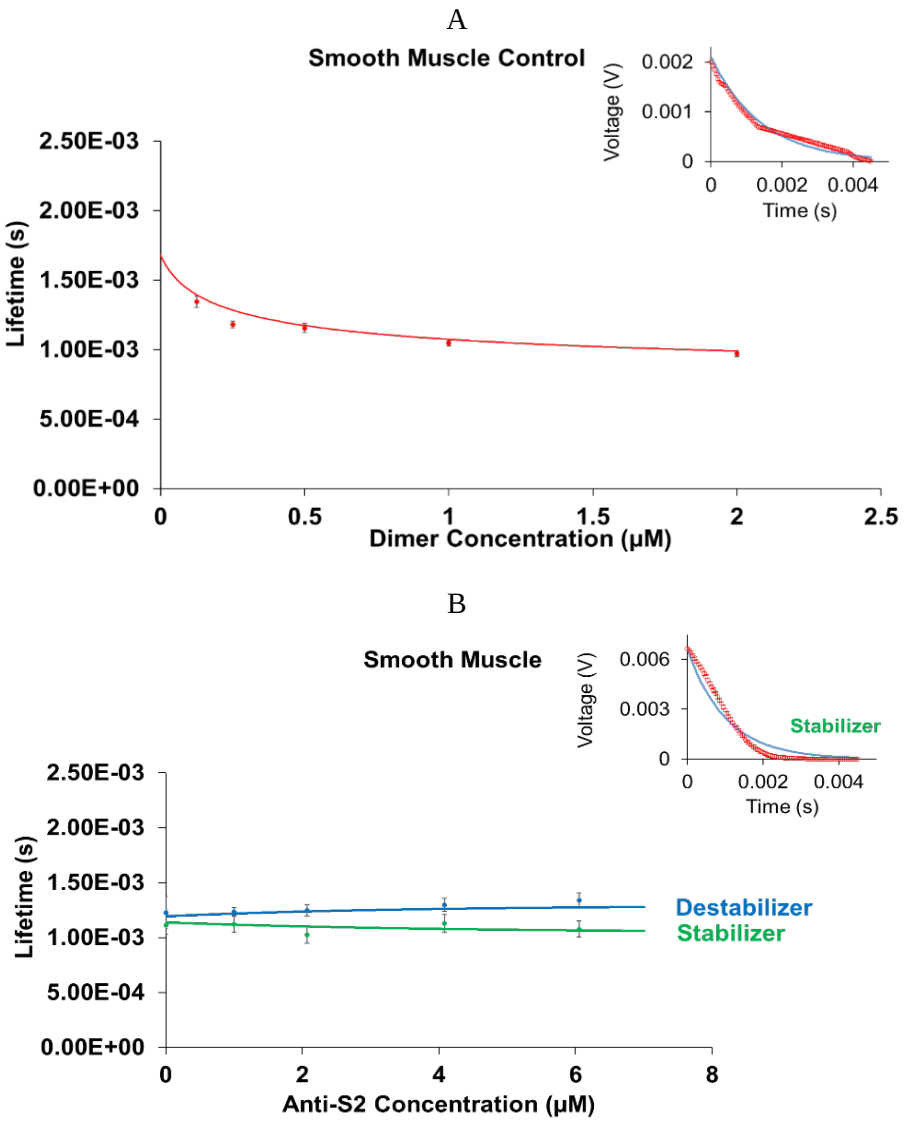

Figure 3.5: The FRET results of MYH11 isoform. (A) Lifetime of smooth muscle myosin S2 donor probe. (B) Lifetime of smooth muscle myosin S2 donor probe treated with the stabilizer (green) and the destabilizer (blue).

Experiment	Dissociation Constant (μM) ± SEM	Correlation Coefficient (R)
Smooth Myosin S2	3.02E-01 ± 2.02E-01	0.78
Skeletal Myosin S2	3.41E-01 ± 2.91E-02	0.89
Skeletal Myosin S2 with Stabilizer	1.97E-02 ± 2.87E-03	0.99
Skeletal Myosin S2 with Destabilizer	1.00E+00 ± 1.38E+00	0.98
Cardiac Myosin S2	3.03E-01 ± 4.42E-02	0.97
Cardiac Myosin S2 with Stabilizer	2.12E-02 ± 6.61E-03	1.00
Cardiac Myosin S2 with Destabilizer	9.97E-01 ± 9.87E-03	0.96
Cardiac Myosin S2 Mutant, ΔE930	1.11E+00 ± 1.15E-01	0.96
Cardiac Myosin S2 Mutant, ΔE930 with Stabilizer	2.38E-01 ± 4.14E-02	0.92
Cardiac Myosin S2 Mutant, E924K	9.42E-01 ± 1.24E-01	0.96
Cardiac Myosin S2 Mutant, E924K with Stabilizer	3.40E-02 ± 4.50E-03	0.98

Table 3.3: Summary of dissociation constant and correlation coefficient of FRET experiments

Summary of Student's t-test on each compared pair of the curve fitted parameters is shown with n = 3 independent experiments performed (Table 3.4). The stabilizer and the destabilizer tests detected a statistically significant difference ($p < 0.05$). This indicates that the myosin S2 isoforms treated with anti-S2 peptides were significantly different.

Controls		P-value (t-test)
	Smooth vs. Skeletal	8.56E-01
	Smooth vs. Cardiac	9.96E-01
	Smooth vs. E924K	5.37E-02
	Smooth vs. ΔE930	2.57E-02
	Skeletal vs. Cardiac	5.09E-01
	Skeletal vs. ΔE930	2.97E-03
	Skeletal vs. E924K	9.06E-03
	Cardiac vs. E924K	8.19E-03
	Cardiac vs. ΔE930	2.85E-03
	E924k vs. ΔE930	3.86E-01
Skeletal		
	Control vs. Stabilizer	4.55E-04
	Control vs. Destabilizer	1.23E-02
	Stabilizer vs. Destabilizer	2.32E-06
Cardiac		
	Control vs. Stabilizer	3.18E-03
	Control vs. Destabilizer	5.87E-03
	Stabilizer vs. Destabilizer	2.29E-03
E924K		
	Control vs. Stabilizer	1.83E-03
ΔE930		
	Control vs. Stabilizer	2.07E-03

Table 3.4: Summary of Student's test for FRET experiments

3.2 Gravitational Force Spectroscopy

3.2.1 Anti-S2 Peptides have an Impact on MYH7

The specificity and activity of the anti-S2 peptides were further tested using GFS. GFS measured the mechanical stability of myosin S2 coiled-coil peptides treated with or without anti-S2 peptides. Anti-S2 peptides were designed with the purpose of binding and stabilizing or destabilizing the myosin S2 coiled coil and increase or decrease the amount of force produced during acto-myosin interaction. The designed anti-S2 peptides are specific to the myosin S2 regions (Singh, R.R., *et al.,* 2018). The peptides were designed computationally to target S2 region of cardiac muscle β-myosin (MYH7). Of the two peptides, one peptide was designed to increase mechanical stability of S2 region and one was designed to decrease.

The mechanical stability of the cardiac muscle myosin S2 coiled coil could be altered when treated with anti-S2 peptides. GFS was performed to uncoil the single molecule of myosin S2 peptide dimer in a direction perpendicular to the coiled coil axis. The myosin S2 molecule was further treated with anti-S2 peptides and mechanical stability was measured. The mechanical stability of coiled coil was measured by the amount of force required to uncoil the coiled coil structure along the length of the molecule.

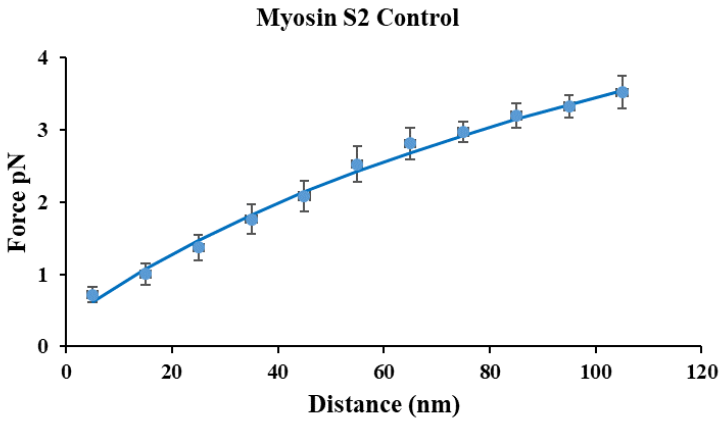

Figure 3.6: Force-distance graph of uncoiling a single molecule of rabbit skeletal myosin (n= 10). It was fit to F = A ln (x + B) + C

The control was performed by tethering G-actin to the edge of both the cover slip and silica beads. The S1 heads of a myosin molecule was suspended by the actin treated coverslip and silica heads. From the force-distance curve fit (Singh, R.R., *et al.*, 2018), the force required to uncoil the myosin molecule for a length of 60 nm was 2.67 ± 0.23 pN with R value of 0.99 (Figure 3.6). Shown result is as observed before (Singh, R.R., *et al.*, 2018).

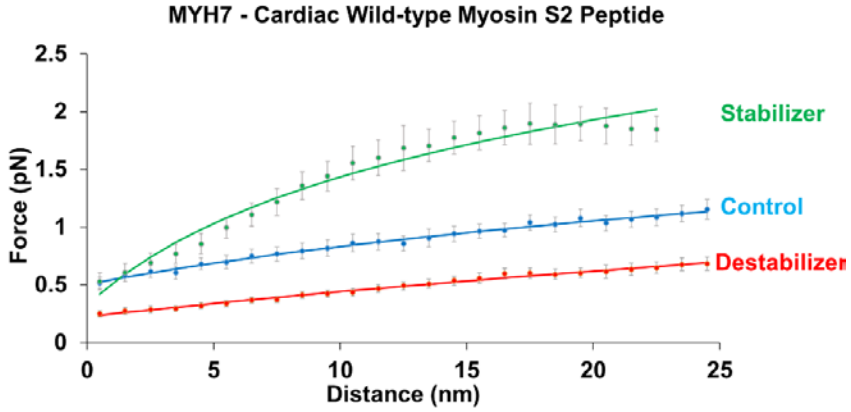

Figure 3.7: The GFS results of MYH7 isoform. Force-distance graph of uncoiling a single molecule of cardiac muscle myosin S2 wild-type isoform, MYH7, in presence of anti-S2 peptides. (Green) Force-distance graph of uncoiling a single molecule in presence of the stabilizer peptide (n=19). (Blue) Force-distance graph of uncoiling a single molecule (control; n=21). (Red) Force-distance graph of uncoiling a single molecule in presence of the destabilizer peptide (n=17)

Next experiment was performed by treating both the coverslip and silica beads with the monomers of cardiac muscle myosin $S2^{pep}$, further allowing dimerization of the monomers to allow the suspension of myosin $S2^{pep}$ between coverslip and silica bead of GFS. Later these S2 dimers were treated with anti-S2 peptides. From the force-distance graph, the force required to uncoil cardiac muscle myosin S2 molecule for a length of 10 nm in absence of anti-S2 peptides was $8.63\times10^{-1} \pm 7.45\times10^{-2}$ pN with R value of 0.98 (Figure 3.7). In presence of anti-S2 peptides (stabilizer and destabilizer respectively) the force required was $1.55 \pm 1.46\times10^{-1}$ pN with R value of 0.98 and $4.36 \times10^{-1} \pm 3.30\times 10^{-2}$ pN with R value of 0.98 (Figure 3.7). The stabilizer anti-S2 peptide increased the amount of force required to uncoil the myosin S2 coiled coil by

1.80 times and an opposite effect observed with the treatment with the destabilizer peptide, the amount of force required decreased by 1.98 times (Table 3.5).

	A (pN)	C (pN)	R	X (nm)
MYH7 - Control	2.25E-01 ± 2.38E-02	4.06E-01 ± 6.09E-02	0.88	0-25
MYH7 + Stabilizer	4.71E-01 ± 3.61E-02	4.16E-01 ± 8.47E-02	0.94	0-25
MYH + Destabilizer	1.32E-01 ± 1.30E-02	1.86E-01 ± 3.12E-02	0.91	0-25
ΔE930	1.48E-01 ± 1.55E-02	1.31E-01 ± 3.87E-02	0.89	0-25
ΔE930 + Stabilizer	2.98E-01 ± 3.37E-02	4.11E-01 ± 5.74E-02	0.93	0-25
MYH11 + Control	1.24E-01 ± 7.80E-03	1.58E-01 ± 1.92E-02	0.96	0-25
MYH11 + Stabilizer	1.32E-01 ± 9.69E-03	1.75E-01 ± 2.35E-02	0.94	0-25
MYH11+Destabilizer	1.63E-01 ± 1.60E-02	1.71E-01 ± 3.94E-02	0.90	0-25
MYH2 + Control	1.44E-01 ± 1.33E-02	9.85E-02 ± 3.17E-02	0.92	0-25
MYH2 + Stabilizer	2.47E-01 ± 2.50E-02	1.49E-01 ± 6.22E-02	0.89	0-25
MYH2 + Destabilizer	3.44E-02 ± 6.16E-03	1.23E-01 ± 1.53E-02	0.76	0-25

Table 3.5: Summary of fitted parameters for GFS experiments correlated with the thermodynamic equation.

The force-distance data is fit to the equation as described previously (Singh, R.R. *et al.*, 2018). The deviation in the force fit for the myosin molecule with the stabilizer and the destabilizer was expected since the binding of the stabilizer to the myosin coiled coil would alter the entropy change in parameter a and binding of the destabilizer to the myosin S2 coiled coil would alter the enthalpy change in parameter c of the logarithmic force fit. The results confirmed

that mechanical stability of MYH7 peptide is increased and decreased with respective anti-S2 peptides.

Fitted parameters in $F = A \ln (x + B) + C$ for the GFS data can be interpreted as $A = vkT$ in which k is Boltzmann's constant (the ideal gas law constant divided by Avogadro's number), T is absolute temperature (typically in Kelvin), and v is a proportionality constant (it appears to be equal to the inverse of the persistence length). The persistence length is a measure of stiffness, but the persistence length extracted from the "A" term is measured perpendicular to the length of the polymer which might make it somewhat different from normal persistence length measurements. Parameter "A" is inversely proportional to this stiffness. The "B" parameter is the linker length in attaching the peptides to the surfaces. The "C" parameter is a measure of change in enthalpy (H) with extension (x) such that $c = -\int dH/\int dx$, and is assumed to be constant with extension. This term would most closely be related to the number of hydrogen bonds that break during extension. In GFS experiments with small peptides, B was zero since a chemical linker was used to attach the peptides to the glass bead and the coverslip unlike actin in full length myosin control experiment mentioned above (figure 3.6). Thus, the force length data was fit to the $F = A \ln (x) + C$. Summary of fitted parameters for GFS experiments correlated with the thermodynamic equation is added to table 3.5. The stabilizer affects entropy (A) and only has a significant effect on enthalpy (C) in the case of the ΔE930. The destabilizer also affects entropy, but it may have a significant effect on enthalpy in the case of the cardiac muscle myosin S2 isoform but not the skeletal muscle myosin S2 isoform. This is in contrast to MyBPC which primarily affected enthalpy, so MyBPC seems to have a different thermodynamic mechanism than the stabilizer.

3.2.2 Stabilizer Peptide has an Impact on MYH7 Mutant Peptide

GFS assay was further performed to test the mechanical stability of cardiac muscle myosin S2 carrying an FHC mutant ΔE930. The mechanical stability of cardiac muscle myosin S2 with ΔE930 mutant was found to be 2.10 times unstable compared to wild type cardiac muscle myosin S2 (Table 3.6). Later the ΔE930 dimer were treated with the stabilizer peptide to increase the stability of an unstable ΔE930 dimer. The force required to uncoil the ΔE930 in presence of stabilizer was greater compared to that in absence of stabilizer (Figure 3.8).

From the force-distance graph, the force required to uncoil ΔE930 myosin S2 molecule for a length of 10nm in absence of the stabilizer peptide was $4.11 \times 10^{-1} \pm 2.97 \times 10^{-2}$ pN with R value of 0.98 (Table 3.6). In presence of the stabilizer peptide the force required was $1.07 \pm 8.28 \times 10^{-2}$ pN with R value of 0.98 (Table 3.6). The stabilizer peptide increased the amount of force required to uncoil the myosin S2 coiled coil by 2.60 times. The results indicate the mechanical stability of ΔE930 dimer is increased in presence of the stabilizer peptide.

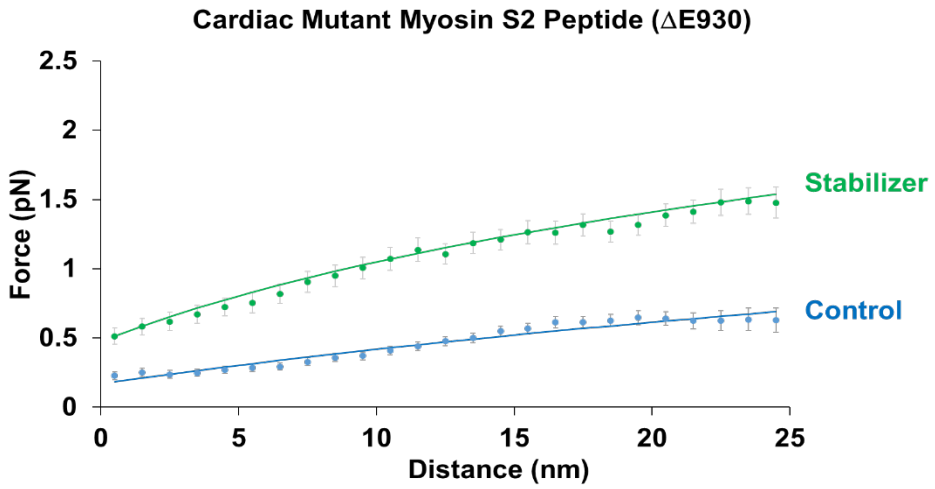

Figure 3.8: The GFS results of mutant MYH7 isoform (ΔE930). Force-distance graph of uncoiling a single molecule of cardiac myosin S2 mutant peptide isoform, MYH7, in presence of anti-S2 peptide. (Green) Force-distance graph of uncoiling a single molecule in presence of the stabilizer peptide (n=27). (Blue) Force-distance graph of uncoiling a single molecule (control; n=28).

3.2.3 Anti-S2 Peptides have an Impact on MYH2

Furthermore, the skeletal muscle myosin $S2^{pep}$ (MYH2) molecule was treated with anti-S2 peptides. GFS was performed to uncoil the myosin dimer as a single molecule treated with or without anti-S2 peptides. The force required to uncoil the skeletal muscle myosin S2 molecule in presence of the stabilizer and the destabilizer was greater and smaller respectively compared to that in absence of the stabilizer or the destabilizer (Figure 3.9).

From the force-distance graph, the force required to uncoil the skeletal muscle myosin S2 molecule for a length of 10 nm in absence of anti-S2 peptides was $4.50 \times 10^{-1} \pm 5.56 \times 10^{-2}$ pN with R value of 0.98 (Table 3.6). In presence of the stabilizer peptide the force required was $6.28 \times 10^{-1} \pm 4.32 \times 10^{-2}$ pN with R value of 0.98 and in presence of the destabilizer peptide force required was $1.84 \times 10^{-1} \pm 4.00 \times 10^{-2}$ pN with R value of 0.99 (Table 3.6). The stabilizer anti-S2 peptide increased the amount of force required to uncoil the skeletal muscle myosin S2 coiled coil by 1.40 times and an opposite effect was observed with the treatment of destabilizer peptide, the amount of force required decreased by 2.45 times. The results indicate that mechanical stability of skeletal muscle myosin S2 can also be altered in similar trend as that of cardiac muscle myosin $S2^{pep}$ with the anti-S2 peptides.

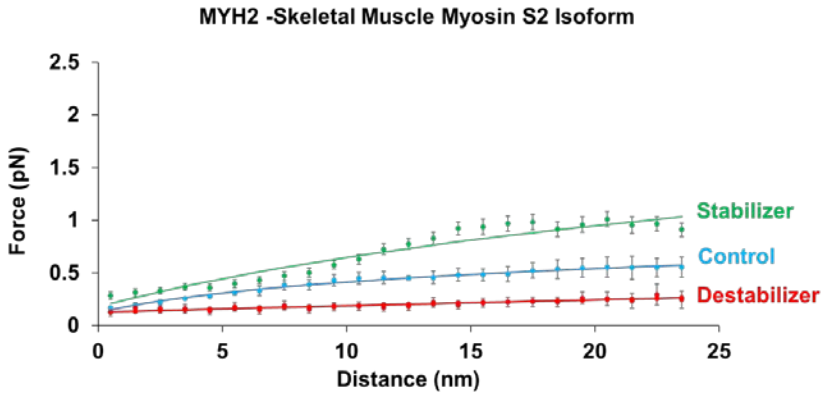

Figure 3.9: The GFS results of MYH2 isoform. Force-distance graph of uncoiling a single molecule of the skeletal myosin S2 peptide isoform (MYH2) in presence of anti-S2 peptides. (Green) Force-distance graph of uncoiling a single molecule in presence of the stabilizer peptide (n=24). (Red)

Force-distance graph of uncoiling a single molecule in presence of the destabilizer peptide (n=23) (Blue) Force-distance graph of uncoiling a single molecule (control; n=22).

3.2.4 Anti-S2 Peptides have No Impact on MYH11

In GFS assay, the results similar to FRET experiments were observed. GFS was performed to uncoil the myosin dimer as a single molecule treated with or without of anti-S2 peptides. This test compared the stability and instability of smooth muscle myosin $S2^{pep}$ to control force distance curve. The results indicate an insignificant change in the force distance curve for a single molecule of smooth muscle myosin S2 dimer and smooth muscle myosin S2 dimer treated with anti-S2 peptides (Figure 3.10). The force required to uncoil the smooth muscle myosin S2 to a length of 10 nm was similar (Table 3.6), and student's test on each compared pair of the curve fitted parameters did not detect a statistically significant difference ($p > 0.05$). Therefore, it could be concluded that the stabilizer and the destabilizer do not have an impact on mechanical stability of smooth muscle myosin S2 peptide.

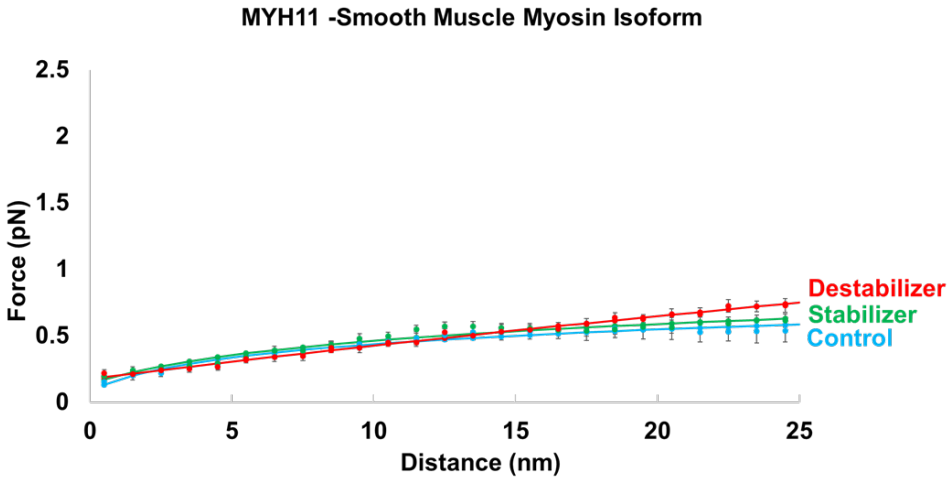

Figure 3.10: The GFS results of MYH11 isoform. Force-distance graph of uncoiling a single molecule of smooth myosin S2 peptide isoforms (MYH11) belonging to myosin heavy chain family in presence of anti-S2 peptides. (Green) Force-distance graph of uncoiling a single molecule in presence of stabilizer peptide (n=19). (Red) Force-distance graph of uncoiling a single molecule in presence of destabilizer peptide (n=19) (Blue) Force-distance graph of uncoiling a single molecule (control; n=14).

Experiment	Length (nm)	Force (pN) ± SEM	No. of molecules	Correlation Coefficient (R)
Smooth Myosin S2	10	4.61 E-01 ±4.25E-02	14	0.99
Smooth Myosin S2 with Stabilizer	10	4.96 E-01 ±7.60E-02	19	0.92
Smooth Myosin S2 with Destabilizer	10	4.51E-01 ±2.98E-02	19	0.93
Skeletal Myosin S2	10	4.50 E-01± 5.56E-02	22	0.98
Skeletal Myosin S2 with Stabilizer	10	6.28 E-01 ±4.32E-02	24	0.98
Skeletal Myosin S2 with Destabilizer	10	1.84 E-01 ±4.00E-02	23	0.99
Cardiac Myosin S2	10	8.63 E-01±7.45E-02	21	0.98
Cardiac Myosin S2 with Stabilizer	10	1.55 E+00±1.46E-01	19	0.98
Cardiac Myosin S2 with Destabilizer	10	4.36 E-01± 3.30E-02	17	0.98
Cardiac Myosin S2 Mutant, ΔE930	10	4.11 E-01±2.97E-02	28	0.98
Cardiac Myosin S2 Mutant, ΔE930 with Stabilizer	10	1.07 E+00±8.28E-02	27	0.98

Table 3.6: Summary of myosin S2 molecular uncoiling length measured with GFS in presence and absence of anti-S2 peptides for all myosin S2 Isoforms and FHC mutant

Stabilizer peptide is specific to cardiac muscle myosin S2 and skeletal muscle myosin S2 peptides. Striated muscles are 87% identical and cardiac muscle myosin S2 and smooth muscle myosin S2 peptides are only 40% identical. Difference of 60% in amino acid sequences is the reason stabilizer has no effect on smooth muscle myosin $S2^{pep}$. It seems like the stabilizer increased the stiffness and had a little effect on H-bonds. Thus, cardiac muscle myosin S2 sequence is stiffer than the skeletal and smooth muscle peptides. The destabilizer also increases stiffness, but greatly reduces the number of H-bonds that need to be broken during extension. Statistical significance were measured using Wilcoxon-Mann-Whitney test; which is a nonparametric test of t-test (Table 3.7).

		P-value (t-test)	P-value (Wilcoxon-Mann-Whitney)
Skeletal			
	Control vs. Stabilizer	<0.001	0.0001
	Control vs. Destabilizer	0.0001	<0.0001
	Stabilizer vs. Destabilizer	<0.0001	<0.0001
Cardiac			
	Control vs. Stabilizer	<0.0001	0.0001
	Control vs. Destabilizer	<0.0001	<0.0001
	Stabilizer vs. Destabilizer	<0.0001	<0.0001
ΔE930			
	Control vs. Stabilizer	<0.0001	<0.0001
Smooth			
	Control vs. Stabilizer	0.7595	0.0821
	Control vs. Destabilizer	0.4895	0.3147
	Stabilizer vs. Destabilizer	0.9049	0.7543

Table 3.7: Summary of P-values of t-test and Wilcoxon-Mann-Whitney test

CHAPTER 4

DISCUSSION

4.1 Myosin Subfragment 2 Regulates the Availability of Myosin Subfragment 1

This study focused mainly on how stability of myosin S2 structure could be altered or changed using small peptide fragments but the emphasis being that myosin S2 regulates the availability of myosin S1 heads to actin thin filaments thus, in retrospect controlling or regulating the amount of contraction in the muscle sarcomere. There has been evidence for how muscle myosin S2 contribute in regulating the myosin S1 heads in striated and non-striated muscle.

There has been very strong evidence where myosin S2 allows for the myosin S1 heads to fold back and rest on the myosin S2 thus appearing to be resting on the backbone of the myosin thick filament. For the smooth muscle it is pretty evident that myosin S1 heads are controlled by activation and inactivation of myosin light chain by myosin light chain kinase so when the myosin light chain is dephosphorylated myosin S1 heads are folded back on to the myosin S2 **(**Figure 4.1). Change in calcium levels within thick filament of smooth muscle initiates muscle contraction. This change in calcium activates calmodulin by calcium binding to it which leads to activation of myosin light chain kinase (Trybus *et al.*, 1982). Calcium-calmodulin complex activates myosin light chain kinase and myosin light chain phosphatase dephosphorylates the myosin light chain (Trybus *et al.*, 1982).

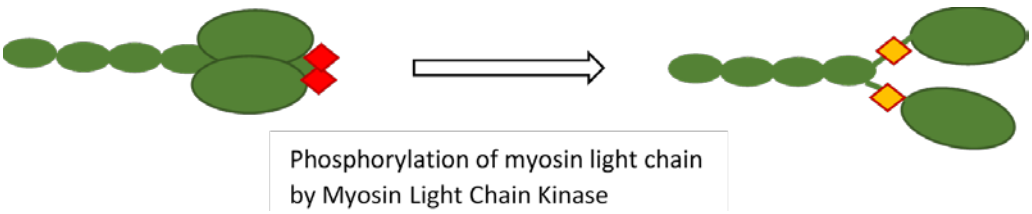

Figure 4.1: Phosphorylation (yellow) of myosin light chain from dephosphorylated one (red) in Smooth muscle myosin by myosin light chain kinase.

This regulation of myosin S1 heads in smooth muscle could be due to involuntary control of these smooth muscles requiring a synchronous contraction and relaxation to allow for the essential functions controlled by smooth muscles for example peristalsis of intestine (Clinton, W. 2003). Thus, myosin S2 along with myosin light chain kinase plays an important role of regulating the myosin S1 heads. Another study where sedimentation of smooth muscle myosin gave two structures namely 6S and 10S, here 10S represents myosin S1 heads folded on to its tail domain (Trybus *et al.*, 1982).

However, for the skeletal muscle system this activation and deactivation of myosin S1 heads by light chain kinase has not been direct. The sedimentation and viscosity experiments looking into the assembly of the myosin minifilaments in skeletal muscle myosin displayed the same 10S and 6S population (found earlier in smooth muscle) representing the dimer and the monomer respectively for myosin (Reisler *et al*., 1986). The 6S and 10S population were found to be in equilibrium with each other stating that these were initial states of assembly for myosin minifilaments (Reisler *et al*., 1986). The 10S myosin population found in the skeletal system, similar to that of smooth muscle, provided that necessary evidence that myosin heads in the skeletal system would probably undergo a bent conformation.

There has been evidence of myosin S1 heads folding back on to the myosin S2 in insect skeletal muscle and chimeras with different light chains. Electron micrographs from Elliott *et. al*; 1978 (Elliott *et al*., 1978) show that myosin S1 heads of skeletal muscles fold back on to its extensive tail. Another study where chimera of HMM from skeletal muscle myosin associated with smooth muscle light chain allowed for the skeletal S1 heads to fold back on to the available S2 region (Sata *et al*., 1997). The theory being that the light chain of the smooth muscle myosin allows for the S1 heads to fold back and rest on to the myosin S2 (Elliott *et al*., 1978). In a study

where overexpression of calcium-calmodulin dependent skeletal myosin light chain kinase allowed for increased force output in fast skeletal muscle fibers (Gittings *et al*., 2015; Ryder *et al*., 2007; Stull *et al*., 2011).

Lately, atomic model studies and cryo-electron micrographs from an invertebrate insect skeletal muscle show that myosin S1 heads can fold back and rest on to the myosin S2 where there is no smooth muscle light chain (Sugi *et al*., 1992). This folding back of myosin S1 heads on to the myosin S2 is related to myosin S1 heads being inactive or in switched off state. The inactivation of myosin S1 heads by folding back on to the myosin S2 have been aided by myosin light chain in smooth muscle. The cardiac myosin light chain kinase has also been found to phosphorylate not only cardiac myosin regulatory light chain but also the cardiac troponin I. The phosphorylation of these two proteins allowed for an increased contractility in cardiac muscle fibers, and it has also been shown to attenuate the cardiac hypertrophy (Chang *et al*., 2016; Sevrieva *et al*., 2020).

To add to this, recently it has been shown that also the N terminal of myosin binding protein C for skeletal and cardiac muscle allows for the inactivation of myosin S1 heads (Singh *et al*., 2017; McNamara *et al*., 2019). The atomic model prediction from Spudich lab speculates that both N terminal cardiac myosin binding protein C and cardiac myosin regulatory light chain interact with each other at the cardia myosin S2 to allow for the myosin S1 heads fold back in to its switched off state (Nag *et al*., 2017). For the myosin binding protein C in skeletal muscle the study showed that the inactivation of heads or low force motility of actin thin filaments was occurring due to binding of myosin binding protein C. The force spectroscopy data showed that myosin S2 was stabilized by the myosin binding protein C. Thus, stating that a molecule or a compound which would increase the stability of myosin S2 would in turn decrease the amount of

force produced by S1 heads. Stability of S2 has been studied previously where antibody to the entire myosin S2 would decrease contractile kinetics and on the other hand where S2 coiled coil was destabilized by laser temperature jump studies resulted in an elevated contractile kinetics (Davis *et al*., 1998; Chang *et al*., 2016).

We have discussed about how S2 regulates the S1 heads in smooth and skeletal muscle. There has been strong evidence that S2 also regulates the S1 heads with the help of cardiac myosin binding protein C in cardiac muscles. Cardiac myosin binding protein C bound to myosin S2 allows for myosin S1 heads to be in their switched off state or also called the super relaxed state (SRX). However, when this cardiac myosin binding protein C is either phosphorylated or has any FHC mutations it allows the myosin S1 heads to go from switched off to a switched on state or to go from super relaxed state to disordered relaxed state (DRX). The theory being that this increased disordered relaxed state of myosin leads to a hypercontractile sarcomere ultimately leading to FHC. To add to the importance of myosin S2 there is a cluster of FHC mutations close to proximal region of myosin S2 which interacts with N-terminal cardiac myosin binding protein C. There has been another theory where a mathematical model predicts that the transition of myosin S1 heads from SRX to DRX in cardiac muscle is force dependent or the passive stiffness of thick filament which contributes to length dependent activation of the cardiac sarcomeres (Campbell *et al*., 2018). This model prediction also answers for constant contraction and relaxation in cardiac muscles with minimal calcium requirement is achieved by modulating the length of the sarcomeres leading to activation and deactivation of myosin heads (Campbell *et al*., 2018). So to put the length activation in terms of myosin S1 heads resting on S2, if the sarcomere length is increased the S2 coiled coil would be stretched along the axis of thick filament, thus allowing the S1 heads to dissociate from S2 and when they are relaxed the S2 pops away from

thick filament allowing the S1 heads to fold back onto the S2. The recent small angel x-ray studies involving the contracting cardiac muscle from rats indicate that peak force during contraction occurs at the C-zone of the sarcomere and during relaxation the myosin S1 heads are folded back and more helically ordered in C-zone supporting the hypothesis of S1 heads folding back on to the S2 or the backbone of thick filament (Brunello *et al*., 2020).

With these properties of myosin S2 in mind where a stable S2 would result in an inactive myosin or switched off myosin and a destable myosin S2 would result in much active myosin or switched on, the Root lab created two peptides specific to cardiac muscle myosin S2, one which could increase the stability of myosin S2 and the other could decrease it. We tested the stability of myosin S2 coiled coil using FRET and GFS assays, we also verified the specificity of these peptides to cardiac muscle myosin S2 by performing control experiments with myosin S2 of skeletal and smooth muscle origin. Next, we also answered if FHC mutations would decrease the stability of cardiac muscle myosin S2 coiled coil and whether the stabilizer peptide would increase the stability across these FHC mutant cardiac myosin S2. The main goal is to regulate myosin S1 heads activity by altering the stability of myosin S2 coiled coil using the designed peptides. Thus, in case of a FHC sarcomere which has hyperactive myosin S1 heads, we could increase the stability of myosin S2 and thus decrease the population of hyperactive S1 heads and help rescue FHC phenotype.

4.2 Fluorescence Resonance Energy Transfer

The major focus of the study was to efficiently measure the effect of a FHC mutation in the myosin S2 and how would it effect the tertiary structure of myosin S2 coiled coil. In the pursuit of the study we also had computationally designed anti-S2 peptides which could enforce and stabilize the myosin S2 coiled coil, while the other could destabilize the coil. These anti-S2

peptides were designed specific to myosin S2 of the MYH7 isoform, hence the next discourse was to test the specificity of these ant-S2 peptides on myosin S2 of skeletal MYH2 and smooth MYH11 muscle isoforms. To embark on this study, FRET was used to test how a FHC mutation could affect the myosin S2 coiled coil. FRET allowed for the distance measurements within labeled myosin S2 coiled coil peptides. For FRET, a myosin S2 monomer was labelled with terbium chelate donor and another myosin S2 monomer was labelled with FITC as acceptor. When these labelled myosin S2 monomers were allowed to dimerize, and if they are dimerized the donor and acceptor probe are in close proximity of each other. And when the donor probe is excited at its respective wavelength of light the energy emitted by donor would excite the acceptor probe and in turn emitting energy at different wavelength of light detected by a photomultiplier tube. Another indication of dimerization would be also a decrease in donors' lifetime when excited due to nearby acceptor probe (fluorescein) able to accept the energy being emitted by donor. For lower or dampened dimerization of myosin S2, the donors' lifetimes would remain constant or minimal decrease due to absence of acceptor probe nearby. Calculation of efficiency of energy transfer was also possible for probes that are within range of 1 nm to 10 nm (Hussain, S. 2009).

First, the stability for coiled coil of cardiac muscle (MYH7) myosin S2 isoform and FHC mutants (E924K & ΔE930) were tested by dilution. The mutants ΔE930 and E924K were decreased 2.67 and 2.11 fold, respectively, in affinity to form a dimer compared to wild type stating the mutants were unstable and could not form an efficient dimer (Table 3.3). In presence of the stabilizer, affinity of the ΔE930 and E924K increased by 10.23 and 0.60 fold respectively, stating that the stabilizer peptide had more impact on ΔE930 and improving dimerization (Table

3.3). Thus, interaction of the stabilizer with FHC mutants (E924K & ΔE930) strongly stabilized the dimer formation and settled the structure of targeted region of muscle myosin S2.

Second, impacts of the destabilizer peptide on muscle myosin S2 isoforms were tested. The destabilizer peptide had binding affinity of 9.97×10^{-1} μM to MYH7 isoform, 1.00 μM to MYH2 isoform, and no impact on MYH11 (Table 3.3). Interaction of the destabilizer peptide with muscle myosin S2 peptides of MYH7 and MYH2 strongly destabilized the dimer formation and disrupted the coiled coil formation (Figures 3.1 and 3.4C).

Our FRET results highly support the hypothesis that different concentrations of the stabilizer and the destabilizer peptides change the efficiency of energy transfer between the two helices of the coiled coil myosin S2 in muscle myosin S2 isoforms and FHC mutants (E924K & ΔE930). The FRET assay also showed that coiled coil structure stability in lieu of FHC mutation could be efficiently measured and how a small compound or peptide in this case could affect the stability. We further used the FRET system to analyze the change in stability of the coiled coil structure in presence and absence of the anti-S2 peptides. The results from FRET confirmed that binding of the stabilizer peptide enhanced the stability and binding of the destabilizer peptide increased flexibility of targeted myosin S2 region of striated muscles. Furthermore, Increase or decrease in lifetime of donor probes with increase in concentrations of the anti-S2 peptides strongly supported interaction of the anti-S2 peptides with targeted region.

FRET experimental data confirmed that FHC mutations (E924K & ΔE930) have more flexible coiled coil myosin S2 structures compared to wild type, thus these mutations impact dimer formation and destabilize the coiled coil structure of the targeted region. FHC mutations disrupt α-helices of the coiled coil structure which leads to instability in the proximal region of myosin S2. Increase in lifetime donor of these mutations indicated energy transfer between donor

to acceptor probe was decreased due to a decrease in peptide dimer concentration. Furthermore, an increase in dissociation constant demonstrated a decrease in dimer formation of FHC mutants compared to wild type. However, in the presence of the stabilizer peptide, improvements in coiled coil formation were observed. A decrease in the donor lifetime of these mutations was detected as energy transfer between donor and acceptor probe was increased due to an increase in peptide dimer concentration. Dissociation constants of mutants treated with stabilizer peptide were almost the same as the dissociation constant of the cardiac muscle myosin S2 wild type peptide.

4.3 Gravitational Force Spectroscopy

Gravitational Force Spectroscopy is a single molecule force spectroscopy which allows one to measure the absolute molecule length and the mechanical stability of the same molecule. The spectroscopy utilizes gravitational force to pull the molecule which thus gives the information about how much force is required to stretch, extend or pull the molecule to a certain length. GFS was used to show that myosin exhibits a much more unstable coiled coil at the myosin subfragment 2 compared to light meromyosin which confirms with the previous study published on the stability of light meromyosin. GFS also showed that when myosin S2 is treated with whole length skeletal myosin binding protein-C, it would stabilize the coiled coil structure by three fold (Singh *et al*., 2017). Hence GFS was used to test stability and flexibility of all muscle myosin S2 isoforms and FHC mutation (ΔE930) for the cardiac muscle isoform treated with and without anti-S2 peptides. (Singh *et al*., 2017). The results from these GFS experiment would validate and supplement the data obtained from the FRET studies. Uncoiling of muscle myosin S2 isoforms and mutations were demonstrated in presence and absence of equimolar of anti-S2 peptides to show their effect on stability of muscle myosin S2 coiled coil isoforms. Upon

treatment of stabilizer peptide to myosin S2 and if it increased the stability of the myosin S2 molecule it would be confirmed by the force required to pull the molecule to a constant distance is higher when compared to force required to pull the molecule to same distance with no treatment. As for the destabilizer peptide, if there is an effect it would lower the amount of force required to pull the myosin S2 molecule to the same constant distance.

The forces required to uncoil muscle myosin S2 dimers of MYH7, MYH11, MYH2, and FHC mutant (ΔE930) were measured. The force required to uncoil muscle myosin S2 peptides in the presence of the stabilizer peptide was more than in its absence in muscle myosin S2 isoforms of MYH7 (1.80 fold higher), MYH2 (1.40 fold higher), and ΔE930 (2.60 fold higher) and no change for MYH11 compared to control. The binding of the stabilizer peptide to the myosin S2 molecule had a stabilizing impact. This impact on MYH7, MYH2, and mutants is due to specificity of this designed peptide to this region of muscle myosin S2 which stabilizes this region (Singh *et al*., 2017). Furthermore, the force required to uncoil muscle myosin S2 in presence of the destabilizer was less than in its absence in both MYH7 (2.00 fold lower) and MYH2 (2.5 fold lower) but the same for MYH11 compared to control. The binding of the destabilizer peptide to the myosin S2 molecule had a destabilizing effect and enhance flexibility of this region. In addition, this flexibility is due to specificity of this designed peptide to this region of muscle myosin S2.

The GFS was performed on a single molecule of muscle myosin S2 of different muscle myosin S2 isoforms in presence and absence of anti-S2 peptides. This assay demonstrated stability of MYH2, MYH7, and mutants in presence of the stabilizer peptide and enhancement of flexibility in MYH2 and MYH7 in presence of the destabilizer peptide. Specificity of anti-S2 peptides altered the stability and flexibility of muscle myosin S2 isoforms. Furthermore, this

assay demonstrated that anti-S2 peptide have no impact on increasing stability or enhancing flexibility of muscle myosin S2 isoform of MYH11.

4.4 Comparison of FRET with GFS

The FRET and GFS assays had similar results. First, dissociation constants (binding affinity) and forces required to uncoil muscle myosin S2 isoforms were measured. Second, the impacts of anti-S2 peptides were tested. In both assays, the stabilizer peptide had impacts on MYH7, MYH2, and FHC mutants (E924K & ΔE930). The stabilizer peptide enhanced dimer formation and stabilizing properties. The destabilizer peptide had an effect on the muscle myosin S2 region of MYH7 and MYH2 by enhancing the flexibly. In both assays, anti-S2 peptide did not have any impact on MYH11 due its differences in amino acid residues within this region of muscle myosin S2 being compared to the striated muscle myosin S2 region.

Anti-S2 peptides are more effective on striated muscle system, cardiac and skeletal, and they were not as effective on non-striated or smooth muscle. Both anti-S2 peptides were designed against cardiac muscle myosin S2 peptide region 921 to 939. The stabilizer peptide is a polycation compound that is rich in positive charge. This polycation compound forms a strong binding to the glutamate rich region of cardiac muscle myosin S2 isoform and forms a sturdy interaction. The skeletal muscle myosin S2 isoform with being 81% identical to the cardiac muscle myosin S2 isoform has similar binding affinity to the stabilizer peptide. Valine, threonine, alanine, and isoleucine are the amino acid that are different between the two striated muscle myosin S2 isoform. However, there are not significant amino acid properties changed within the skeletal and cardiac muscle myosin S2. Additionally, in presence of the stabilizer peptide, the skeletal muscle myosin S2 isoforms requires 1.40 fold more force to uncoil the dimer while the cardiac muscle myosin S2 isoforms required 1.80 fold more force compared to

their controls. The GFS states that stabilizer peptide was more effective to the cardiac myosin S2 when compared to skeletal myosin S2. The binding affinity indicated by the dissociation constant showed that K_d of stabilizer peptide was higher for skeletal myosin S2 while significantly lower for the cardiac myosin S2. On the other hand, smooth muscle myosin S2 isoform with being only 41% identical to the cardiac muscle myosin S2 isoforms has no binding affinity to the stabilizer. Within the smooth muscle amino acids, due to glutamine, amino acid with polar uncharged side chain, and leucine, amino acid with hydrophobic side chain, the binding does not form at all. Also, with GFS there was minimal to no effect observed on the change in force required to uncoil the smooth muscle myosin S2.

Similarly, the destabilizer peptide affected the striated muscle system (cardiac and skeletal) but had no effect to the smooth muscle system. The destabilizer, 19 residue peptide, designed computationally against cardiac muscle myosin S2 region 921 to 939. This peptide has high binding affinity to this region of myosin. One molecule of the destabilizer peptide would bind to one α-helix of the muscle myosin S2 coiled coil and disrupts the natural coiled coil formation. Effectiveness of the destabilizer peptide on the skeletal muscle myosin S2 isoform was similar. However, between the two striated muscles, dissociation constant of the destabilizer peptide bound to skeletal muscle myosin S2 isoform was lower compared to the cardiac muscle myosin S2 isoform. This high binding affinity could be due to change from non-critical amino acid to a critical amino acid (asparagine $\rightarrow$threonine). Skeletal muscle myosin S2 isoform lacks asparagine and methionine which are available in cardiac muscle myosin S2 isoform and these two amino acids have and extra chargeable amino group which are lacking in skeletal muscle myosin S2 isoform which that could be reason for the change in affinity of the destabilizer peptide towards skeletal muscle myosin S2 isoform. Also, in presence of the destabilizer, the

skeletal muscle myosin S2 isoform required 2.5 fold less force to uncoil the dimer compared to the cardiac muscle myosin S2 isoform that required 2 fold less force compared to their non-treated controls.

Smooth muscle myosin is less than 50% identical to its skeletal and cardiac isoforms. Myosin S2 coiled coil regions of smooth muscle do not have the same distribution of polar and nonpolar amino acids for its heptad repeats compared to skeletal and cardiac muscle myosin S2. However, the skeletal and cardiac muscle myosins, being more than 80% identical, have the same distribution of polar and non polar amino acids in its heptad repeats to form the myosin S2 coiled coil. Hence the computationally designed stabilizer and destabilizer had an impact on skeletal and cardiac muscle myosin and not that on smooth muscle. Another mode of difference between and non-striated (smooth) and striated (cardiac and skeletal) muscle is the sequestration of myosin S1 heads on to the myosin S2. In smooth muscle the dephosphorylated myosin regulatory light chain is sufficient to sequester the myosin S1 heads. However for skeletal and cardiac system the sequestration of myosin S1 heads actively occurs in the C zone by dephosphorylated myosin binding protein C. Myosin light chain kinase is essentially required to activate the myosin S1 heads in smooth muscle, however no such system is required in skeletal and cardiac muscle intrinsically, even though myosin light chain kinase do have an effect on these muscles. The difference of charges seen in myosin S2 region of striated and non-striated could be that striated muscles have a system which does not require active sequestration of myosin S1 heads throughout the sarcomere of muscles but concentrated in certain zone like C zone is cardiac sarcomere. And non-striated muscle requires synchronous activation and deactivation of myosin S1 heads which could be chalked up to smooth muscle function being under involuntary control for the essential function performed by the smooth muscle.

Heterodimers of the mutant and wild type would behave more like the homodimer of the mutants rather than the homodimer of wild type due to one strand of α-helix being defective. The coiled coil is formed by the repeating units of the heptad repeats of two single α-helix, where a and d position are hydrophobic residues while the f position is hydrophilic or charged residue. In case of the heterodimer where one α-helix is of wild type while the other helix has a FHC mutation, as result of which the heptad repeat of the FHC mutant will be out of sync and when the coiled coil is formed between these two the coiled coil would be staggered and unstable. The binding cannot hold together to form a proper coiled coil; thus, it would cause instability of this region and hyper contractility. On the other hand, the homodimer of the FHC mutants would be unstable compared to its heterodimer and wild type counterpart.

In this study, I tested the stability of E924K and ΔE930 FHC mutations, and FRET and GFS data corroborated the hypothesis where both the FHC mutations were highly unstable, since in FRET the lifetime signal at donor was higher compared to wild type, and with GFS less force was required to uncoil the FHC mutant dimer when compared to wild type. We also were able to improve the stability of these FHC mutant dimers with the stabilizer peptide. FHC muscle usually demonstrates a hypercontractile nature in sarcomere where the ensemble force is elevated. The use of stabilizer peptide would allow for increased stability of myosin S2 coiled coil and decreased availability of myosin S1 heads thus rescuing the hypercontractile phenotype.

The FHC mutation, R453C, causes hypercontractility (Sommese *et al*., 2013). This hypercontraction is caused by instability of the myosin S2 coiled coil by increasing number of myosin S1 heads available for actomyosin interaction. The stabilizer peptide would be helpful to counteract it by regulating myosin S1 heads available. In addition, R403Q, FHC mutation, results in disarrayed actomyosin interaction which has faster rates of cross-bridge relaxation

(Nag *et al*., 2015; Volkmann *et al*., 2007; Witjas-Paalberends *et al*., 2014). Availability of myosin S1 heads can be controlled by altering stability of myosin S2 coiled coil region. On the other hand, the destabilizer peptide could be useful in a phenotype where the contractile force or the ensemble force of the sarcomere is dampened. Destabilizer can be used in heat failure with reduced ejection fraction or systolic ejection failure or hearts suffering dilated cardiomyopathy. Destabilizer can increase the amount of S1 heads by increasing the flexibility of myosin S2 coiled coil. The stabilizer can also be used in diastolic dysfunction of the heart or heart failure with preserved ejection fraction by decreasing the available S1 heads. The myosin S2 region is an ideal region that can be improved to change the cross-bridge kinetics. For muscles with cross bridge formation deficiencies at this region can be targeted for potential therapeutics. Since both the stabilizer and destabilizer peptide were effective in skeletal muscle system, I can also use them to treat the disorders arising from increased or decreased muscle function in skeletal muscle function. For example, a skeletal myosin binding protein C genetic disorder Distal Arthrogryposis Type 1 results in the hypercontracted state of the limbs and phalanges. In this case I can utilize the property of the stabilizer peptide to improve the hypercontracted state of the skeletal muscles of the limbs. The timing and effective dose of stabilizer peptide needs to be validated but still it could be a viable therapy. While the destabilizer would be effective in disorders arising from muscular dystrophy where the muscle function is attenuated. The treatment of these muscle could allow more myosin S1 heads to be available thus increasing the muscle function in the skeletal muscles. These effects of the therapeutic peptides require efficient testing with right animal models and systemic dosage.

4.5 The Effect of Anti-S2 Peptides on Skinned Human Cardiac Ventricle Muscle Fibers

Most importantly, to substantiate the effect of anti-S2 peptides, our collaborators treated

the human cardiac skinned ventricles muscle tissue and these peptides were able to significantly alter calcium sensitivity and force produced in these cardiac muscle fibers (Bertrand *et al*., 2019). The human cardiac ventricle muscle fibers were skinned to allow to dissolve the cell membrane, now the sarcomeres are easily available to be treated with the anti-S2 peptides. The skinned muscle was then cycled through buffer containing increasing amount of calcium (Stelzer *et al.,* 2006). With the infusion of calcium, the muscle contracts and produces force. The force produced increases with increasing calcium (pCa 6.0 to 5.5) and saturates at calcium concentration at pCa 5.4 and beyond, and maximal at pCa 4.5. The force-pCa curve thus plotted will provide the sensitivity of skinned muscle to calcium at its pCa_{50}. If the force produced is higher at each pCa than its control, the force-pCa curve would shift towards the left of the control thus indicating the higher calcium sensitivity than the control. If the force produced is lower at each pCa than its control, the force-pCa curve would shift towards the right of the control thus indicating the lower calcium sensitivity than the control. The stabilizer was able to decrease the calcium sensitivity in the skinned muscle fibers where more calcium was required to produce the force with increase the concentration of calcium. As expected, the stabilizer was able to decrease the amount of force in human cardiac ventricle. With the destabilizer, an appositive effect was observed where the calcium sensitivity was increased stating that lower amount of calcium was required to produce maximal force, thus the destabilizer was able to increase the amount of force in human cardiac ventricles hence effectively demonstrating the designed and purpose of these anti-S2 peptides and their efficacy to influence the amount of force produces in human cardiac ventricle (Bertrand *et al*., 2019; Stelzer *et al.,* 2006). The effect was seen at both lower and higher sarcomere length (1.9 and 2.3 μM). Cardiac muscle fibers display a length dependent activation where increase in sarcomere length in a muscle fiber increases the amount

of force produced compared to force produced by the same muscle fiber with lower sarcomere length. Even with the increased sarcomere length the anti-S2 peptides was still effective in the skinned cardiac muscle fibers (Bertrand *et al*., 2019). The stabilizer caused a greater effect at longer sarcomere lengths while the destabilizer had a greater impact at shorter sarcomere lengths. Indeed, the pCa_{50} change due to destabilizer was only statistically significant at the shorter sarcomere length. These results are consistent with simulations by published computational models of the sarcomere published by our collaborator Dr. Campbell.

4.6 Conclusions

In conclusion, in presence of the stabilizer peptide, stability of muscle myosin S2 isoforms of MYH7, MYH2, and FHC mutants (E924K & ΔE930) could be altered. In presence of the destabilizer peptide, the flexibility of muscle myosin S2 isoforms of MYH7 and MYH2 could be enhanced. These alterations had an impact on dissociation constant and force required uncoil the dimers.

Both assays show that the stability and flexibility of muscle myosin S2 coiled coil could be altered with a small peptide. The stabilizer peptide improved stability of this region and the destabilizer peptide enhanced flexibility. Increase in dissociation constant and force required to uncoil the muscle myosin S2 peptide, the more stable this region and vice versa, in presence the stabilizer and the destabilizer respectably.

The measured force-distance curves indicate the changes in disorder due to entropy as indicated by extension of molecule, the change in enthalpy remains fairly constant, if this was not the case the graph would not fit the logarithmic GFS curve fit as indicated by the below formula. The stabilizer affects entropy (A) and only has a significant effect on enthalpy (C) in the case of the ΔE930. The destabilizer also affects entropy, but it may have a significant effect

on enthalpy in the case of the cardiac muscle myosin S2 isoform but not the skeletal muscle myosin S2 isoform. This is in contrast to MyBPC which primarily affected enthalpy, so MyBPC seems to have a different thermodynamic mechanism than the stabilizer (Singh *et al*., 2018).

$$F = a \ln (x + b) + c$$

The changes in the stability along the myosin S2 coiled coil should show up as altered or different enthalpy component resulting to deviate from the logarithmic fit of the force-distance curve. The stabilizer peptide thus would increase the enthalpic component and the destabilizer peptide would increase the entropy component of the logarithmic fit for the force curve. Hence the stabilizer peptide would measure a high force fit the same distance and on the other hand the destabilizer would allow the force fit to be lower for the same distance fit.

It has been shown that the myosin S1 heads of an invertebrate skeletal muscle myosin folds back on to the myosin S2 backbone using Cryo-electron microscopy (Woodhead *et al*., 2005; Alamo *et al*., 1973; Pinto *et al*., 2012). The N-terminal region of the muscle myosin S2 region is a key region for myosin S2 heads to bind along with MyBPC (Nag *et al*., 2017). Therefore, one can anticipate that the myosin S2 region regulates the availability of myosin S1 heads by altering their stability and flexibly. A stable myosin S2 leads to a supervised number of S1 heads available and a flexible myosin S2 leads to an increase in availability of myosin S1 heads for actomyosin interaction.

These assays supported importance of the role of myosin S2 coiled coil in striated muscle contraction. Due to the function of myosin S2 coiled coil in actomyosin interaction and contraction, mutations within this region would lead to lethal cardiomyopathies. The proposed anticipation of myosin S1 heads folding back on to the stable myosin S2 coiled coil could be

tested in presence and absence of anti-S2 peptides using techniques such as electron microscopy or cryo-electron microscopy.

A molecular level study helped us better understand stability and flexibility of proximal region of muscle myosin S2 isoforms and FHC mutants (E924K & ΔE930) in presence or absence of anti-S2 peptides. FRET and GFS experiments with synthetic peptides facilitated us with better indulgent of this region. Experimental results bring anticipation that such a small molecule could potentially be an answer to cure this disease and reverse the impact of mutations.

Animal models of wild type and FHC mutant treated with anti-S2 peptides would be an ideal model to better understand actomyosin interaction and test expected results. The FHC human engineered heart tissues would be another probable application to focus on. These peptides could be the answer to the untreatable lethal disease and potential drug. By targeting stability and flexibility of myosin S2 coiled coil, other muscle contraction parts do not have to altered directly. Although targeting muscle myosin S2 coiled coil impacts other parts of muscle contraction such as ATPase activity or availability of myosin S1 heads.

Although there are no compounds to prevent FHC completely, there have been number of non-sarcomeric targets. Non-sarcomeric targets such as calcium signaling, beta-blockers, or the ion channel are ways of preventing FHC progression and they are the current therapeutic therapy for FHC mutations (Tardiff *et al*., 2015). However, these drugs have long term impact and side effects. For example, number of beta-blockers have vasodilating effects and these beta blockers cannot be used for obstructive FHC (Sherrid *et al*., 2016). Alternative to current treatment are our designed stabilizer and the destabilizer peptides. These peptides are specifically designed to myosin coiled coil structure whose specificity and efficacy have been tested. These structural designed peptides are only targeted to bind to muscle myosin in the sarcomere. The designed

peptides have minimal to no binding to non muscle myosin as observed through confocal imaging performed in the lab (Singh *et al*., 2017). The advantages of these designed peptides are that it won't interact or interfere with calcium signaling nor ion channels thus mitigating any side effects as caused by the other ionotropic agents.

This study helps to show that we can use therapeutic agent compounds or small proteins to either target the structure of the sarcomere proteins or protein - protein interaction to rectify the cardiovascular disorders like FHC caused by the mutations within the sarcomere. These structural therapeutics unlike the calcium signaling, beta-blockers, or the ion channel targeting drugs would have less of side effects and much better efficacy.

In summary:

1. FRET and GFS assays demonstrated that both anti-S2 peptides have impacts on the cardiac muscle myosin S2 isoform. In FRET assays, lower lifetime values in presence of the stabilizer and higher lifetime values in presence of the destabilizer were observed. In GFS assays, more force was required to uncoil cardiac muscle myosin S2 isoform in presence of the stabilizer and less force was required to uncoil the dimer in presence of the destabilizer.

2. FHC mutations (E924K and ΔE930) showed higher lifetime values in FRET assays and lower force required to uncoil coiled coil myosin S2 in GFS assays, demonstrating the elevated instability in these FHC mutations. This instability was improved by treating the FHC mutants with stabilizer, as a result lifetime values decreased in FRET assays and more force was required to uncoil FHC myosin S2 coiled coil in GFS assays.

3. FRET and GFS assays also concluded that both anti-S2 peptides have impacts on skeletal muscle myosin S2 isoform. In FRET assays, lower lifetime values in the presence of the stabilizer and higher lifetime values in presence of the destabilizer were seen. In GFS assays,

more force was required to uncoil the cardiac muscle myosin S2 isoform in presence of the stabilizer and less force was required to uncoil the dimer in presence of the destabilizer.

4. FRET and GFS assays also confirmed that both anti-S2 peptides do not have any impact on the smooth muscle myosin S2 isoform. In FRET assays, there was no significant difference in lifetime values in presence or absence of anti-S2 peptides. In GFS assays, there was no significant difference in the force required to uncoil the dimer in presence or absence of the anti-S2 peptides.

In conclusion, the study successfully demonstrated that mechanical stability of myosin S2 coiled coil in striated muscle system can be altered using the S2 specific anti-S2 peptides. Also, the stabilizer anti-S2 peptide was efficacious in increasing the mechanical stability of an already unstable FHC myosin S2 coiled coil. This increased stability might be used to treat the hypercontractile nature of FHC hearts, thus paving a new way to treat the cardiovascular or skeletal muscular disorders by targeting the structural properties of muscle proteins.

REFERENCES

Alamo, L., Wriggers, W., Pinto, A., Bártoli, F., Salazar, L., Zhao, F.Q., Craig, R., and Padrón, R. (2008) Three-dimensional reconstruction of tarantula myosin filaments suggests how phosphorylation may regulate myosin activity. *J Mol Biol.* 384, 780- 797.

Barsheshet, A., Brenyo, A., Moss, A.J., and Goldenberg, I. (2011). Genetics of sudden cardiac death. *Current Cardiology Reports*, 13(5), 364-76.

Bertrand T, Campbell K, Qedan M, Aboonasrshiraz N, Quedan D, Awinda P, Bernardino Schaefer A, Root D. (2019). Anti-S2 Peptides Modulate Myosin Coiled-Coil Structure and Shift Force-pCa Curves in Human Cardiac Muscle. *Biophysical Journal*. 116, 263a

Brunello, E., Fusi, L., Ghisleni, A., Park-Holohan, S. J., Ovejero, J. G., Narayanan, T., and Irving, M. (2020) Myosin filament-based regulation of the dynamics of contraction in heart muscle. *Proc Natl Acad Sci U S A*, 117, 8177-8186

Campbell, K. S., Janssen, P., & Campbell, S. G. (2018). Force-Dependent Recruitment from the Myosin Off State Contributes to Length-Dependent Activation. *Biophysical journal*, *115*(3), 543–553.

Chang, A. N., Mahajan, P., Knapp, S., Barton, H., Sweeney, H. L., Kamm, K. E., & Stull, J. T. (2016). Cardiac myosin light chain is phosphorylated by Ca2+/calmodulin-dependent and -independent kinase activities. *Proceedings of the National Academy of Sciences of the United States of America*, *113*(27), E3824–E3833.

Cho, K.W., Lee, J., and Kim, Y. (2016) Genetic variations leading to familial dilated cardiomyopathy. *Mol Cells. 39*, 722-727.

Cirino, A. L., and Ho, C. (2008). Familial hypertrophic cardiomyopathy overview. *GeneReviews™*,

Clegg, R.M. (1992) Fluorescence resonance energy transfer and nucleic acids, *Methods Enzymol. 211*, 353-388.

Clinton Webb, R. (2003) Smooth Muscle Contraction and Relaxation. *Advances in Physiology Education*. 27:4, 201-206.

Colegrave, M. Peckham, M. (2014). Structural implications of β-cardiac myosin heavy chain mutations in human disease. Anat. *Rec. 297*, 1670–1680.

Cooke, P. (1976) A filamentous cytoskeleton in vertebrate smooth muscle fibers, *J. Cell Biol. 68*, 539–556.

Crilley, J. G., Boehm, E. A., Rajagopalan, B., Blamire, A. M., Styles, P., McKenna, W. J., OstmanSmith, I., and Clarke, K. (2003). Hypertrophic cardiomyopathy due to sarcomeric gene mutations is characterized by impaired energy metabolism irrespective of the degree of hypertrophy. *Journal of the American College of Cardiology*, *41(10)*, 1776-82.

Davis, J.S., and Harrington, W.F. (1998) Force generation by muscle fibers in rigor: a laser temperature-jump study. *Proc Natl Acad Sci U S A. 84*, 975-979.

Ebashi, S., Endo, M. and Ohtsuki, I. (1969) Control of Muscle Contraction. *Q. Rev. Biophys. 2,* 351-384.

Elliott, A., and Offer, G. (1978) Shape and flexibility of the myosin molecule. J. *Mol. Biol. 123,* 505-519.

Erdmann, J., Daehmlow, S., Wischke, S., Senyuva, M., Werner, U., Raible, J., Tanis, N., Dyachenko, S., Hummel, M., Hetzer, R., Regitz-Zagrosek, V. (2003) Mutation spectrum in a large cohort of unrelated consecutive patients with hypertrophic cardiomyopathy. *Clin. Genet. 64,* 339-349.

Fabiato, A. (1988). Computer programs for calculating total from specified free and free from specified total ionic concentrations in aqueous solutions containing multiple metals or ligands. *Methods Enzymol.* 157:378–417.

Förster, T. (1948). Intermolecular energy migration and fluorescence, Annals of Physics, 2, 55 75.

Gittings W, Aggarwal H, Stull JT, Vandenboom R. 2015. The force dependence of isometric and concentric potentiation in mouse muscle with and without skeletal myosin light chain kinase. Can. *J. Physiol. Pharmacol*. 93(1): 23-32

Goldman, Y.E. (1987) Kinetics of the Actomyosin ATPase in Muscle Fibers. *Annu. Rev. Physiol. 49,* 637-654.

Goodson, H.V. and Spudich, J.A. (1993) Molecular Evolution of the Myosin Family: Relationships Derived from Comparisons of Amino Acid Sequences. *Proc. Natl. Acad. Sci. U.S.A. 90,* 659- 663.

Gundapaneni, D., Xu, J., and Root, D.D. (2005) High flexibility of the actomyosin crossbridge resides in skeletal muscle myosin subfragment-2 as demonstrated by a new single molecule assay. *J Struct Biol. 149,* 117-126.

Hill, R. W., Wyse, G. A., & Anderson, M. (2008). Animal physiology. Sunderland, MA: *Sinauer Associates*.

Hussain, Syed Arshad. (2009). An Introduction to Fluorescence Resonance Energy Transfer (FRET). *Energy*. 132.

Huxley, A.F. (1964) Muscle. *Annu. Rev. Physiol. 26,* 131-152.

Huxley, A.F. and Niedergerke, R. (1954) Structural Changes in Muscle During Contraction; Interference Microscopy of Living Muscle Fibres. *Nature 173,* 971-973.

Jean, M. (2003) How to Subdue a Swelling Heart. *Science. 300,* 1492-1496.

Kron, S.J., Toyoshima, Y.Y., Uyeda, T.Q.P., and Spudich, J.A. (1991) Assays for actin sliding movement over myosin-coated surfaces. *Methods Enzymol. 196,* 399-446.

Lymn, R.W. and Taylor, E.W. (1971) Mechanism of adenosine triphosphate hydrolysis by actomyosin. *Biochemistry 10,* 4617–4624.

Maliwal, B.P., Kusba, J., Lakowicz J.R. (1994) Fluorescence energy transfer in one dimension: Frequency-domain fluorescence study of DNA–fluorophore complexes. Biopolymers, 35, pp. 245-255

Marieb, E.N., Smith, L. (12th Edition) Human Anatomy & Physiology Laboratory Manual, *Main Version*.

McNamara, J. Singh, R., & Sadayappan, S. (2019). Cardiac myosin binding protein-C phosphorylation regulates the super-relaxed state of myosin. *Proceedings of the National Academy of Sciences*. 116. 201821660.

Nag, S., Sommese, R.F., Ujfalusi, Z., Combs, A., Langer, S., Sutton, S., Leinwand, L.A., Geeves, M.A., Ruppel, K.M., and Spudich, J.A. (2015) Contractility parameters of human β-cardiac myosin with the hypertrophic cardiomyopathy mutation R403Q show loss of motor function. *Sci Adv*. 1.

Nag, S., Trivedi, D.V., Sarkar, S.S., Adhikari, A.S., Sunitha, M.S., Sutton, S., Ruppel, K.M., and Spudich, J.A. (2017) The myosin mesa and the basis of hypercontractility caused by hypertrophic cardiomyopathy mutations. *Nat Struct Mol Biol. 24*, 525- 533.

Pinto, A., Sánchez, F., Alamo, L., and Padrón, R. (2012) The myosin interacting-heads motif is present in the relaxed thick filament of the striated muscle of scorpion. *J Struct Biol. 180,* 469-478.

Price, H.M. (1963) The skeletal muscle fiber in the light of electron microscope studies. A review. *Am J Med. 35,* 589-605.

Rayment, I., and Holden, H.M. (1994) The three-dimensional structure of a molecular motor. *Trends Biochem Sci. 19,* 129-34.

Rayment, I., Smith, C., and Yount, R. G. (1996) The active site of myosin. *Annu. Rev. Physiol. 58*, 671–702.

Redwood, C.S., Moolman-Smook, J.C., and Watkins. H. (1999). Properties of mutant contractile proteins that cause hypertrophic cardiomyopathy. *Cardiovascular Research, 44,* 20-36.

Rees, M.K., and Young, M. (1967) Studies on the isolation and molecular properties of homogeneous globular actin. Evidence for a single polypeptide chain structure. *J. Biol. Chem. 242,* 4449-4458.

Reisler, E., Cheung, P., and Borochov, N. (1986) Macromolecular assemblies of myosin. *Biophys. J. 49,* 335-342.

Richard, P., Charron, P., Carrier, L., Ledeuil, C., Cheav, T., Pichereau, C., Benaiche, A., and Isnard, R. (2004). Hypertrophic cardiomyopathy: Distribution of disease genes, spectrum of mutations, and implications for a molecular diagnosis strategy. *Circulation, 109(25),* 3258.

Richard, P., Charron, P., Carrier, L., Ledeuil, C., Cheav, T., Pichereau, C., Benaiche, A., Isnard, R., Dubourg, O., Burban, M., Gueffet, J.P., Millaire, A., Desnos, M., Schwartz, K., Hainque, B., and Komajda, M. (2003) Hypertrophic cardiomyopathy: distribution of disease genes, spectrum of mutations, and implications for a molecular diagnosis strategy. *Circulation 107,* 2227-2232.

Robyt, J. F, and White, B. J. (1987). Biochemical techniques: theory and practice. Monterey (Calif.): Brooks/Cole

Root, D. D. (1997) In situ molecular association of dystrophin with actin revealed by sensitized emission immuno-resonance energy transfer. *Proceedings of the National Academy of Sciences. 94*, 5685–5690.

Root, D. D., Yadavalli, V. K., Forbes, J. G., and Wang, K. (2006). Coiled coil nanomechanic and uncoiling and unfolding of the superhelix and a-helices of myosin. *Biophysical Journal. 90(8),* 2852-2866.

Ruppel, K.M., and Spudich, J.A. (1996) Structure-function analysis of the motor domain of myosin. *Annu Rev Cell Dev Biol. 12,* 543-73.

Ryder, J., Lau, K., Kamm, K., & Stull, J. (2007). Enhanced Skeletal Muscle Contraction with Myosin Light Chain Phosphorylation by a Calmodulin-sensing Kinase. *The Journal of biological chemistry*. 282. 20447-54.

Sata, M., Stafford, W., Mabuchi, K., and Ikebe, M. (1997) The motor domain and the regulatory domain of myosin solely dictate enzymatic activity and phosphorylation-dependent regulation, respectively. *Proc. Natl. Acad. Sci. U.S.A. 94,* 91-96.

Schiller, P. W. (1975). In Biochemical Fluorescence: Concepts. ed. R. F. Chen, H. Edelhoch, 1:285-303. New York: Dekker. 408 pp.

Selvin, P. R. (1995). Fluorescence resonance energy transfer. *Methods in enzymology*, *246*.

Semsarian, C., Ingles, J., Maron, M.S., Maron, B.J. (2015) New perspectives on the prevalence of hypertrophic cardiomyopathy. *J. Am. Coll. Cardiol. 65,* 1249-1254.

Semsarian, C., Ingles, J., Wilde, A.A. (2015) Sudden cardiac death in the young: the molecular autopsy and a practical approach to surviving relatives. *Eur. Heart J. 36,* 1290-1296.

Sevrieva, I. R., Brandmeier, B., Ponnam, S., Gautel, M., Irving, M., Campbell, K. S., Sun, Y. B., & Kampourakis, T. (2020). Cardiac myosin regulatory light chain kinase modulates cardiac contractility by phosphorylating both myosin regulatory light chain and troponin I. *The Journal of biological chemistry*, *295*(14), 4398–4410.

Sherrid M. V. (2016). Drug Therapy for Hypertrophic Cardiomypathy: Physiology and Practice. *Current cardiology reviews*, *12*(1), 52–65.

Siemankowski, R. F., Wiseman, M. O. and White, H. D. (1985) ADP Dissociation from Actomyosin Subfragment 1 is Sufficiently Slow to Limit the Unloaded Shortening Velocity in Vertebrate Muscle. *Proc. Natl. Acad. Sci. U.S.A. 82,* 658–662.

Singh, R. R., Dunn, J. W., Qadan, M. M., Hall, N., Wang, K. K., & Root, D. D. (2018). Whole length myosin binding protein C stabilizes myosin S2 as measured by gravitational force spectroscopy. *Archives of Biochemistry and Biophysics*, *638*, 41–51.

Singh, R.R, Qadan, M.M., Aboonasrshiraz, N., Quedan, D.M., Wang, D., and Root D.D. (2017). Peptides designed to destabilize the myosin coiled coil enhance myofibril shortening while peptides that stabilize the coiled coil inhibit myofibril shortening. *Biophysical Journal*. 112, 557a.

Singh, R.R., Dunn, J.W., Qadan, M.M., Hall, N., Wang, K.K., and Root, D.D. (2017) Whole length myosin binding protein C stabilizes myosin S2 flexibility as measured by gravitational force spectroscopy. *Archives of Biochemistry and Biophysics*.

Sommese, R.F., Sung, J., Nag, S., Sutton, S., Deacon, J.C., Choe, E., Leinwand, L.A., Ruppel, K., and Spudich, J.A. (2013) Molecular consequences of the R453C hypertrophic cardiomyopathy mutation on human β-cardiac myosin motor function. Proc Natl Acad Sci U S A. 110, 12607-12612

Spudich, J.A. and Watt, S. (1971) The regulation of rabbit skeletal muscle contraction. I. Biochemical studies of the interaction of the tropomyosin-troponin complex with actin and the proteolytic fragments of myosin. *J. Biol. Chem. 246,* 4866–4871.

Stelzer, J. E., Fitzsimons, D. P., & Moss, R. L. (2006). Ablation of myosin-binding protein-C accelerates force development in mouse myocardium. *Biophysical journal*, *90*(11), 4119-4127.

Stull, J. T., Kamm, K. E., & Vandenboom, R. (2011). Myosin light chain kinase and the role of myosin light chain phosphorylation in skeletal muscle. *Archives of biochemistry and biophysics*, *510*(2), 120–128.

Sugi, H, Kobayashi, T., Gross, T., Noguchi, K., Karr, T., and Harrington, W.F. (1992) Contraction characteristics and ATPase activity of skeletal muscle fibers in the presence of antibody to myosin subfragment 2. *Proc. Natl. Acad. Sci. U. S. A. 89*, 6134-6137

Taei, N., Root, D.D. (2013) "Synthetic peptides model instability of cardiac myosin subfragment-2." *University of North Texas*.

Tardiff, J. C., Carrier, L., Bers, D. M., Poggesi, C., Ferrantini, C., Coppini, R., Maier, L. S., Ashrafian, H., Huke, S., & van der Velden, J. (2015). Targets for therapy in sarcomeric cardiomyopathies. *Cardiovascular research*, *105*(4), 457–470.

Taylor, E.W. (1977) Transient phase of adenosine triphosphate hydrolysis by myosin, heavy meromyosin, and subfragment 1. *Biochemistry 16,* 732-740.

Tesson, F., Richard, P., Charron, P., Mathieu, B., Cruaud, C., Carrier, L., Dubourg, O., Lautié, N., Desnos, M., Millaire, A., Isnard, R., Hagege, A.A., Bouhour, J.B., Bennaceur, M., Hainque, B., Guicheney, P., Schwartz, K., and Komajda, M. (1998) Genotype-phenotype analysis in four families with mutations in beta-myosin heavy chain gene responsible for familial hypertrophic cardiomyopathy. *Hum Mutat. 12,* 385-392.

Trybus, K. M., Huiatt, T. W., & Lowey, S. (1982). A bent monomeric conformation of myosin from smooth muscle. *Proceedings of the National Academy of Sciences of the United States of America*, *79*(20), 6151–6155.

Vibert, P., Craig, R., and Lehman, W. (1997). Steric-model for activation of muscle thin filaments. J. *Mol. Biol.* 266, 8–14.

Volkmann, N., Lui, H., Hazelwood, L., Trybus, K.M., Lowey, S., and Hanein, D. (2007) The R403Q myosin mutation implicated in familial hypertrophic cardiomyopathy causes disorder at the actomyosin interface. *PLoS One*. 2, e1123

Waldmüller, S., Sakthivel, S., Saadi, A.V., Selignow, C., Rakesh, P.G., Golubenko, M., Joseph, P.K., Padmakumar, R., Richard, P., Schwartz, K., Tharakan, J.M., Rajamanickam, C., and Vosberg, H.P. (2003) Novel deletions in MYH7 and MYBPC3 identified in Indian families with familial hypertrophic cardiomyopathy. *J Mol Cell Cardiol. 35, 623-636*.

Walker, S.M., and Schrodt, G.R. (1967) Contraction of skeletal muscle. *Am J Phys Med. 46,* 151-72

Wang, K. (1985) Sarcomere - Associated Cytoskelatal Lattices in Striated Muscle. *Cell Muscle Motil.*, 315-369. Springer US, New York

White, H. D. and Taylor, E. W. (1976) Energetics and Mechanism of Actomyosin Adenosine Triphosphatase. *Biochemistry* 15, 5818–5826.

Wigle, E. D., Rakowski, H., Kimball, B. P., and Williams, W. G. (1995). Hypertrophic cardiomyopathy: Clinical spectrum and treatment. *American Heart Association Journals*, 92(7), 1680-1692.

Wilson, K., & Walker, J. (Eds.). (2010). Principles and Techniques of Biochemistry and Molecular Biology. Cambridge: Cambridge University Press.

Witjas-Paalberends, E.R., Ferrara, C., Scellini, B., Piroddi, N., Montag, J., Tesi, C., Stienen, G.J., Michels, M., Ho, C.Y., Kraft, T., Poggesi, C., and van der Velden, J. (2014) Faster cross bridge detachment and increased tension cost in human hypertrophic cardiomyopathy with the R403Q MYH7 mutation. *J Physiol*. 592, 3257-3272

Woodhead, J.L., Zhao, F.Q., Craig, R., Egelman, E.H., Alamo, L., and Padrón, R. (2005) Atomic model of a myosin filament in the relaxed state. *Nature* 436, 1195-1199.

Xu, J., and Root, D.D. (2000) Conformational selection during weak binding at the actin and myosin interface. *Biophys* J. 79, 1498-1510.